The Screamin' Dingo

An Investigation and Adventure into

Competitive Aerobatic Light Sport Aircraft

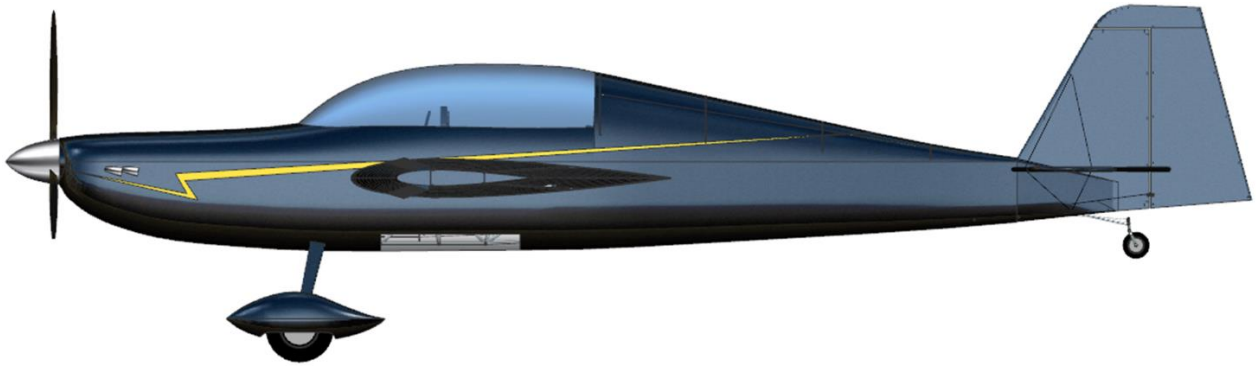

AIAA Undergraduate Team Aircraft Design Competition

2015 - 2016

Jefferson Vlasnik

Joel Eppler

Liam Murphy

Riley Sprunger

Michael Gritsch

Justin Fox

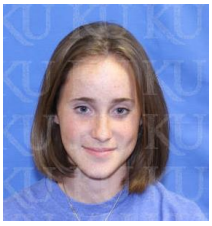

Taylor George

Joel Kennedy

Cameron Clanchy

Team Member	Nationality	AIAA Number	Signature
Cameron Clanchy	AUS	688036	
Joel Eppler	USA	688495	
Justin Fox	AUS	687865	
Taylor George	USA	665629	
Michael Gritsch	AUS	592050	
Joel Kennedy	AUS	687576	
Liam Murphy	AUS	687950	
Riley Sprunger	USA	464114	
Jefferson Vlasnik	USA	688450	
Team Advisors	**Nationality**	**AIAA Number**	**Signature**
Dr. Ron Barrett	USA	022393	
Cees Bil	AUS	077937	

Acknowledgments

The team would like to extend their gratitude towards those who lent their time and expertise throughout this design process:

University of Kansas Representatives:

Dr. Ron Barrett – Faculty Advisor

Dr. Richard Hale

Royal Melbourne Institute of Technology University Representatives:

Dr. Cees Bil – Faculty Advisor

DARCorp Representatives:

Dr. Jan Roskam

Dr. Willem Anemaat

U.S.A. 2015 Unlimited Aerobatic Team:

Mark Norwosielski

Alligator Inc.:

Ron Renz

Federal Aviation Administration:

Marv Nuss

Wes Ryan

OzAero Pty. Ltd.:

David Pilkington

All who attended the 2nd Annual "Snowbird Classic" Aerobatic Contest in Dunnellon, Florida for allowing us to observe, participate, and ask many questions.

Table of Contents

Page No.

List of Symbols

Symbol	Definition	Units
AR_h	Aspect Ratio of the Horizontal Stabilizer	~
AR_v	Aspect Ratio of the Vertical Stabilizer	~
AR_w	Aspect Ratio of the Wing	~
b_h	Horizontal Stabilizer Span	ft
b_v	Vertical Stabilizer Span	ft
b_w	Wing Span	ft
C_D	Coefficient of Drag	~
C_{D_O}	Zero-Lift Coefficient of Drag	~
C_{D_u}	Coefficient of Drag due to Variation in Speed	~
C_{D_α}	Coefficient of Drag due to Angle of Attack	deg^{-1}
C_L	Coefficient of Lift	~
C_{L_O}	Zero Angle of Attack Coefficient of Lift	~
C_{L_u}	Coefficient of Lift due to Variation in Speed	~
C_{L_q}	Coefficient of Lift due to Pitch Rate	deg^{-1}
C_{L_α}	Coefficient of Lift due to Angle of Attack	deg^{-1}
C_{l_p}	Coefficient of Rolling Moment due to Roll Rate	deg^{-1}
C_{l_β}	Coefficient of Rolling Moment due to Sideslip Angle	deg^{-1}
$C_{l_{\delta_a}}$	Coefficient of Rolling Moment due to Aileron Deflection	deg^{-1}
$C_{l_{\delta_r}}$	Coefficient of Rolling Moment due to Rudder Deflection	deg^{-1}
C_{m_O}	Zero-Lift Coefficient of Pitching Moment	~

C_{m_q} ..... Coefficient of Pitching Moment due to Pitching Rate ..... deg^{-1}
C_{m_u} ..... Coefficient of Pitching Moment due to Variations in Speed ..... ~
C_{m_α} ..... Coefficient of Pitching Moment due to Angle of Attack ..... deg^{-1}
$C_{m_{\delta_e}}$ ..... Coefficient of Pitching Moment due to Elevator Deflection ..... deg^{-1}
C_{n_p} ..... Coefficient of Yawing Moment due to Roll Rate ..... deg^{-1}
C_{n_β} ..... Coefficient of Yawing Moment due to Sideslip Angle ..... deg^{-1}
$C_{n_{\delta_a}}$ ..... Coefficient of Yawing Moment due to Aileron Deflection ..... deg^{-1}
$C_{n_{\delta_r}}$ ..... Coefficient of Yawing Moment due to Rudder Deflection ..... deg^{-1}
c_r ..... Wing Root Chord Length ..... ft
c_t ..... Wing Tip Chord Length ..... ft
C_{y_β} ..... Coefficient of Side Force due to Sideslip Angle ..... deg^{-1}
D_{prop} ..... Propeller Diameter ..... ft
e ..... Oswald Efficiency Factor ..... ~
E ..... Young's Modulus ..... Msi
F_{cy} ..... Compressive Yield Stress ..... ksi
F_{tu} ..... Tensile Ultimate Stress ..... ksi
F_{ty} ..... Tensile Yield Stress ..... ksi
I ..... Moment of Inertia ..... in^4
L/D ..... Lift to Drag Ratio ..... ~
MM ..... Maneuver Metric ..... ~
M_{prop} ..... Propeller Mach Number ..... ~
n ..... Load Factor ..... ~
P ..... Power ..... hp
S_H ..... Horizontal Stabilizer Area ..... ft^2
s_L ..... Landing Run Length ..... ft
s_{to} ..... Takeoff Run Length ..... ft
S_V ..... Vertical Stabilizer Area ..... ft^2
S_W ..... Wing Area ..... ft^2
S_{wet} ..... Wetted Area ..... ft^2
T ..... Thrust ..... lb
TVC ..... Tail Volume Coefficient ..... ~
V ..... Velocity ..... kts. or ft/s
W_{ae} ..... Aerobatic Weight ..... lb
W_e ..... Empty Weight ..... lb
W_{oe} ..... Operating Empty Weight ..... lb
W_{to} ..... Takeoff Weight ..... lb
X_{CG} ..... X-Direction Center of Gravity Location ..... ft
λ ..... Taper Ratio ..... ~
ρ ..... Air Density ..... $slugs/ft^3$
ϕ ..... Roll Rate ..... deg/s

List of Acronyms

Acronym	Description
AAA	Advanced Aircraft Analysis
AIAA	American Institute of Aeronautics and Astronautics
ASI	Airspeed Indicator
ASTM	American Society for Testing and Materials
BTU	British Thermal Unit
CAD	Computer Aided Design
CAS	Calibrated Air Speed
CG	Center of Gravity

EIS ..... Entry into Service
EFIS ..... Electronic Flight Information System
FAA ..... Federal Aviation Administration
FAR ..... Federal Aviation Regulations
FAI ..... Fédération Aéronautique Internationale
GA ..... General Aviation
GAMA ..... General Aviation Manufacturers Association
HP ..... Horsepower
IAC ..... International Aerobatic Club
ISA ..... International Standard Atmosphere
KU ..... University of Kansas
LL ..... Low Lead
LSA ..... Light Sport Aircraft
mgc ..... Mean Geometric Chord
MSL ..... Mean Sea Level
NACA ..... National Advisory Committee for Aeronautics
RC ..... Rate of Climb
RFP ..... Request for Proposal
RMIT ..... Royal Melbourne Institute of Technology University
RPM ..... Revolutions per Minute
S&C ..... Stability and Control
SFC ..... Specific Fuel Consumption
STAMPED ..... Statistical Time and Market Predictive Engineering Design
TEL ..... Tetraethyl-Lead
TO ..... Takeoff
TOFL ..... Takeoff Field Length
VG ..... Vortex Generators
VSI ..... Vertical Speed Indicator
WWI ..... World War I
WWII ..... World War II

List of Tables

Page No.

List of Figures

Page No.

Executive Summary

With the rewrite of FAR 23 regulations currently going through the review process and looking to be implemented early in 2017, the market for small aircraft will see an incredible influx in innovation and design. This rewrite also includes new rules for how light sport aircraft will be certified, with the goal being to bring LSAs to market faster and at a lower cost. In this new environment, there is space to create family of aircraft that combines the thrill and excitement of aerobatics with the affordability and accessibility of the LSA market. The family consists of a single and two seat aircraft. The single must be competitive in the intermediate category of International Aerobatic Club (IAC) Competition, while the two seat should be geared toward general aviation and aerobatic training. Both aircraft have their own performance metrics which they must meet, but both must fall within the FAR 14 definition of an LSA.

To determine the most competitive design, 7 Class I concepts were conceived and researched. A down selection resulted in a final aircraft to be carried through Class II design. This design was adapted for both single and two seat variants, in order to achieve 75% commonality by structure. The aircraft have a length of 320 in., a wingspan of 360 in., and a maximum takeoff weight of 980 lb. and 1,200 lb. for the single and two seat, respectively. The wings are made from a symmetric airfoil, and utilize vortex generators to achieve the lift required to meet the stall speed requirement of 45 kts. Flaps are not required for takeoff or landing. For ease of storage, the wings are removable from the aircraft by a pinned connection. Flight controls are fully reversible, employing push-rods for maximum feedback to the pilot, and direct connection cables for the rudder. Both aircraft are longitudinally and laterally stable. The aircraft will be manufactured from a chrome-moly truss, aluminum panels, and fabric overlays. It will be offered as both a kit and a fully assembled aircraft. Market price will be $95,000 for the fully assembled single seat, and $100,000 for the fully assembled two seat.

Compliance Matrix

Description	*Requirement*		*Compliance*		*Section*
	Single	*Two*	*Single*	*Two*	
Maximum W_{TO}	1,320 lb		980 lb.	1,200 lb.	9.3
Stall Speed	≤45 kt.		45 kt.		5.1
Max Speed	≤120 kt CAS		116 kt. CAS		11.5
Engines	1		1		6.2
Propeller	Fixed Pitch/Ground Adjustable		Fixed Pitch		6.2
Landing Gear	Fixed		Fixed		9.2
Ferry Range	300 nmi + 30 min.	250 nmi + 30 min	460 nmi	327 nmi	11.4
Climb Rate	1,500 fpm	800 fpm	2,250 fpm	2,170 fpm	11.1
TOFL 5,000' MSL, ISA + 10°C	1,200 ft.	1,500 ft.	680 ft.	1,010 ft.	11.2
Roll Rate	180°/s	---	184.5°/s	---	11.3
Payload	30 lb., 4 ft^3	30 lb., 6 ft^3	30 lb., 6.5 ft^3		11.4

Aircraft 3-Views

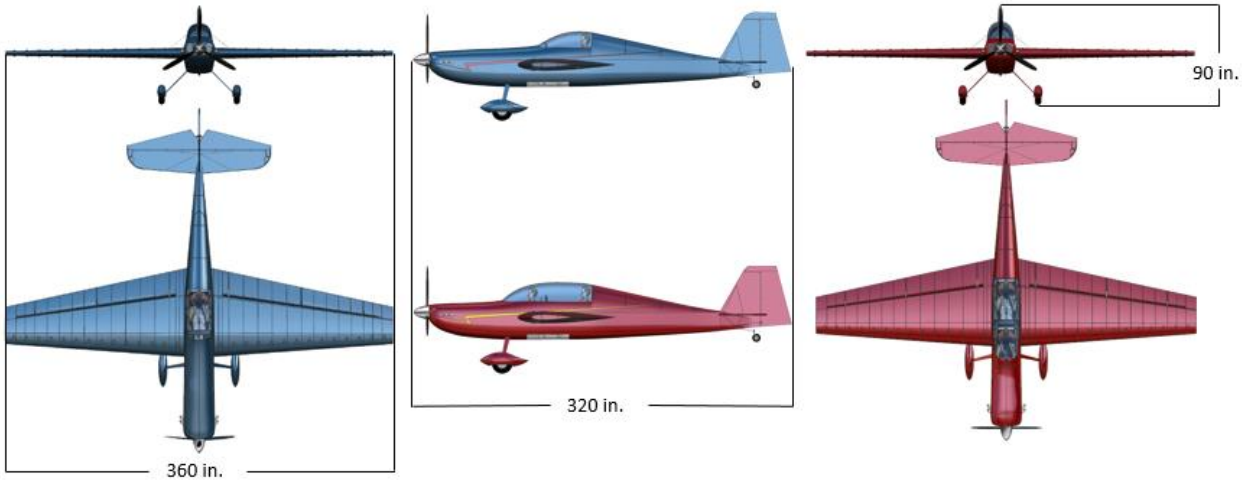

1. Mission Specification and Profile

The Aerobatic Light Sport Aircraft Family RFP [1] provided by the AIAA for the Undergraduate Team Aircraft Competition details the following requirements:

Table 1.1: RFP Requirements

Performance Requirements		
	Single Seat	Two Seat
Limit Loads	+6/-5	+6/-3
Ferry Range	300 nmi + 30 min. reserves	250 nmi + 30 min. fuel reserves
Climb Rate	1,500 fpm	800 fpm
Takeoff/Landing Distance*	1,200 ft.	1,500 ft.
Cargo	Pilot: 230 lb + 15 lb parachute Payload: 30 lb, 4 ft^3	Pilots: 200 lb + 15 lb parachute Payload: 30 lb, 6 ft^3
Max Gross Takeoff Weight	1320 lb	
Max Stall Speed	45 kts	
Max Speed (Level Flight)	120 kts CAS	
Inverted Flight	5 minutes minimum	
Flight Qualities	Similar to other aerobatic aircraft	
Configuration Constraints		
Propeller	Fixed/ground adjustable	
Cabin	Unpressurized	
Landing Gear	Fixed	
Design Objectives		
Structure	Reuse 75% structure and systems by weight between single and two seat variants	
Engines	One - Must meet LSA ASTM standards by EIS	
Systems	Meet LSA ASTM standards by EIS	
Maintainability/Reliability	Similar to comparable aircraft	
Styling	Make aircraft visually appealing for marketability	

*must be shown for sea level ISA + 10°C, 5,000 ft. MSL ISA + 10°C

From the given requirements, two mission profiles are defined. The first mission profile is an aerobatic mission. This profile is of short duration, lasting no more than 1 hour. The aircraft will takeoff, loiter for 10-20 minutes prior to competition, perform the aerobatic routine, and proceed to land. This profile is optimized for competition. The second profile is for cruise flight. This uses the given range and reserves requirements for both the single and two seat. The mission profiles are displayed on the following page.

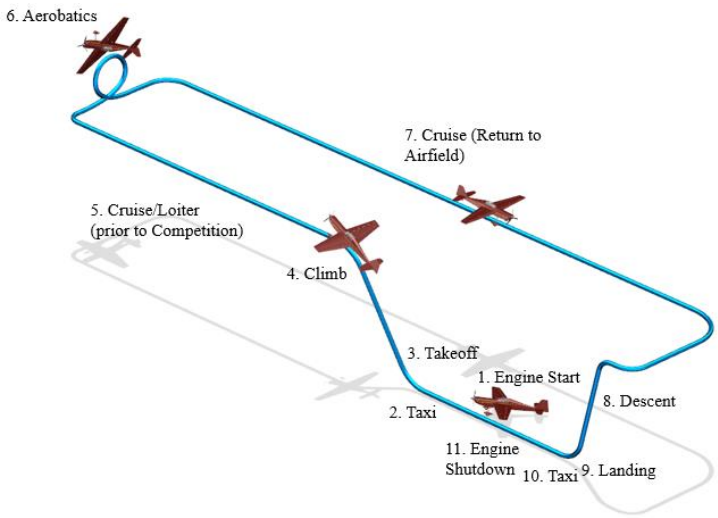

Figure 1.1: Mission Profile for Aerobatics

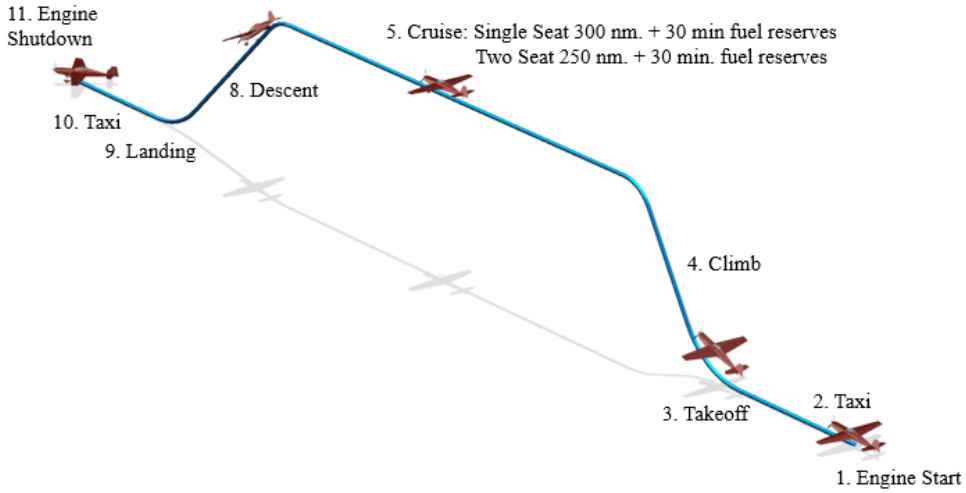

Figure 1.2: Mission Profile for Cruise

2. Historical Overview of Aerobatic Aircraft

Modern light sport aircraft and aerobatic competitions didn't develop overnight. The history and standardization of modern aerobatic competitions has a length that rivals that of flight itself. The earliest aerobatic maneuver was recorded by the Wright Brothers: a simple 360° turn. This move was considered difficult at the time, due to the common focus on stability rather than control. From this humble beginning, along with the advancement of flight control technology, stunt flying began to excite pilots and spectators alike. These basic stunt pilots became the pioneers of aerobatic flight, pushed strongly by the challenges of the First World War.

2.1 World War I

Early stunt pilots were recruited by militaries around the world as early reconnaissance officers and fighter pilots. As aerial engagements increased in frequency, certain techniques became more deadly than others. One of the first aerobatic combat maneuvers involved flying at your enemy from out of the sun or from underneath, followed by a quick aerobatic turn to escape. This hit and run technique allowed the underpowered Fokker Eindecker (shown in Figure 2.1) to dominate air combat early in the war. To combat and develop these techniques, pilots began teaching themselves and their fellow pilots more complex dogfighting maneuvers that became available as the engine power increased and aircraft were designed with maneuverability in mind. Aircraft such as the Fokker Albatross and the Sopwith Camel (shown in Figure 2.2) allowed for the development of many aerobatic maneuvers. These aerobatic maneuvers, such as the split-s and the Immelmann, became the tricks that continue to be performed in modern aerobatic competition. Once military commands began understanding the importance of aerobatic flight in dogfighting, the first training regiments for aerobatic flying began in 1916, leading to the development of a large base of aerobatic pilots.

Figure 2.1: Fokker Eindecker [2]

Figure 2.2: Sopwith Camel [3]

2.2 Post War Barnstorming

After the conclusion of the First World War, the aerobatic dogfighting pilots were left missing the daring adrenaline of the war. Many pilots began purchasing military surplus aircraft, and flying their wartime maneuvers for crowds of spectators. The Curtiss “Jenny” JN-4 was popular. Eventually, the competitive nature of these pilots began to show. As engine power and aircraft design began to advance in technology, so did the maneuvers possible: from simple loops and barrel rolls to the avalanche (a roll on top of a loop) to sustained inversion. The first negative g-force loop, referred to as an outside loop since the pilot is outside the loop, was performed by a Curtis P-1 in 1927. These post war pilots inspired aerobatic traveling airshows that were the precursors to today’s modern aerobatic competitions.

One of the key lessons to take away from the aircraft developed during WWI and WWII was how designs evolved to beat other aircraft. This meant that aircraft more easily maneuverable by pilots were the aircraft on which new designs were based. If a design wasn't able to outmatch previous aircraft, then it wasn't considered a good investment. The reason that aircraft are designed the way they are today with longitudinal and lateral control surfaces in the rear and the wing in the middle of the aircraft is because those designs were the best in the war. An expanded discussion on configuration layout is presented in Section 4.

2.3 Competitions and Modern Developments

Worldwide aerobatic competitions began to take hold in 1960. These competitions began as mainly freestyle events, with judges basing their rankings off of the impressiveness and riskiness of a pilots' routine. The Aerobatic Club of America that was established in 1962 would eventually become the International Aerobatic Club (IAC) that is the main proprietor of aerobatic competitions today. One of the more important aspects of Aerobatic competition today was developed in 1964 by Jose Louis Aresti, a Spanish aerobatic pilot. He developed a standardized system of shorthand notation for aerobatic routines. In modern competition, each of the standardized maneuvers is given a difficulty rating, and each pilot is judged on their ability to precisely fly those maneuvers. However, the spirit of the barnstorming days is still present in today's competitions during the freestyle portion: where pilots can push their bodies and airframes to the limits for the most exciting thrills.

The first aircraft to rise to dominance in these aerobatic competitions was the Pitts S-2S. This biplane was designed immediately following World War II and is designed specifically to be highly maneuverable with characteristics such as a high roll rate. Important design features include a symmetric airfoil for inverted flight, lightweight wood and fabric wings, control rods for nearly instantaneous control response, a fuel tank along the centerline to lower the moment of inertia and chrome-moly steel tubing fuselage to support a cockpit containing only the essentials. According to all the pilots the authors spoke with, aerobatic flying is an exhausting sport, and the hard aluminum seat with only a parachute for a cushion proves this point. As is common with other aerobatic aircraft, many Pitts are

Figure 2.3: Stephens Akro [4]

homebuilt, as many pilots who fly aerobatics as a hobby prefer to build their aircraft. This biplane is still a common sight at competitions of today, although it no longer places at the top.

The aircraft that ended the dominance of the Pitts and is the basis for future monoplane aerobatic aircraft is the Stephens Akro. Until 1972, the conventional thought was that an aerobatic aircraft had to be a biplane, while racing planes were monoplanes. Like the Pitts, the Akro was typically homebuilt with a chrome moly steel tubing and fabric covered fuselage. It also has a plywood covered wing with a 7-ply wooden railroad tie for the spar. As is clearly visible if the airframes are placed side by side, current unlimited class aircraft such as the Zivko Edge 540 and the Extra 330 trace the basis for their designs back to the Stephens Akro.

Also of note is the Champion Aircraft Citabria, later on known as the Super Decathlon. These aircraft are the trucks of the aerobatic world, with high wings and a tube and fabric construction. According to Mark Norwosielski, aerobatic pilots learn to fly on either a Pitts or a Super Decathlon. While it can put on an excellent show in the right pilot's hands as the authors witnessed at the Snowbird Classic Aerobatic Competition, the disadvantage to this aircraft is that it has a high wing and is therefore too inherently stable.

Figure 2.4: American Champion Super Decathlon

2.4 Design Research Trip

To gain firsthand experience with aerobatic planes similar to the RFP, the authors from the University of Kansas travelled to Dunnellon, Florida for the Snowbird Classic Aerobatic Contest. This contest featured competitors in the primary, sportsman, intermediate, and advanced categories. Along the way, the authors stopped in Mexico, Missouri to tour the Zenith Aircraft factory and gain insight into how they build their aircraft. Between Mexico and Dunnellon, the authors stopped in Warner Robins, Georgia to visit the U.S. Air Force Museum of Aviation.

At the Zenith Aircraft factory, the authors were able to tour the factory floor and see the process the Zenith uses to build their kit planes. Insight was gained on the size and scale of their operation, as well as the process for manufacturing the stock pieces for their many kit planes. The visit culminated with the authors taking flights in Zenith CH 650.

Figure 2.5: Zenith CH 650 [5]

At the Warner Robins U.S. Air Force Museum of Aviation, the authors gained general knowledge of aircraft, most of which was not directly applicable to the LSA specification. The most relevant knowledge gained was how the Flying Tigers utilized the power and speed of their P-40 Warhawk's to outfly the more maneuverable Japanese Zero's during World War II.

In Dunnellon Florida, the authors were able to talk to and interview many of the pilots who were competing. During the competition, the authors were able to see the competing aircraft and question the pilots about the most important design features of each. At the contest there were examples of a Pitts, Extra 330, Edge 540, Yak-53, Super Decathlon, Panzl S-300 and several other aircraft. One of the competing pilots was Mark Norwosielski, a current member of the U.S. Unlimited Aerobatic Team. He competed in the FIA World Aerobatic Championship in 2015, assisting the national team to take 3rd place overall. He currently flies an Edge 540. The authors were able to acquire many important details of aerobatic design from this seasoned aerobatic pilot. Once competition began, the authors were able to sit among the judges as they scored routines, and assist in taking down scores gaining valuable insight into the requirements to win competitions.

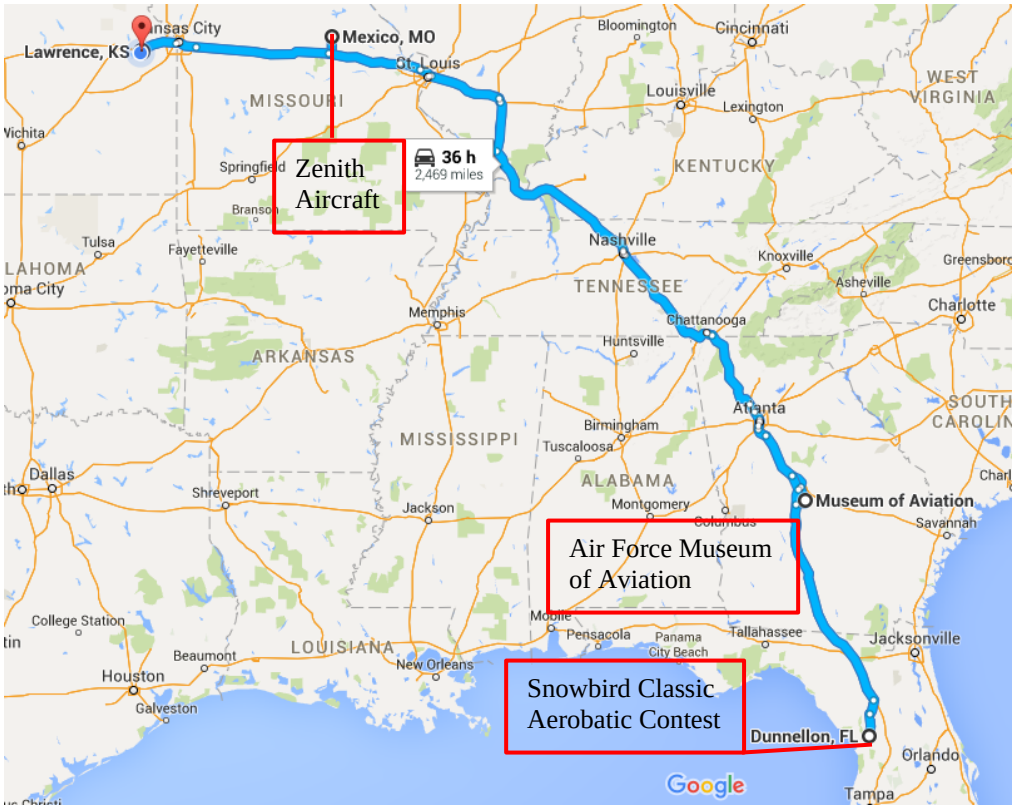

Figure 2.6: Route of Design Research Trip

3. STAMPED Vector Analysis, Initial Sizing

The STAMPED Vector Analysis is a method used to plot the change in a variable over a given length of time. Using data collected from the current and past market, a plot can be made of how a variable can change with respect to time. By plotting key design variables, a trend can be plotted to show where key design variables will be given a future date. During the market research, the team realized that many aerobatic aircraft are built specifically for aerobatics, and with little regard to LSA specifications. Few planes contain aspects from both Light Sport Aircraft as well as Aerobatic Aircraft. Therefore, it was decided that a design philosophy that contains aspects from both Light Sport Aircraft and Aerobatic Aircraft would be utilized for initial sizing. To begin the sizing process, a linear trend projecting the preferred takeoff weight from market of one seat Light Sport Aircraft was found. This trend is shown in Figure 3.1 as the black set of data with a black trend line.

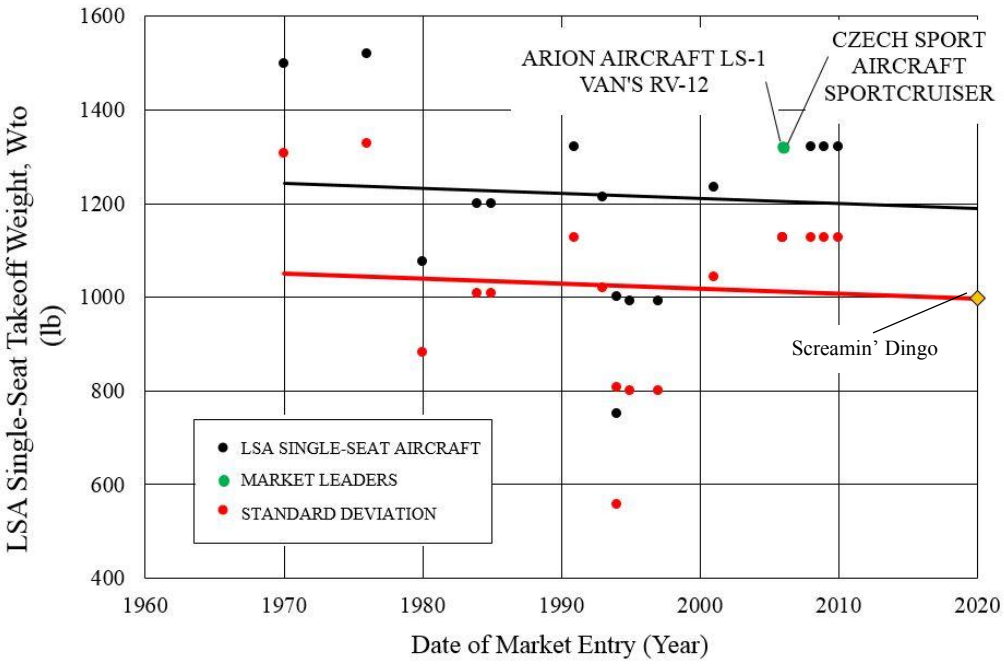

Figure 3.1: LSA Single Seat Takeoff Weight

The resulting takeoff weight for a one seat aircraft following the market trends in the year 2020 would be about 1,190 lbs. This weight was deemed to be too large to accommodate a two seat variant that would still be within the Light Sport Aircraft designation of 1,320 lbs. It was therefore determined that moving one standard deviation below the projected market in 2020 would be a statistically acceptable move. This placed the one seat variant takeoff weight at 1,000 lbs. This trend is shown as the red set of data in Figure 3.1, with the trend line shown in red. The

design point for this aircraft is shown as a gold diamond in Figure 3.1. The weight of the two seat variant was determined by removing an assumed smoke kit, weighing 40 lbs, removing a larger pilot, changing from 230 lbs to 200 lbs, adding an additional pilot, at 200 lbs, adding an additional parachute at 15 lbs, and lastly adding an assumed seat and structure weighing 95 lbs. The net change in weight between the one seat and two seat variant results at +240 lbs. This places the resulting takeoff weight for the two seat variant aircraft at 1,240 lbs.

The next two parameters that were determined were the ratios of: aerobatic competition weight to takeoff weight and empty weight to takeoff weight. For these parameters, the team determined that data from relevant aerobatic aircraft would be the most efficient way to size for more aerobatic performance. The linear trend for the above two parameters is shown in Figure 3.2 and Figure 3.3, with the trend line shown in black. The resulting design points are shown as gold diamonds. The resulting values determined from this trend at an aerobatic to takeoff weight of .870 and an empty weight to takeoff weight of .649. These two parameters allowed the aerobatic and empty weights to be estimated from the takeoff weights of the two variants. The resulting aerobatic and empty weights are shown in Table 3.1.

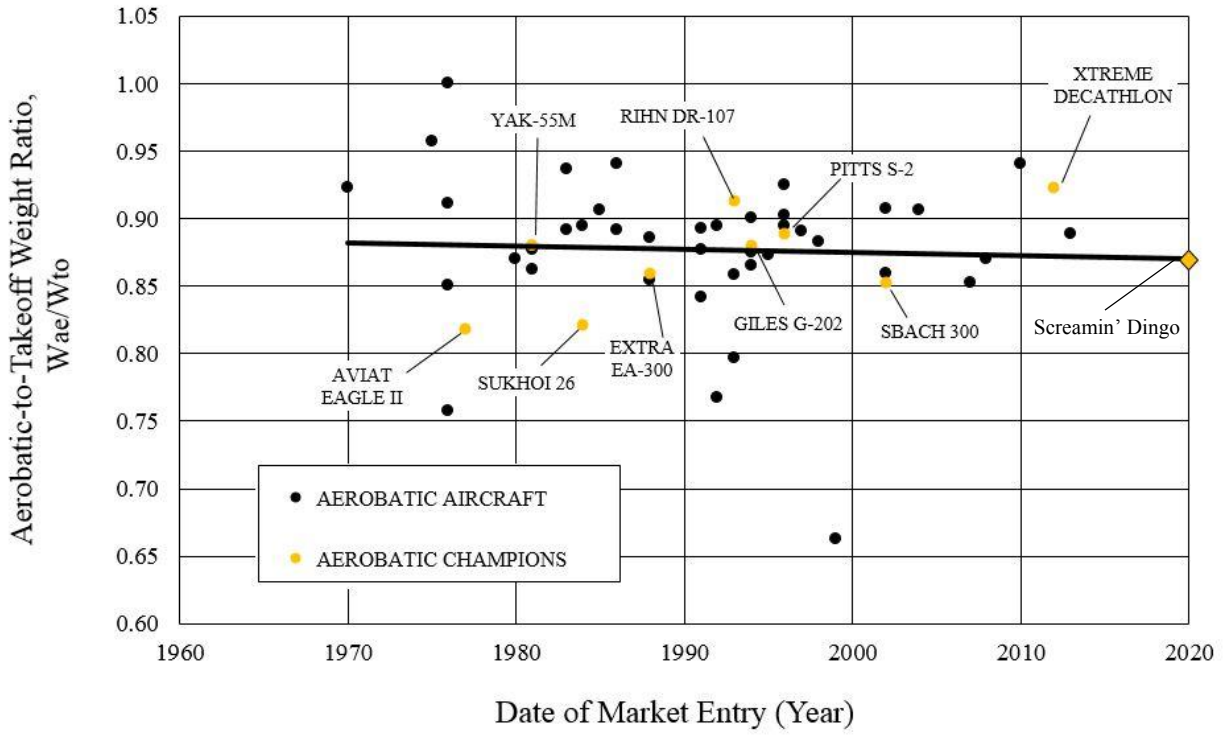

Figure 3.2: Aerobatic to Takeoff Weight

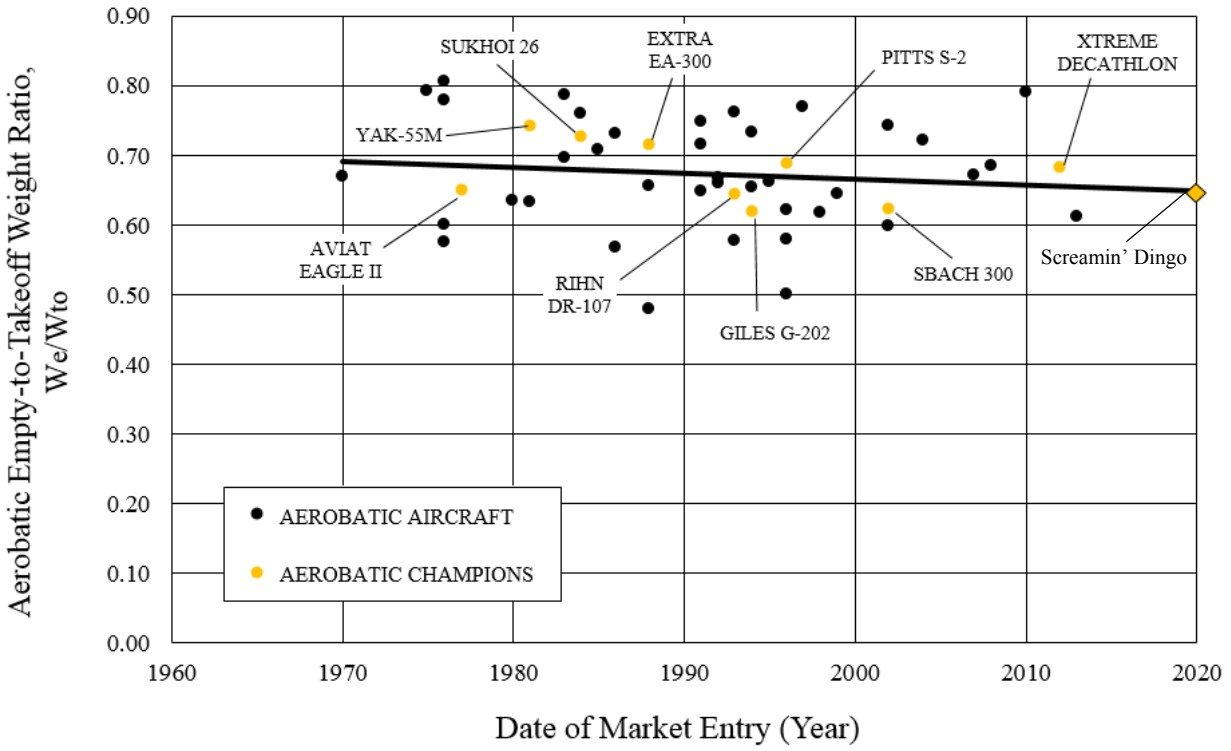

Figure 3.3: Aerobatic Empty to Takeoff Weight

The next parameter that was calculated using linear market trends was aircraft takeoff power loading, W_{to}/hp. The market that was used for this trend was one seat LSA aircraft, since the level of power loading for aerobatic loading was determined to be too low (engines too powerful). This is because a majority of the aerobatic planes researched are rated to fly in the unlimited category, rather than the intermediate category. The data trend for the power loading of single seat aircraft is shown in Figure 3.4. The trend line for this data is shown in black, with the design point following the trend line shown as a gold diamond. The value that was determined to be appropriate for power loading was determined to be 10.75 lbs/hp. Using this value, a required engine horsepower was calculated for both the one seat and two seat variants. The engine horsepower that was required for the one seat variant was 93 hp, and the engine horsepower that was required for the two seat variant was 115 hp. For increased commonality between the two aircraft, the engine requirement for both aircraft was determined to be 115 hp. The resulting power loading values for both variants is shown in Table 3.1.

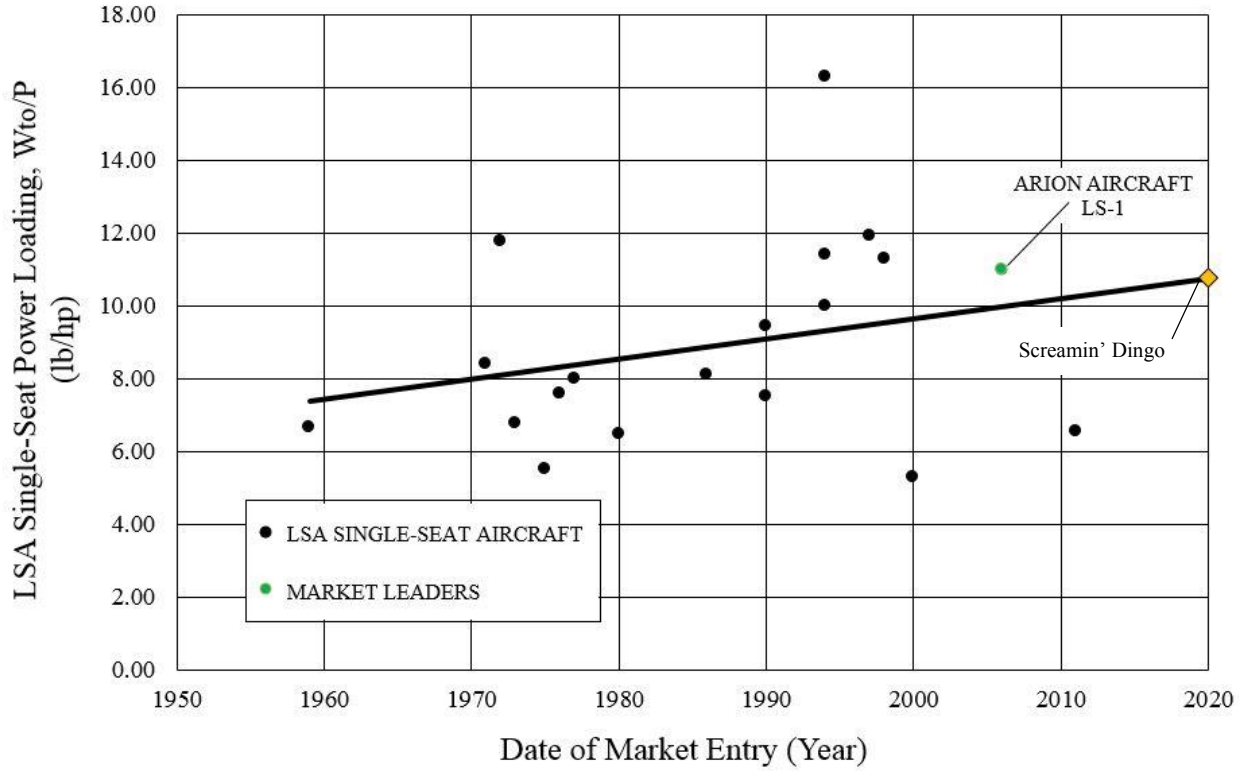

Figure 3.4: LSA Single Seat Power Loading

The wing loading is the next parameter to be predicted using market trend data. To achieve an approximate sizing appropriate for Light Sport Aircraft, data from the one and two seat LSAs were examined. Since the trend data showed that the two seat LSA aircraft required a lower wing loading (and therefore a larger wing), the data for the two seat LSA aircraft were used to create an initial sizing for this design. The trend line and data for the two seat LSA aircraft are shown in Figure 3.5. The trend line is shown in black, with the design point shown as a gold diamond.

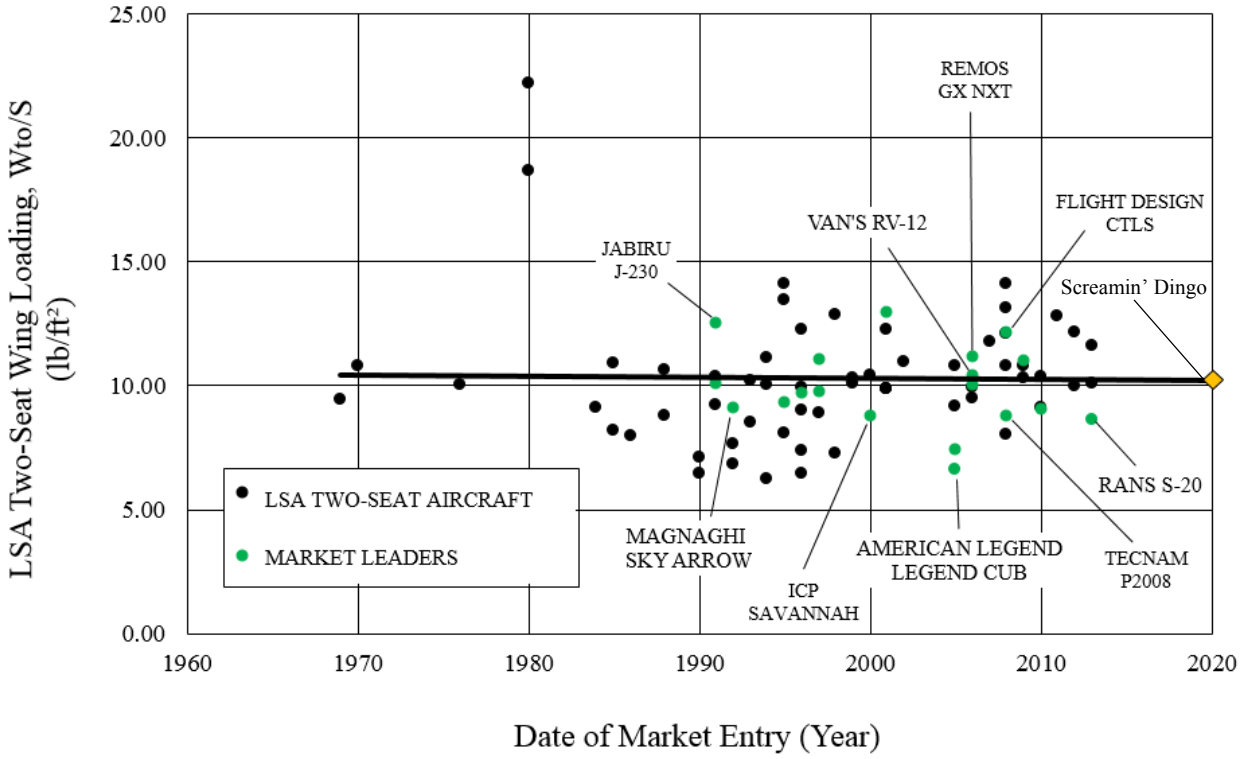

Figure 3.5: LSA Two Seat Wing Loading

The resulting wing loading that was determined to fit the LSA market in 2020 was found to be 10.20 lbs/ft². Using this value, approximate wing areas were determined for both the one seat and two seat variants. These values were 98.0 ft² and 121.6 ft², respectively. Since the two seat variant wing area controls the sizing, and commonality is deemed imperative for the wings, a wing area of 121.6 ft² will be used for both the one seat and two seat variants.

To appropriately size the wingspan, an aspect ratio was determined using market data. The market data that was deemed the most relevant for aspect ratio was the aerobatic aircraft market. This was because the aircraft will be required to have aerobatic performance in roll, and an aspect ratio similar to current aerobatic aircraft was deemed the most appropriate direction for the highest potential to be competitive in the intermediate category. The data utilized to determine this trend is shown in Figure 3.6, with the linear trend line shown in black, and the design point shown as a gold diamond. Using this trend data, the aspect ratio that was determined for this aircraft was 6.0. Using the wing area of 121.6 ft^2 found above, the wingspan was found to be 26.7 ft.

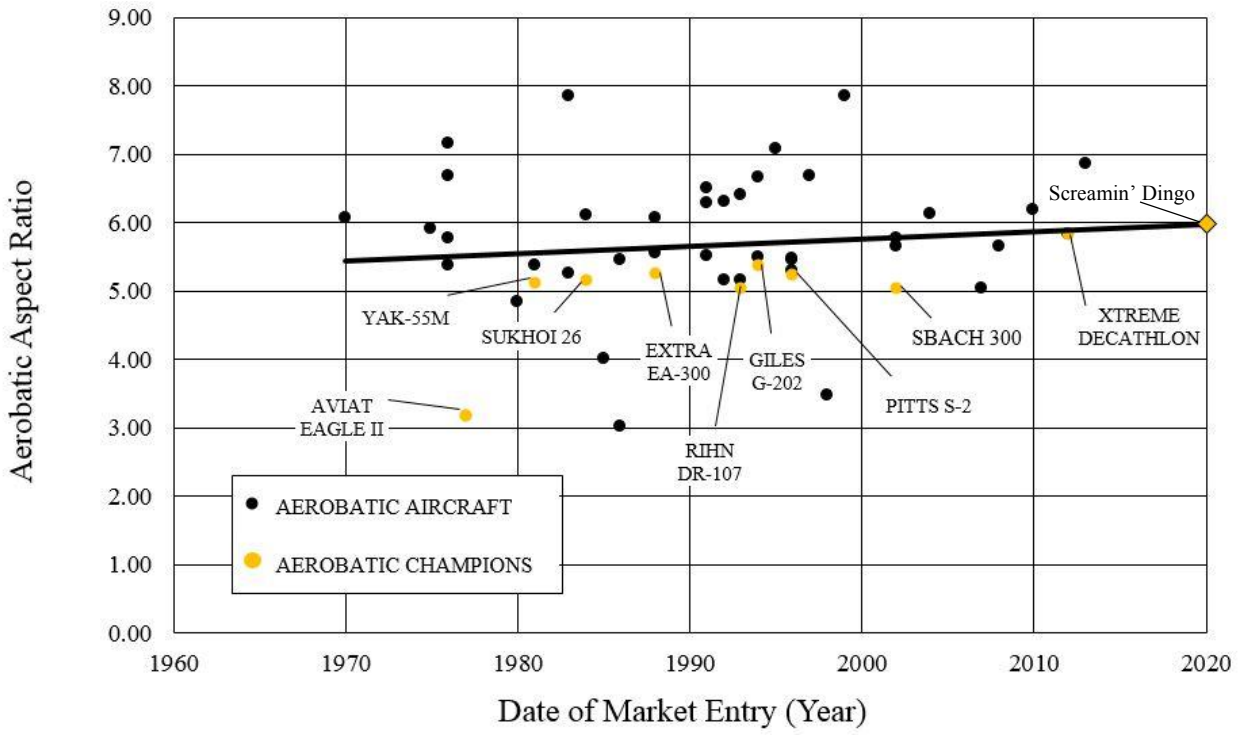

Figure 3.6: Aerobatic Aspect Ratio

The next parameter that was found using a linear trend line was the maneuver metric, defined as the thrust of an aircraft divided by the weight. This is a direct measurement to determine how maneuverable the aircraft is, and how must thrust will need to be produced by the engine and propeller. The data utilized to determine this trend is shown in Figure 3.7, with the linear trend line shown in black, and the design point shown as a gold diamond. This trend line was found using aerobatic aircraft, since this will help our Light Sport Aircraft reach better aerobatic performance. The linear trend line for the maneuver metric data for the year 2020 was determined to be 0.616.

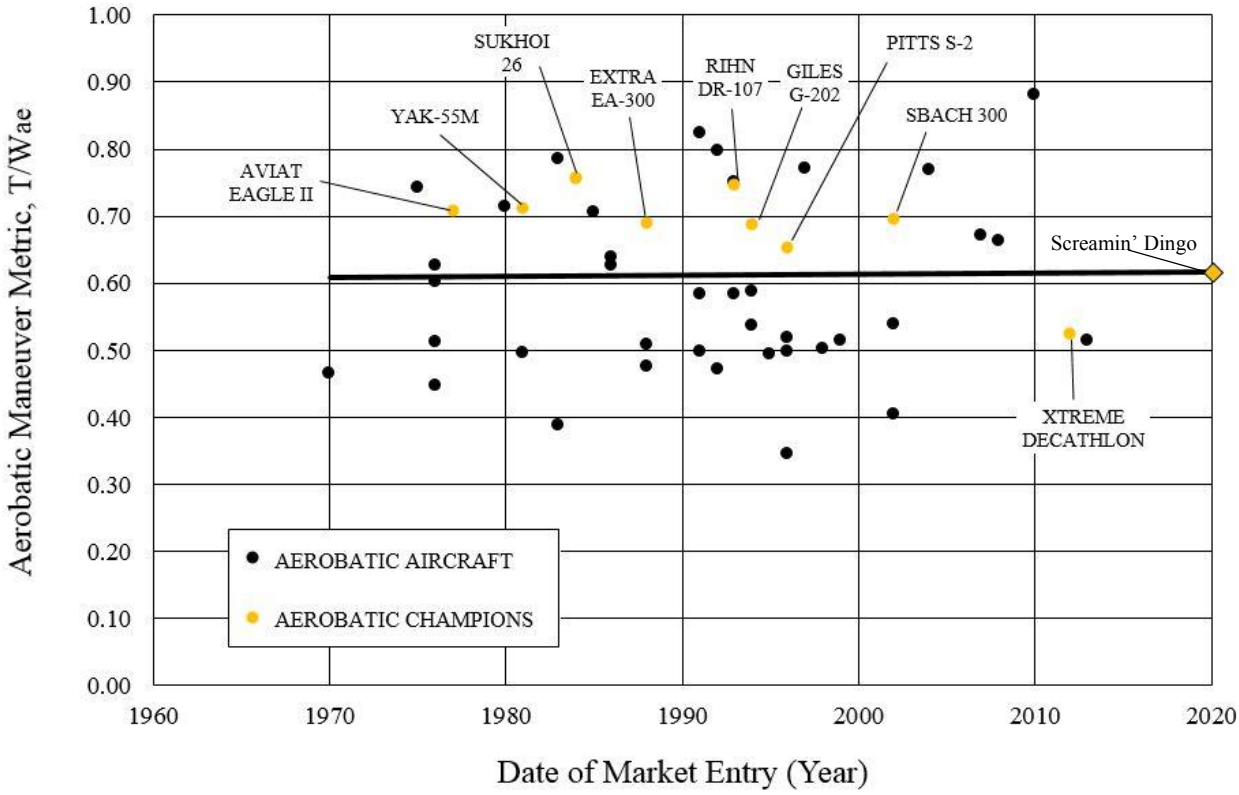

Figure 3.7: Aerobatic Maneuver Metric

To achieve this parameter at a minimum for both variants, the two values of required thrust were determined to be 536 lbs for the one seat variant and 664 lbs for the two seat variant. Since the required thrust is controlled by the two seat variant, the team aimed to achieve a thrust value of 664 lbs for both variants. Using the combination of the engine horsepower of 115 hp and the required thrust of 664 lbs, an estimation of propeller size can be determined. Assuming the aircraft was flying at 5,000 ft in standard atmosphere, propeller momentum theory was used to determine an initial propeller size:

$$D_{prop} = \sqrt{\frac{4 * (Thrust)^3}{2 * \pi * \rho * {M_{prop}}^2 * \left(HP * 550\ {}^{ft * lb}/_{hp}\right)^2}} = \sqrt{\frac{4 * (664\ lbs)^3}{2 * \pi * .00204\ {}^{lb * s^2}/_{ft^4} * (.72)^2 * \left(115\ hp * 550\ {}^{ft * lb}/_{hp}\right)^2}} \approx 6.5\ ft$$

Utilizing propeller momentum theory, a propeller that is sized at 6.5 feet in diameter will achieve the appropriate thrust values required for the one and two seat variants. The summarized basic sizing information for both the one and two seat variants is shown in Table 3.1.

Table 3.1: Summary of Initial STAMPED Sizing

	One Seat Variant	Two Seat Variant
Takeoff Weight, W_{TO}	1000 lbs	1240 lbs
Aerobatic Weight, W_{AE}	930 lbs	1080 lbs
Empty Weight, W_E	650 lbs	805 lbs
Engine Horsepower, HP	115 hp	
Propeller Diameter, D_{prop}	6.5 ft	
Thrust Attainable, T	664 lbs	
Wing Area, S_W	122 ft²	
Wingspan, b_W	27 ft	
Aspect Ratio, AR	6	
Takeoff Power Loading, W_{TO}/HP	8.7 lbs/hp	10.8 lbs/hp
Takeoff Wing Loading, W_{TO}/S	8.2 lbs/ft²	10.2 lbs/ft²
Maneuver Metric, T/W_{AE}	0.76	0.62

To determine the approximate C_{Lmax} values that would need to be achieved by the aircraft, a sizing chart was plotted and graphed. The sizing chart was created with the two-seat aircraft in mind, assuming that the C_{Lmax} achieved by the two seat would be adequate for the single seat. When performing the calculations to generate the curves, performance parameters for the single and twin seat were compared, and the more limiting factor was taken (i.e. taking the 1,200 ft. takeoff and landing distance of the single seat vs. 1,500 ft. for the twin). Sample aircraft are plotted on the sizing chart to display how current LSA and aerobatic aircraft compare to where our design point lands.

In order to find a direction for where the LSA market will be at the EIS, a linear trend line tracking W/S and W/P through the years was plotted. To generate this line, the W/S and W/P values for both single and twin LSAs were collected and sorted based on the year the aircraft came to market. Using the linear regression of these two data sets, a vector plotting W/P to W/S was charted through time, beginning at 1970 and ending at our EIS date for single seat, 2020. This was done in order to best size for an aircraft that can accommodate both single and twin seat variants. Figure 3.8 displays the sizing chart for the aircraft. It also displays LSA market leaders and intermediate aerobatic competition champions to show where the design point falls in the current market.

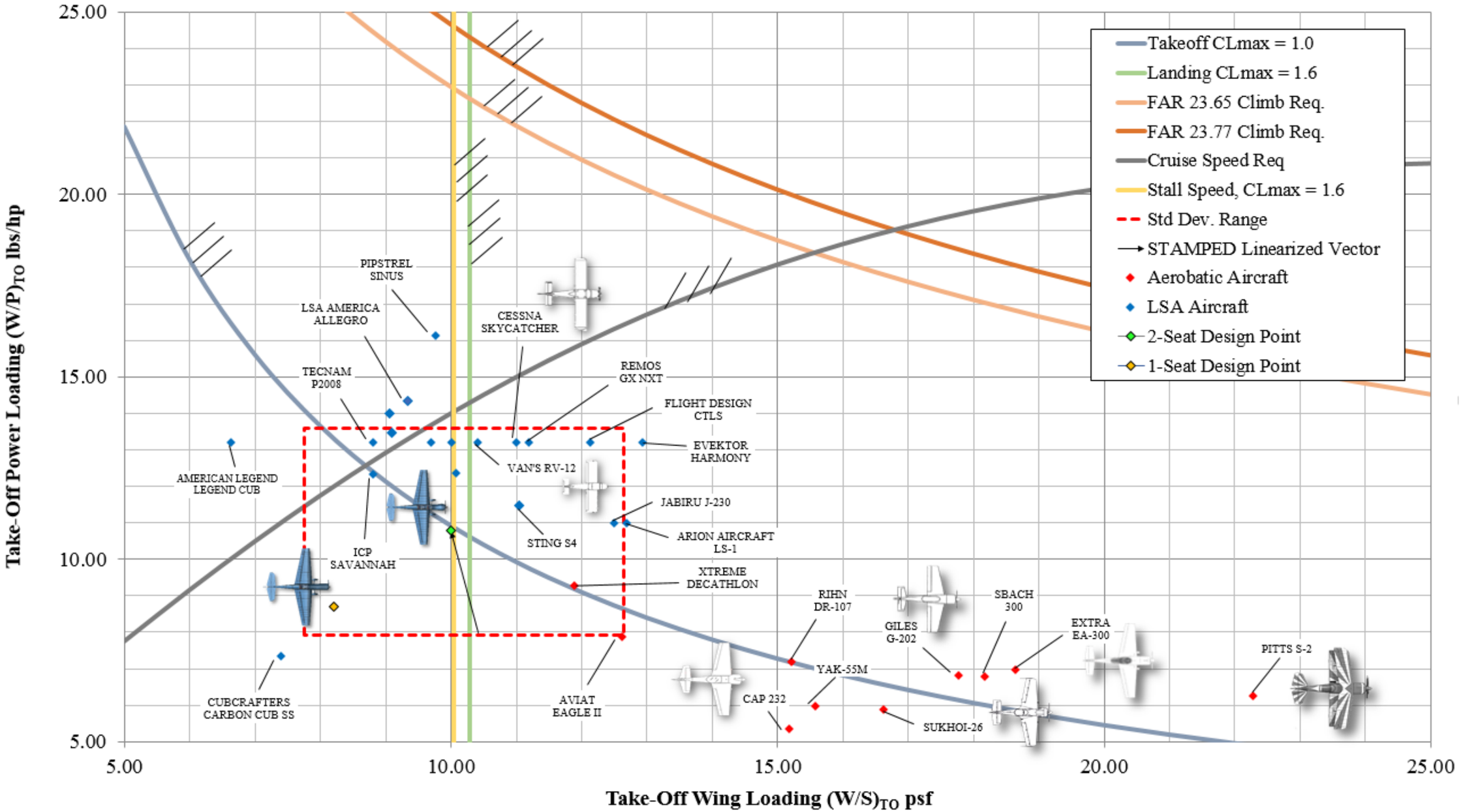

Figure 3.8: Sizing Chart with STAMPED Information

4. Class I Configuration Selections

The first stage of the design process was to determine a handful of configurations on which to perform Class I analysis. Initial Class I configurations were selected to fulfill the requirements of both the LSA category and the aerobatic category requirements. The primary restriction from the LSA requirements is the 1,320 lb. weight limit. However, since the aerobatic requirements are the most rigid, the configuration is primarily designed to meet the performance requirements for competition maneuvers. To assist in determining a feasible configuration, the IAC official competition rules were consulted, as well as advice from native Kansas aerobatic pilot Ron Renz.

The specification allows for the possibility of a powered land based airplane, seaplane or glider. While the IAC does hold aerobatic competitions for gliders, this configuration was not considered in detail because the cruise requirements would require adding a removable engine, increasing complexity and weight. Also, gliders make up a smaller portion of the market. Seaplanes are allowed a higher weight in the LSA category, but this is used to accommodate the floats and additional structure, which will have a negative impact on the aerobatic performance. Both the floats and mounting the engine away from the water would increase the moment of inertia and decrease roll rate. For these reasons, the main aircraft configuration to be considered is a single engine land based aircraft.

To assist in the down selection process, a criteria matrix was created to show all options considered. Various metrics including Acquisition Cost, Life Cycle Cost, Aerobatic Performance, Cruise Performance, Ease of Assembly, and Market Preference were used to determine the optimal set of configurations to move forward with in this design. To determine which designs would be appealing to many different design theories and eventually pilots, local aerobatic pilot Ron Renz was also consulted in this process. Ron Renz owns and operates Alligator Inc., an engineering consulting firm specializing in design, modification, flight testing, and certification of aircraft components and systems. He has been a test pilot for the Boeing 737 and has logged over 4,000+ hours in 60+ aircraft. He flew and delivered Aviat Eagle II's for over 10 years, and owns his own for recreational aerobatic flight. His opinion was consulted in the form of separate weighting factors. Designs that "won" in the different configurations of weighting factors were considered more viable designs. The major categories that were used to examine different configurations were fuselages, wings, landing gear, propeller location, engine type, empennage, and materials. Scores highlighted in green represent configurations chosen for Class I analysis.

Figure 4.1: Ron Renz [41]

Table 4.1: Criteria Matrix for Class I Selection

		Metrics							
		Cost		Performance		Market Preference	Ease of Assembly		
		Acquisition	Life Cycle	Aerobatic	Cruise				
	Team Initial Weight Factors	20%	10%	25%	15%	15%	15%		
	Ron Renz Weight Factors	12%	5%	47%	1%	12%	23%		
Component Category	Configuration Option	Scores (1-5, 5 is the highest)						Total Score (Team)	Total Score (Renz)
Fuselage	Twin Body, Side by Side	2	2	1	1	1	1	1.30	1.17
	Single Body, Tandem Seating	5	5	5	5	5	5	5.00	5.00
	Single Body, Bench Seating	5	5	4	4	5	5	4.60	4.52
	Single Body, Twin Boom	3	2	2	3	3	3	2.65	2.48
Wing	Bi-Plane	5	3	4	3	4	3	3.80	3.83
	Low Monowing	4	5	5	5	5	5	4.80	4.88
	Middle Monowing	4	5	5	5	5	5	4.80	4.88
	High Monowing	5	4	2	4	3	4	3.55	3.06
	Box Wing	2	1	1	3	1	2	1.65	1.37
	X-Wing	3	2	2	2	1	1	1.90	1.77
Landing Gear	Quadruple	1	1	2	2	1	1	1.40	1.48
	Tandem/Outrigger	2	1	2	2	1	1	1.60	1.60
	Tricycle	3	4	4	4	5	4	3.95	4.00
	Tail Dragger	5	5	5	5	4	5	4.85	4.88
	Pontoons	2	3	1	1	2	3	1.85	1.80
Propeller Location	Pusher	5	3	3	5	4	4	4.00	3.61
	Tractor	5	5	5	4	5	5	4.85	4.99
	Twin Propeller	2	1	1	3	1	1	1.50	1.14
Engine Type	Opposed	5	5	4	3	5	5	4.45	4.51
	Wankel	2	2	3	3	1	5	2.70	3.05
	Diesel	4	4	4	3	3	5	3.85	4.10
	Electric	1	4	5	5	3	5	3.80	4.23
Empennage	T	3	4	4	4	4	3	3.65	3.65
	Cruciform	3	4	4	4	2	4	3.50	3.64
	Conventional	5	5	5	4	5	5	4.85	4.99
	Grid Fin	1	2	3	2	1	3	2.05	2.46
	V	4	3	2	5	3	3	3.25	2.67
	H	2	4	3	3	2	2	2.60	2.58
	X	2	1	1	3	1	2	1.65	1.37
	Canard	5	4	3	4	3	4	3.80	3.53
	3-Surface	2	2	2	3	1	2	2.00	1.89

4.1 Fuselage Configuration

For the fuselage, a couple ideas were considered. A twin boom arrangement was considered with the idea in mind to make a modular aircraft. For a single seat variant, two wings would plug into one fuselage. The two seat variant would have two fuselage sections that were connected side by side with wings on the outside. This was deemed to be too complex, and separation of the pilots in their own fuselage pods would lessen the joy of flying with others.

A twin boom configuration would be the ideal choice if a pusher arrangement was decided on. In Section 4.5, pusher and tractor configurations were considered, and a tractor arrangement is chosen. While a twin boom can be done with a tractor, it is not a traditional design, and has never succeeded in aerobatic competition.

The final choice came down to bench seating vs. tandem. While bench seating is the preferred option for many general aviation aircraft, it would make 75% structural commonality difficult. In transitioning from a single to a two seat design, the fuselage/cockpit area would need to be reshaped, unless the space was repurposed. If the pilots had a large difference in weight, or if a single pilot flew the two seat, the aircraft would not roll around the centerline of the fuselage unless ballasts were used. To best keep the weight distribution of the fuselage on the centerline, a tandem arrangement was chosen.

4.2 Wing Configuration

The wing configurations to be considered for Class I design are low wing monoplane, mid wing monoplane and biplane. High wing monoplane is not considered because its roll stability is too large, and it would require greater structural support likely needing struts to support the wings. The only high wing aircraft to place in the intermediate class is the American Champion Decathlon, which placed 7th. Based on competition victories and conversations with different aerobatic pilots at the Snowbird Classic, a high wing like the Decathlon would not be competitive in intermediate competition.

Biplanes are competitive as aerobatic aircraft because the shorter wings allow for a lower moment of inertia and a higher roll rate. They are also structurally stable because of the box shape and therefore can have lighter wings. However, they do have more drag and are becoming less popular in aerobatic competitions. The reason for this is they are harder to judge in competition. This is because the duel wing is less clear and the short wingspan makes the aircraft harder to see in the sky.

Low wing and mid wing monoplanes are important to consider because all of the recent winners of intermediate class aerobatic competitions fall into this category. These aircraft have high roll rates and lower drag than other configurations. They have the most direct routing for controls, reducing complexity and saving weight. These configurations also have cleaner lines than biplanes. From the judges' point of view, a maneuver by a monoplane will score higher than the exact same maneuver by a biplane. Other configuration possibilities were considered such as three surface, flying wing and joined wing. However, in consultations with Ron Renz and other aerobatic pilots, these ideas were discounted based on their unfamiliarity and less predictable dynamics.

4.3 Landing Gear

For landing gear arrangement, quadruple and tandem outrigger were listed, but since those are mainly used for large aircraft with non-conventional designs or configurations, there was no need for them to be considered. Pontoons were considered to create an option for a seaplane, but aerobatic seaplanes would likely be unable to compete in competitions that take place at airports. The aerobatic champions are all taildraggers, and most of the aircraft that are used as aerobatic trainers are taildraggers. However, taildraggers require special certification, and are harder to handle than tricycle gear. The pilots at the Snowbird Classic expressed a desire for a tricycle aerobatic aircraft that would be easier to handle on the ground. Both options were chosen to go forward into Class I design.

4.4 Tail Configuration

The tail design is one of the most important aspects of the aerobatic aircraft design. The ability to precisely control the aircraft in all axes of motion is required to win aerobatic competitions. According to aerobatic pilot Ron Renz, for a pilot to have full control of the aircraft to successfully complete maneuvers, the controls for roll, yaw and pitch should be decoupled. This sentiment was echoed by the competitors at the Snowbird Classic Aerobatic Contest. This decoupling is key in performing one of the most basic aerobatic maneuvers: A snap roll. This maneuver is enacted by with full rudder deflection and then pulling back on the stick. This yaws the aircraft right or left and then loads the wing by pitching up. This effectively increases the sweep angle on one side of the wing, causing it to stall before the other side, and inducing a roll. The best pilots can perform this maneuver and stop exactly at intervals of 90° or 45°. Since this requires decoupled controls, this eliminates the possibility of a V-tail and any other out-of-plane positioning

of the tail surfaces. T-tails and H-tails are not considered viable because of a higher structural weight and a higher moment of inertia.

Both a conventional tail and a canard configuration were also considered. The canard configuration was discounted because a canard configuration is not capable of performing a clean snap roll, and aerobatic pilots are not used to flying aerobatic canard configured aircraft. This would limit the effectiveness of this aircraft since skills that are learned in conventionally configured aircraft would not be transferable to canard based aircraft. Across all categories of aerobatic competition, the aircraft that win competitions have conventional tails. Therefore, a conventional tail is selected for its precise controls, lower weight, and similarity to other aerobatic aircraft.

4.5 Engine Configuration

The two possibilities for engine placement are tractor and pusher. The tractor configuration is typically used because many aerobatic aircraft are taildraggers. Pushers are inherently more stable and will place the pilot closer to the CG position. In aerobatic flight, it is preferred that the pilot be away from the CG position so that he can feel how the aircraft is maneuvering. Almost all aerobatic planes place the pilot behind the CG; if the pilot is ahead of the CG, it will feel different from aircraft they are used to and possibly make aerobatics disorienting. A pusher suggests a canard configuration which has already been discussed as less than ideal. Another configuration placed under consideration was the idea of powering two propellers on the tips of the wings from one engine. To stay within the cost requirements of the LSA category, the twin propellers would be driven by belts. The main advantage to this design would be to allow the aircraft to have a maneuver metric greater than 1. This would allow the aircraft to hang on its propeller, a feat which only aircraft with large engines can currently perform. Using a smaller engine suited for the LSA market means that the additional thrust would be provided by large diameter propellers. Ultimately, this idea was down selected because it would prevent the aircraft from performing other maneuvers which make up a significant portion of the competition. The roll rate is reduced, and without P-factor, which is an advantage for one roll direction, this configuration could have difficulty with all rolls throughout the competition. Also, the twin propellers would greatly increase weight and complexity.

Of the possibilities, a tractor configuration has the most advantages in terms of maneuvering and satisfying the preferences of pilots. Using the configuration decisions made here, seven initial Class I designs were developed to consider in greater detail.

4.6 Class I Configurations

The following configurations will be considered for Class I design. These designs are the result of consultations with aerobatic pilots and a desire to keep the aircraft as simple as possible for reliability and maintainability. Note that these CAD figures are merely representative of overall configuration, and have not been through any preliminary or Class I sizing.

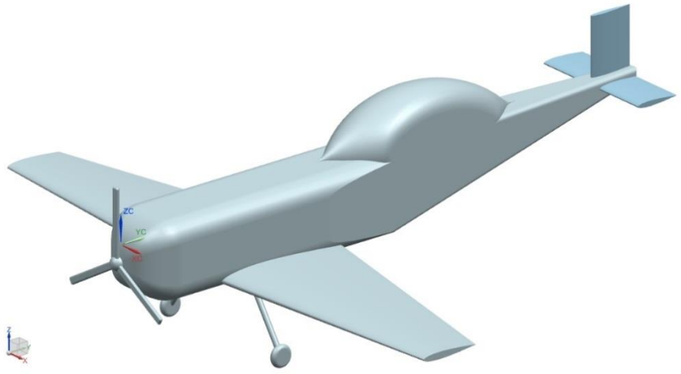

Low Wing Conventional Gear

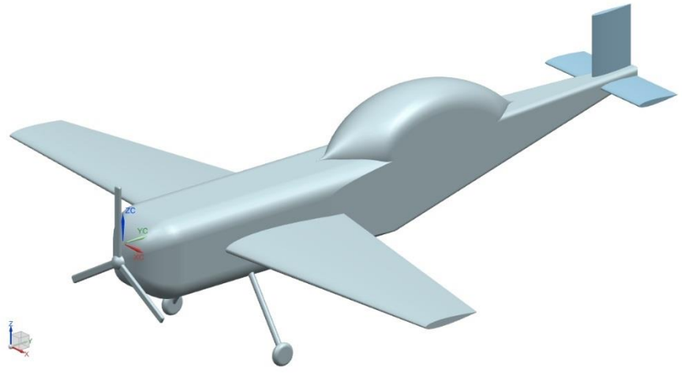

Mid Wing Conventional Gear

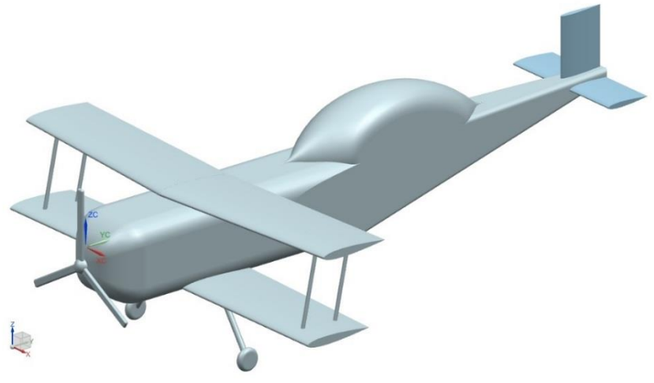

Biplane Conventional Gear

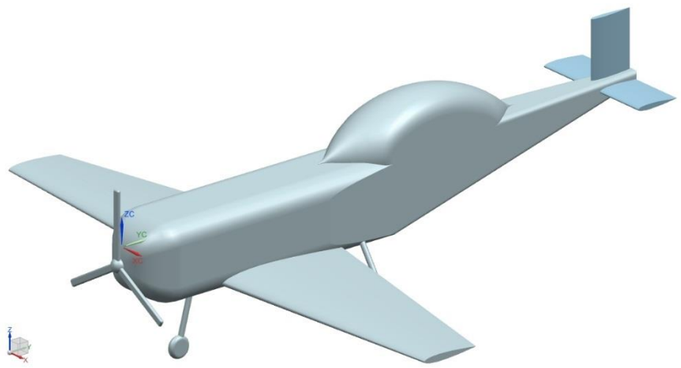

Low Wing Tricycle Gear

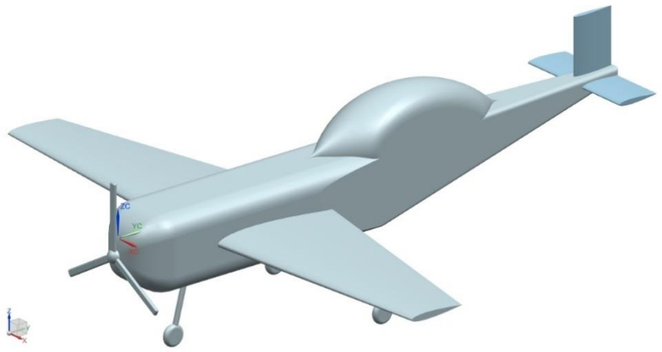

Mid Wing Tricycle Gear

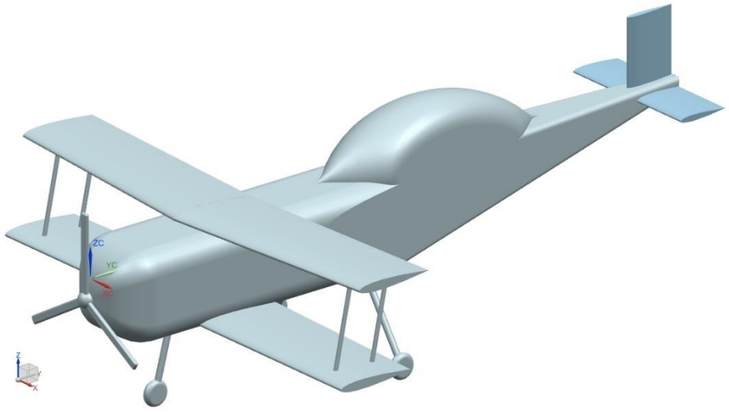

Biplane Tricycle Gear

To take aim at the 'innovative and original' aspect of the RFP, the RMIT team considered the implications of an unconventional ducted fan design. It was expected that the control surfaces located immediately aft of the fan could increase the maneuverability of the aircraft. It was also expected that visibility would be increased due to the lack of propeller in front of the cockpit. A Class I design analysis was performed on the aircraft to explore the possibility of a ducted fan design. It was discounted due to the restricted timeframe of the competition whereby issues surrounding weight and balance, control and stability, and the lack of literature and general uncertainty about ducted fan design did not have time to be solved.

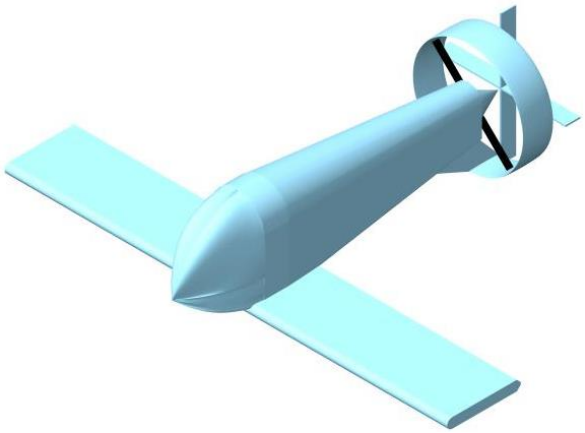

Figure 4.2: RMIT Ducted Fan Concept

5. Class I Design Procedure

The following section details the Class I design performed for each of the aircraft presented in Section 4.6. The configurations are all analyzed with a rough CAD model to determine the performance metrics of each. The final configuration is selected at the end.

5.1 Wing Layout

To achieve aerobatic performance in both the standard and inverted flight portions of the IAC competitions, a symmetric airfoil was chosen for Class I wings of the monoplane and biplane designs. This requirement was strongly recommended by local aerobatic pilot Ron Renz, who claims "Any aerobatic airplane having camber loses performance." This drove the team to select the NACA 0012 for the wings, a classic airfoil with large amounts of data available. Taper ratios for the monoplane and the biplane were chosen to follow other competition aircraft: $\lambda = 0.4$ for the mono-wing, and $\lambda = 0.9$ for the bi-plane. Similarly, zero quarter chord sweep was chosen due to the low speeds, low stall requirements, and similarity to other competition aircraft.

From the sizing chart shown in Figure 3.8, our aircraft needs to achieve an aircraft lift coefficient of about 1.7 to ensure that the aircraft can safely fly with a 45 kt (76 ft/s) stall speed and achieve an aerobatic performance of 6 g's of pull up. Since the NACA 0012 only achieves a section coefficient of lift of about 1.5 at the Reynold's number of this aircraft, the current location of wing loading is not suitable to satisfy all design constraints. Calculations were performed using the maximum section lift coefficients for the NACA 0012 to determine a wing loading value that would achieve the desired stall and aerobatic requirements. In initial calculations, the wing was determined to be over 200 square feet, leading to significantly lower wing loading than the market or similar aircraft currently have. This was determined to be a direct cause of finding a combination of two separate markets: Light Sport and Aerobatic Aircraft.

To compensate for this deficiency, vortex generators are implemented onto the wing section to boost the maximum lift of the section. Wheeler Wishbone Vortex Generators [7] are placed on the wing to create additional vortices to boost the lift of the wing section. However, the exact size and location of these vortex generators was determined to be an experimental value. One piece of the puzzle was found through Dr. Ron Barrett's thesis [8]. In the thesis, placing the vortex generators at the 10% chord throughout the wing energizes the boundary layer the most. This design parameter was selected for the vortex generators, but the exact size and pitch must be determined in flight testing to tailor the aircraft to a 45 kt (76 ft/s) stall speed.

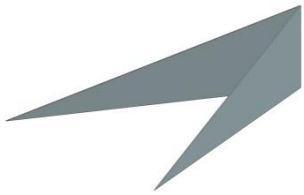

Figure 5.1: Example Vortex Generator

Other systems of inherent wing warping, automatic moving gurney flaps, and t-strips were also considered. To gain insight as to how feasible this would be to certify, the team talked to Marv Nuss, an FAA veteran of over 20 years, and now teaches short courses to industry professionals. He stated that to satisfy LSA clean stall speed requirements, sections of the wing cannot have moveable lift enhancing devices, regardless of whether or not the pilot has control over them. This led the team to select non-moving vortex generators to enhance the lifting ability of the aircraft.

This technology is assumed to increase the section lift coefficients of the wing to allow for a 45 kt (76 ft/s) stall speed. By using the following equations, an acceptable wing loading to satisfy stall and aerobatic requirements was found using the above technologies. It was found that the aerobatic condition restricted the design in the two seat aircraft. This lead to a wing loading of 6.7 lb/ft² for the monoplane and 6.5 lb/ft² for the bi-plane. The calculated wing loading values are shown in Table 5.1.

$$\frac{W_{ae}}{S} = \frac{\rho V^2 C_{L_{\max W}}}{2 * n}$$

Table 5.1: Calculated Wing Loadings

	Mono-Wing	Bi-Wing
$(W_{ae}/S)_{1\ seat}$	6.7 lb/ft²	6.5 lb/ft²
$(W_{to}/S)_{1\ seat}$	5.8 lb/ft²	5.6 lb/ft²
$(W_{ae}/S)_{2\ seat}$	8.3 lb/ft²	8.1 lb/ft²
$(W_{to}/S)_{2\ seat}$	7.2 lb/ft²	7.0 lb/ft²

$$\frac{W_{to}}{S} = \frac{1}{2}\rho V^2 C_{L_{\max W}}$$

Based on the values in Table 5.1, the wing loading of the aerobatic two seat controls. Because of this, those values were used to calculate a wing area. The wing areas for the two variants are shown in Table 5.2.

Table 5.2: Calculated Wing Areas

	Mono-Wing	Bi-Wing (total area)
S	149 ft²	154 ft²

It was determined that the stall speed requirement must be followed to properly size the wing. Utilizing the aspect ratio as described in initial sizing for the mono-wing as well as both wings of the bi-plane, the wingspan and chords of the root and tip can be calculated. Table 5.3 summarizes the characteristics of the wings of both types: mono-wing and bi-wing.

Table 5.3: Wing Characteristics

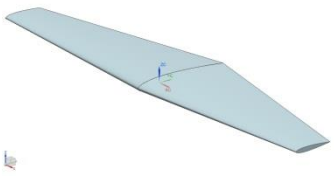

	Mono-Wing	Bi-Wing
S_W	149 ft²	154 ft² (77 ft² each)
AR	6	6 (each)
b	31 ft	22 ft
c_R	7.3 ft	3.9 ft
c_T	2.9 ft	3.5 ft
$Airfoil$	NACA 0012	

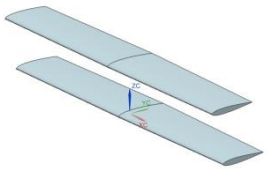

In regards to takeoff and landing requirements, the vortex generators will be engaged at all times during aerobatic flight. This allows the characteristics assumed during stall to apply to takeoff and landing. Additionally, the bottom set of vortex generators will be removed for cruise flight. This is to reduce drag and increase flight efficiency. Since the takeoff speed is specified at 20% above the stall speed and the landing speed is specified at 30% above the stall speed for this aircraft, no additional lift will be needed to safely takeoff and land the aircraft in either configuration. This translates to no flap sections needed for the wing.

5.2 Empennage Sizing

For analysis of the empennage, a NACA 0009 is used, as it is a common airfoil used in empennage construction. However, it was also observed that on some light sport aircraft, a flat plate with no aerodynamic shape is used in place of an airfoil. This is likely done to simplify the construction of the tail, and will be considered as a method of construction in the final configuration.

Figure 5.2: Flat Plate Horizontal and Vertical Stabilizer [9]

To determine a preliminary size for the horizontal and vertical tails, the method of tail volume coefficients was used. The tail volume coefficient is derived from other LSA based on their geometry. This method is outlined in Ref. 12. These sizes were determined to be preliminary, to be refined by a stability and control analysis. The values were used for a Class I Weight and Balance analysis to ensure the aircraft's static margin.

Table 5.4: Preliminary Class I Empennage Sizing

	Biplane		Monoplanes	
	Horizontal	Vertical	Horizontal	Vertical
Aspect Ratio	4	3	4	3
Sweep (deg)	0	30	0	30
Taper Ratio	0.9	0.5	0.5	0.5
Area (ft^2)	20	8	29	12.7

5.3 Undercarriage Integration

For the low wing, mid wing, and biplane Class I design configurations, both tricycle and taildragger landing gear options were considered. Based on the location of the CG calculated in the weight and balance analysis, the landing gear is configured to satisfy lateral tip-over criteria of 55° and longitudinal tip-over criteria of 15°. The lateral tip-over criteria applies to the most forward CG position for tricycle landing gear and most aft CG position for taildragger landing gear. The longitudinal tip-over applies to the most forward CG position for taildragger landing gear and the most aft CG position for tricycle landing gear. The landing gear is also sized to satisfy the minimum lateral ground clearance angle of 5°. In addition, the tricycle configurations are sized to satisfy a maximum 15° rotation on takeoff for longitudinal ground clearance. Of the constraints placed on the landing gear size, the propeller diameter is the main driver of the strut length for all designs considered. A ground clearance of 13" or 1/6 the diameter of the

propeller is used to prevent a ground strike. All Class I configurations were sized to meet these criterion, and examples are shown in Figure 5.3.

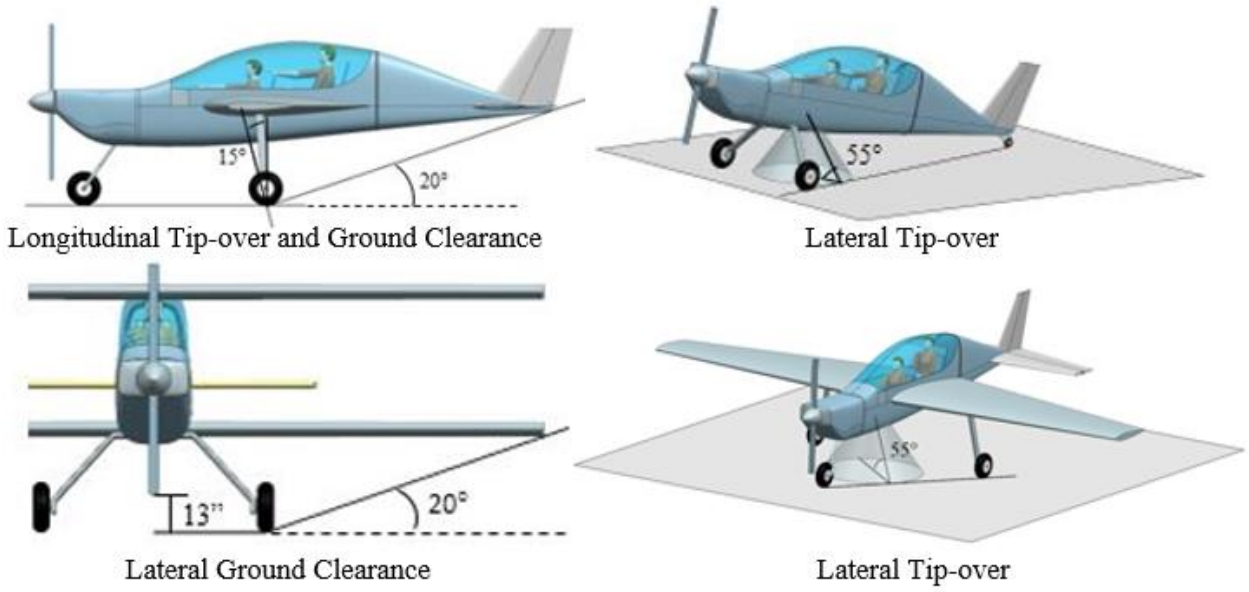

Figure 5.3: Class I Landing Gear Geometric Criteria

The landing gear strut loads were calculated using the distance from the CG position as the moment arm, and the estimated loads are given Table 5.5. Only one tire will need to be attached to each strut because the magnitude of the loads placed on the landing gear is small. Based on the calculated loadings and using data from Ref. 12, it is estimated that the taildragger landing gear will require a 15"x 6" main tire and a 9"x 3.5" tail wheel. The tricycle configurations are estimated to require a 12"x 5" tire for both the main and nose gear.

Table 5.5: Class I Landing Gear Strut Loads

	Taildragger		Tricycle	
Biplane	Main Wheel	505 lb	Main Wheel	390 lb
	Tail Wheel	230 lb	Nose Wheel	450 lb
Low Wing Monoplane	Main Wheel	520 lb	Main Wheel	375 lb
	Tail Wheel	200 lb	Nose Wheel	490 lb
Mid Wing Monoplane	Main Wheel	510 lb	Main Wheel	400 lb
	Tail Wheel	225 lb	Nose Wheel	445 lb

5.4 Weight and Balance

To determine the impact that different configurations would have on weight and balance, a sensitivity analysis was performed. The mid and low monoplanes were found to be identical in every respect except for the z-direction displacement of the wing. The mid wing kept the wing in line with the horizontal tail, giving a displacement between the two lifting surfaces of 0. This distance is 10 inches on the low wing. The overall effect on the static margin was determined to be about 0.5% for every 10 inches of wing displacement. Based on this, the low and mid wing configurations were determined to have the same static margin characteristics, and will be presented as such. Furthermore, it was found that moving from a taildragger to a tricycle configuration only changed the weight and balance of the aircraft by less than 5%. Therefore, the weight and balance for the tricycle and taildragger will be presented in the same section. To summarize, 2 configurations will be presented: The biplane (representing tail and tricycle gear), and the monoplane (representing low and mid wing, tail and tricycle gear).

For both classes of aircraft, the procedure to determine the weight and balance was taken from Ref. 12. In order to estimate the weight fractions, information from the Bede BD5 and the Cessna 150 was taken from Ref. 14. Known weight fractions such as engine, fuel, and payload were calculated, and components such as wing, fuselage, and landing gear were estimated using the 150 and BD5. The length to each component was measured in CAD or approximated based on techniques presented in Ref. 14. The following table displays the weights and locations of each component for the taildragger biplane and monoplane are shown below in Table 5.6. Note the coordinate system is set to 50 in. in front of the nose in X-axis, along the centerline in Y-axis, and 65 in. below centerline in Z-axis.

Table 5.6: Weight and X_{CG} Location for Aircraft Components

		Biplane		Monoplane	
		Weights (lbf)	X_{cg} (in)	Weights (lbf)	X_{cg} (in)
1	Wing	161	135	174	150
2	Horizontal Tail	17	280	17	280
3	Vertical Tail	8	288	8	288
4	Fuselage	155	115	143	115
5	Nacelle	9	67	9	67
6	Landing Gear - Main	42	87	42	87
7	Landing Gear - Tail	7	294	7	294
8	Engine	164	60	164	65
9	Fixed Equipment	72	147	94	147
10	Trapped Fuel & Oil	7	60	7	65
11	Fuel	115	135	115	152
12	Pilot 1	215	187	215	187
13	Pilot 2	215	147	215	147
14	Payload	30	202	30	202

The following charts show the weight and balance travel of the aircraft. It is assumed that empty weight is comprised of items 1-9 in Table 5.6. The operating empty weight included the trapped fuel and oil, as well as the first pilot. It should be noted that first pilot refers to the pilot in the most rearward seat, as the weight and balance characteristics are most favorable with a pilot in the rearward seat. The takeoff weight includes all items in Table 5.6, and the operating empty weight plus pilot and payload excludes only the fuel. The single pilot weight and balance is calculated the same way as the two pilot, minus the pilot in the front seat. The overall travel during flight (W_{to} and $W_{oe+pilot+payload}$) in terms of mean geometric chord is approximately 2% centered at 35% of mgc for the biplane, and 2% centered at 10% mgc on the monoplane.

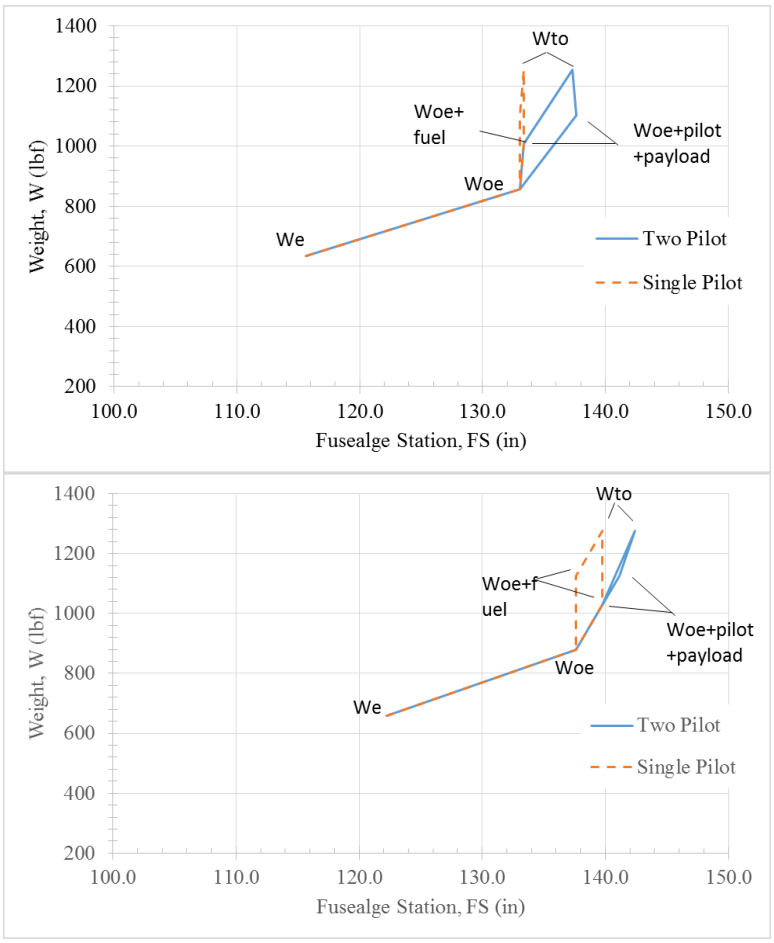

Figure 5.4: CG Excursion for Biplane (Top) and Monoplane (Bottom)

5.5 Longitudinal Stability

Based on the chosen design philosophy, two characteristics were desired for the aircraft: that it be inherently stable and that it be very controllable for novice pilots. To achieve these two, a static margin of 10% was chosen as the goal for each Class I design. This was to give the aircraft a very predictable and reliable nature, but still be maneuverable enough that aerobatic maneuvers could be performed.

Using the methods outlined in Section 11 of Ref. 12, the longitudinal stability was determined as a function of horizontal tail area.

The static margin plots for the biplane and the monoplane are shown in Figure 5.5. The most aft and most forward flight worthy CG locations were plotted alongside the aircraft's aerodynamic center. A vertical line showing the area sized by tail volume coefficient is shown for perspective.

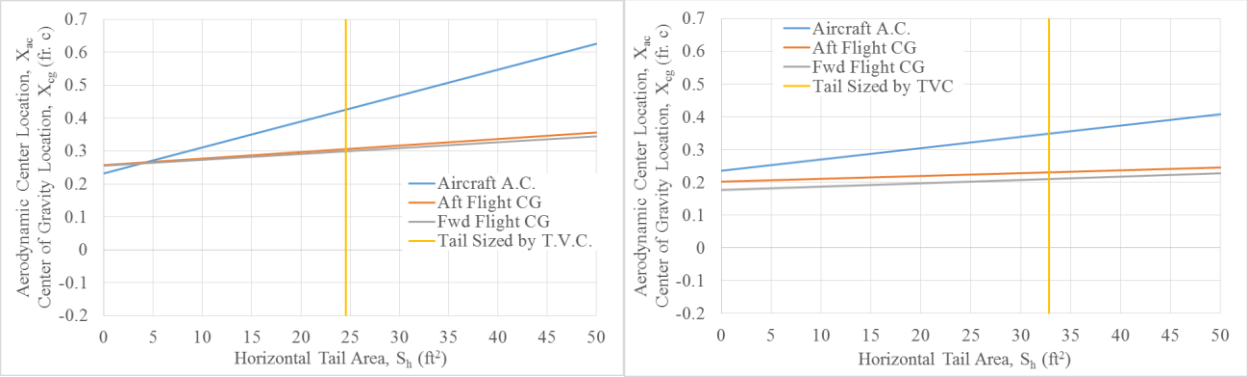

Figure 5.5: Static Margin Plots for the Biplane (Left) and Monoplane (Right)

The monoplane requires a larger horizontal tail because the wing is further back, requiring a larger surface area to account for a reduced moment arm. The equations used to generate the plots were used to determine the horizontal tail area that gave a static margin of 10%. For the biplane, the area was 21 ft^2, and for the monoplane, the area was 31 ft^2. The vertical and horizontal tail areas for both aircraft fall within 10% of the area predicted by the tail volume coefficient; therefore the horizontal tails were resized to achieve the 10% static margin.

5.6 Lateral Stability

For the lateral stability, a stable aircraft is defined as having a $C_{n\beta} = 0.0010$ per deg [12]. Using the method outlined in Ref. 12, the vertical tail area was plotted with respect to $C_{n\beta}$. The vertical tail size was determined based on the intersection between the $C_{n\beta}$ as a function of S_v and $C_{n\beta} = 0.0010$ per deg. The vertical tail area for the biplane

was 11 ft^2 and the monoplane was 14 ft^2. Because each value was within 10% of the area predicted by the tail volume coefficient, the vertical tails were resized to these values for the desired lateral stability.

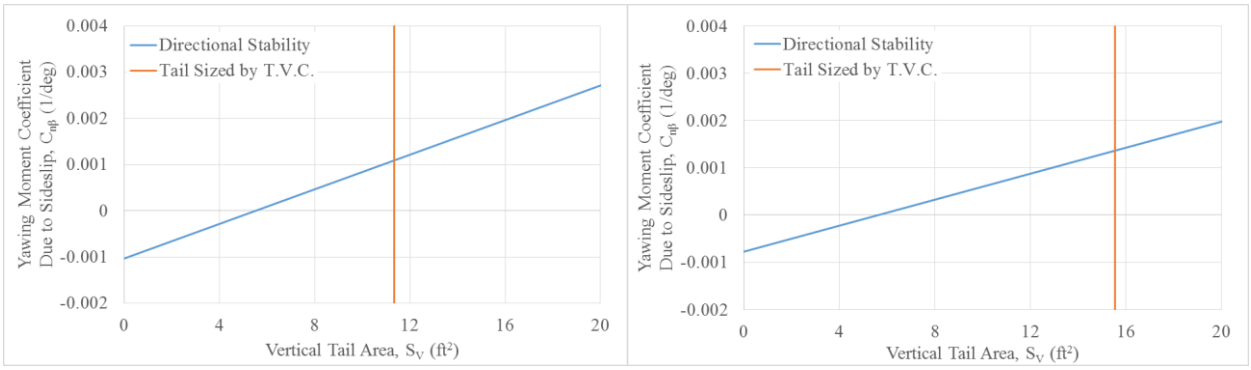

Figure 5.6: Lateral Stability Plots for the Biplane (Left) and Monoplane (Right)

The table below summarizes the final values chosen for the vertical and horizontal area.

Table 5.7: Summary of Empennage Areas for Class I S&C

	Biplane	Monoplane
Horizontal Tail Area (ft^2)	21	31
Vertical Tail Area (ft^2)	11	14

5.7 Drag Polars

To further determine flight characteristics of the preliminary aircraft designs for down selection, Class I drag polars were created for each of the preliminary designs. Since the mid and low mono-wing designs are assumed to have the same drag properties, they were evaluated equally during preliminary drag polar build up. It was found during the development of the drag polars that the drag difference between the monoplane and biplane was <5%. It was then determined to only show one drag polar to represent both wing configurations. Drag build up was performed by first finding a standard wetted area for the biplane and monoplane designs. This wetted area was found utilizing a CAD program, Siemens NX. Utilizing the wetted areas, a corresponding parasite area was found for each aircraft from Dr. Jan Roskam's Aircraft Design Series, Part I, page 120, Figure 3.21c [11]. By taking the ratio of this parasite drag and the wing area of each design, an assumed zero lift drag coefficient was determined. In addition to the standard zero lift drag coefficient, the advanced technology being employed on this design increased the zero lift drag coefficient. From Dr. Ron Barrett's thesis on vortex generators [8], the set increases the zero lift drag coefficient by about .005, and is dependent on the size that will be determined during flight testing. For the current set up, 2 sets of vortex generators are being employed. Since these increases in drag are significantly detrimental, specifically for a cruise

flight, the designers began looking at the possibility of creating a cruise configuration and still retaining requirements. The solution that was determined was to specify no inverted flight during cruise, and remove the set of vortex generators from the bottom of the wing. A skin friction coefficient of .010 was assumed for this aircraft, since it is similar in creation to a Cessna 172. The Oswald efficiency factor was determined to be 0.85 for both the aerobatic configuration and the cruise configuration. The characteristics that are described in the previous paragraphs are summarized in the following tables and graphs that show the drag polars for the preliminary designs, in addition to the equation used to plot the drag polars.

Table 5.8: Drag Polar Characteristics

$C_D = C_{D_0} + \frac{(C_L)^2}{\pi Ae}$	Configuration	Wetted Area (ft²)	Parasite Area (ft²)	C_{D0}
	Aerobatic	572	6	.060
	Cruise			.065

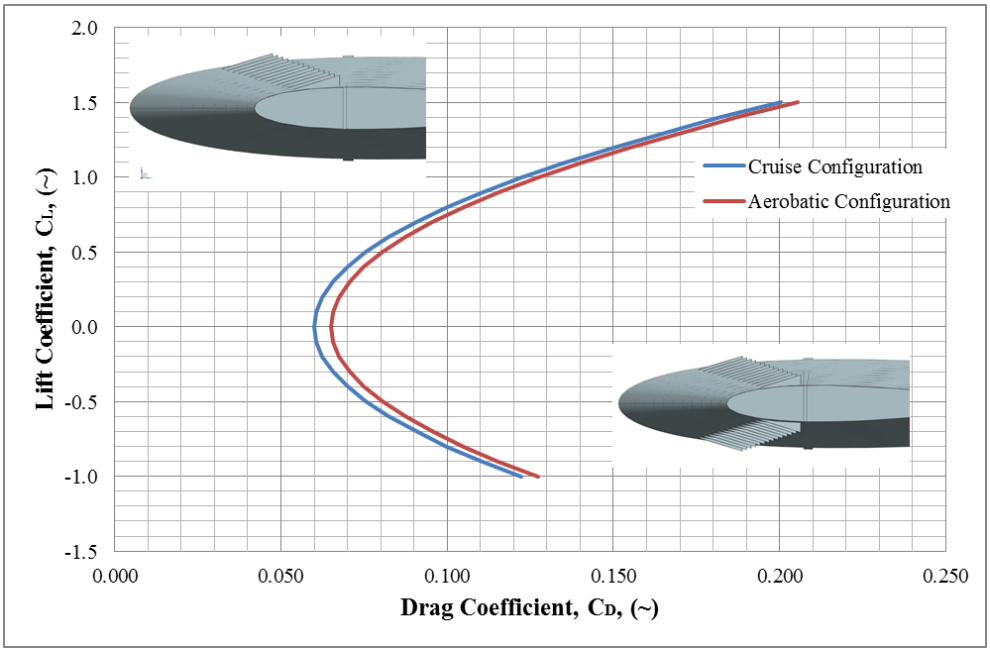

Figure 5.7: Class I Drag Polars

From this preliminary drag polar, it can be see that the cruise configuration has slightly less drag than the aerobatic configuration. This ratifies the goals laid out to reduce cruise drag.

The last set of information that can be determined from the drag polar information are maximum lift to drag values; they are summarized in Table 5.9, along with the equation used to determine those values. It is assumed lift to drag ratio is maximized when parasite drag is equal to induced drag. The equation used to determine the maximum lift to drag ratio that is found from this relation is shown on the following page. The weights of the different flight

situations are shown, since the maximum lift to drag ratio is dependent on it as well. In addition, the takeoff, cruise, and landing speeds are shown since they are also utilized in this calculation. The takeoff speed is assumed to be 20% above stall speed while the landing speed is assumed to be 30% above the stall speed. The cruise speed is assumed to be 120 kts, or 202.5 ft/s. The next component that is necessary for this calculation is the air density. For the takeoff and landing configurations, the air density is assumed to be sea level. The aerobatic air density is assumed to be for 5000 ft. It should also be noted that the cruise C_{D0} is used for takeoff and landing, while the aerobatic C_{D0} is used for the aerobatic calculations.

$$\left(\frac{L}{D}\right)_{max} = \frac{W}{C_{D0} * \rho * V^2 * S}$$

Table 5.9: Maximum Lift to Drag Ratios

Mode	Weight (lb)	ρ_{air} (slugs/ft^3)	V (ft/s)	$(L/D)_{max}$
Single, TO	1000	0.002377	91.1	5.64
Single, AE	930	0.002048	202.5	4.84
Single, L	650	0.002377	98.7	3.12
Double, TO	1280	0.002377	91.1	7.22
Double, AE	1080	0.002048	202.5	5.62
Double, L	805	0.002377	98.7	3.87

6. Class I Propulsion System Layout and Integration

A wide range of energy sources were considered for their suitability by 2020 and beyond. A summary of the fuel type and their associated properties is provided in the following sections.

A range of aviation engines were surveyed and considered for the aircraft application. Two engines were selected for further analysis. The engine selected for use is the Rotax 915 iS.

6.1 Potential Fuel Sources

A variety of fuel sources were investigated for this aircraft. This includes 100LL, Mogas, Avgas, Jet A-1, Bio-fuels, and Electric.

6.1.1 100LL

100 LL is the most commonly used form of aviation gasoline (avgas) for internal combustion engines. High specific energy (18,702 BTU/lb [28]) and consistent power output combined with wide use and availability makes it suitable for use in high performance aircraft engines, such as those used by an LSA. The downside is that it contains .0004 lbs. per gallon of lead and tetraethyl-lead (TEL), a toxic additive that is used to prevent knocking.

Currently the (FAA) is seeking an unleaded alternative suitable for aviation use. As of 2016, the FAA is currently in phase 1 of testing and are sampling four formulations. The outcome of these tests is expected in December 2018 whereby the roadmap to phase out leaded fuels will be updated with a potential phase out date. It should be noted that any Continental and Lycoming engines based around 80/87 avgas can used 100LL; however, they will suffer from lead build-up, which can lead to lead fouling of the spark plugs.

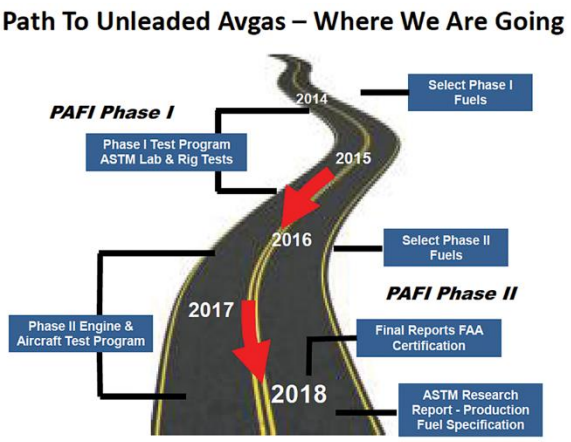

Figure 6.1: FAA Leaded Fuels Replacement Schedule [10]

This fuel is suitable for use and will remain unchanged by 2020 with an uncertain future.

6.1.2 Motoring gasoline (Mogas)

87 octane general automotive gasoline based fuel is unleaded, has no ethanol additives and is the most commonly used fuel type worldwide for automobiles. Manufacture of this fuel type is governed by ASTM D4814 for use in automobiles and has been accepted by the FAA as an acceptable standard for use in general aviation internal combustion engines.

Mogas in general aviation is generally used by aircraft with engines that run on 80/87 avgas and have been modified specifically for mogas operation. Some engine manufacturers such as Rotax and Lycoming have engines designed specifically around it, mainly for the LSA category.

Mogas has a higher specific energy than 100LL (20,202 BTU/lb [28]) and is cheaper than 100LL in most parts of the US ($4.67/gal for 100LL, $3.72/gal for 87 octane mogas [29]). Fuel systems need to be designed to prevent the higher vapor pressure of 87 octane mogas from causing vapor lock and preventing damage to pumps and valves.

This fuel is suitable for use and will remain largely unchanged in 2020, prices will rise but it is expected that mogas will remain cheaper than 100LL avgas.

6.1.3 Jet A-1

Jet A-1 is kerosene based fuel designed for use in turbine engines. It ignites at much higher temperatures and is much more stable at lower temperatures than gasoline-based fuel, making it unsuitable for use in spark ignited internal combustion engines. Jet A-1 has a specific energy similar to that of 100LL (18,400 BTU/lbs [28]). Jet-A1 is considered more environmentally friendly when compared to Avgas or Mogas due to the lower levels of particulate in the exhaust. The potential for a single use fuel in aviation is high and it is expected that this fuel will be Jet A-1

Jet A-1 fuel is suitable for use by 2020 in the LSA market.

6.1.4 Bio Fuels

Bio Fuels are forms of diesel-based fuel produced from biological sources. Due to the similarity with kerosene based fuels, biofuel are mainly developed for use with turbine engines. The properties that it shares with kerosene jet fuel makes it unsuitable for use in spark ignited internal combustion engines.

This fuel is not suitable for use, however should the design move to an aviation diesel engine biofuel would be suitable and further development would only increase its effectiveness by 2020.

6.1.5 Electric

The two most common sources of electrical power that have been considered for aviation are solar power and battery power. In the case of an LSA, solar power is incapable of generating the desired current levels to drive the motor at its maximum power output, leaving battery power as the only viable source.

However, even battery power is not a worthwhile power source for an LSA compared to gasoline and diesel based systems as it lacks the level of energy density of gasoline and diesel fuels (20,180 BTU/lb [28]) for generic gasoline, (730.87 BTU/lb) for LiO_2 solutions [30]) and requires additional cooling systems to keep the operating temperatures within a very narrow range (50-140 ^{0}F) to maintain peak power output.

As can be seen in the graph below, the history and future trend of a 5% increase in LiO_2 energy density year-to-year shows that batteries will not even come close to providing the energy levels that gasoline and diesel fuels can provide per unit of weight that the batteries will add to the aircraft.

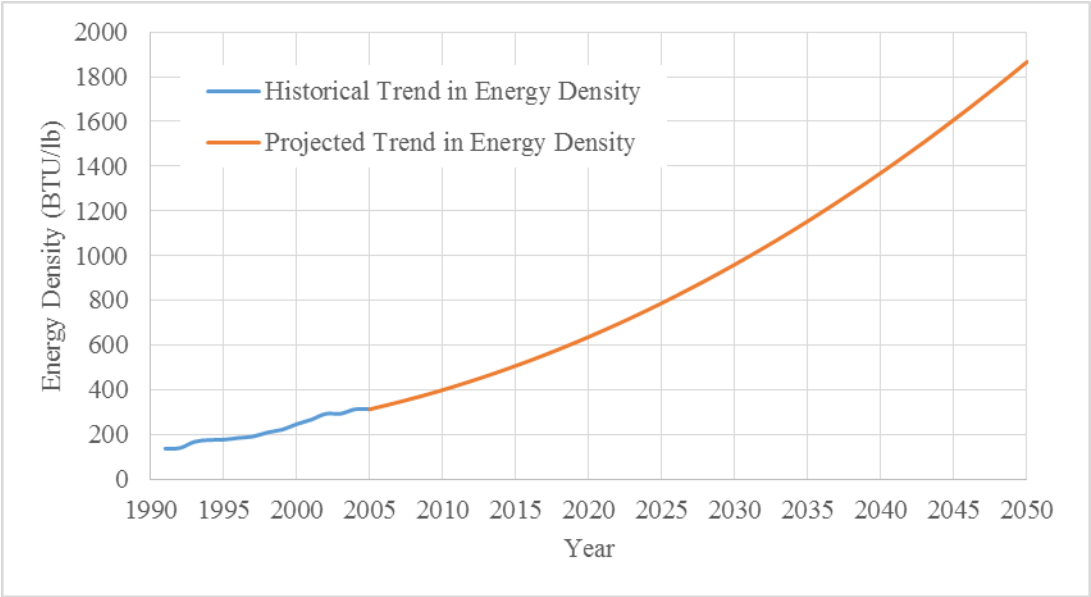

Figure 6.2: LiO_2 Energy Density History and Future Trend to 2050 [30]

Even through to 2050 LiO_2 will not see a significant increase in energy density compared to fuels. It is possible that other solutions such as Al_2O_3 (Aluminium Oxide or Aluminium-Air) will provide a significant boost in energy density for battery systems - potentially up to six times that of LiO_2. However, alternative battery technologies are unlikely to be fully developed and tested in an operating environment like one that would be experienced by GA aircraft or an LSA by the EIS date.

LiO_2 and Al_2O_3 are very volatile substances that are quite sensitive to changes in temperature and pressure, and as such are particularly unsafe for use in aircraft unless special measures are taken to ensure pressure fluctuations are kept to a minimum [30]. Until these issues are rectified and/or acceptable engineering measures are put in place to mitigate the safety issues associated with these types of batteries, they are unlikely to be certified for use by any aviation authorities across the US, Australia, and the European Union between now and 2020.

6.2 Powerplant Selection

A market analysis was performed on a range of aircraft engines. From the engines surveyed, 70 met the minimum 115 hp power output criteria determined in Section 3. The five-minute requirement of inverted flight

necessitated further consideration and it was determined that the engine must have a direct-injection fuel delivery system to maintain fuel flow, and be equipped with an oil system that utilizes a dry sump to maintain adequate lubrication. This limited the number of possible powerplant candidates to 54.

Another key criteria in engine selection is the weight of the powerplant itself. Stability and performance requirements place restrictions on the weight of the powerplant due to required center of gravity location and maximum take-off weight restrictions. If the engine is too heavy the center of gravity will be too far forward, which will orchestrate the need for changes in fuel positioning, passenger seating and potentially wing positioning to ensure adequate handling qualities. To meet requirements, a weight limit of 185 lbs was set to ensure that the aircraft will exhibit required stability and performance characteristics. Implementing these requirements on the available powerplants, it was determined that only 10 were still viable for use.

Power-to-weight ratio is another important powerplant characteristic. An engine with a high power-to-weight ratio generally corresponds to a low fuel consumption, which is an essential requirement for the future market due to rising fuel costs. On comparison of power to weight it was found that only 6 engines had comparably acceptable performance.

To reduce the complications associated with designing, manufacturing and operation of a new aircraft, an established manufacturer will be selected. The selected manufacturer is required to have credible reputation and a steady financial revenue to guarantee continued adoption, product support, maintainability and acquisition over the life of the aircraft.

Figure 6.3: Rotax 915iS Engine [31]

From these selection criteria, the Rotax 915 iS was selected. Although limited information is available at this stage, it is the successor to the Rotax 914 UL, which exhibites superior qualities when compared to the other applicable engines from the database. The 915 iS has been designed to be superior to the 914 UL in almost every way. It has 15% more power, weighs 11% less, and is expected to be significantly more fuel efficient than its predecessor. With the Rotax 915 iS being a newer engine, it would allow for the aircraft to perform better later in its lifetime, compared to an engine that would be outdated by the time the aircraft enters service. This should increase the aircrafts' useful life and reduced the need for future powerplant upgrades.

Using a newer engine also allows for new replacement parts to be purchased direct from the manufacturer without worrying about stock shortages. The aircraft will be inherently more reliable, cheaper to maintain and have the ability to perform consistently. Exploiting the newer engines performance qualities allows for the aircraft to be a viable contender in the future LSA market.

It should be noted that the engine bay will be designed to allow for changes to powerplant selection as the design matures, and new emerging technology becomes available due to the aforementioned leaded fuel replacement

6.3 Leaded Fuel Replacement: Consideration

When considering the leaded fuel replacement requirements, the 135 hp Rotax 915 iS (Mogas/Avgas) and 120 hp Wilksch Airmotive WAM-120 Diesel (Jet A) were selected for direct comparison, as they exceed the 115 hp requirement, are both able to be operated inverted, and have an expected entry into service (EIS) date preceding 2020. Initially considering market reputation, Wilksch Airmotive is relatively unknown, with few operational examples and do not offer a global support network. This is in stark comparison to Rotax who operate a vast global support network and have accrued over 45 million flight hours on a worldwide fleet of 4-stroke engines [32].

When considering weight, the 915 iS weighs 100 lb less than the WAM-120 with an increase of 15 hp over the WAM-120, corresponding to a much higher power to weight ratio.

The possibility of utilizing multiple fuels such as 100LL avgas or 87/95 octane mogas aids in the longevity of the 915 iS. 100LL avgas is currently the most common fuel available at general aviation airports, with mogas generally available in society due to the proliferation of the automotive petrol station. Although the current market primarily caters for petrol engines, future developments could lead to wide spread adoption of biodiesel fuels which, with minor modifications, can be used as a diesel fuel replacement.

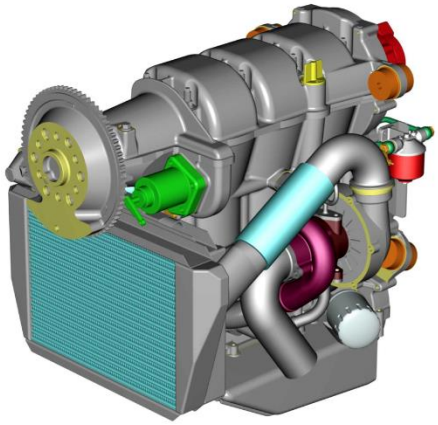

Figure 6.4: WAM - 120 Diesel [25]

Although the WAM-120 may operate using a cheaper fuel source, the historical acquisition costs of diesel engines place the WAM-120 outside the acceptable cost range for LSA operation. Rotax indicates to have the 915 iS both FAR 33 and ASTM F2339-6 certified by 2017 increases the marketability of the aircraft over the WAM-120 which does not have current plans to certify.

For this application, the selected powerplant is still the Rotax 915 iS as exhibits greater performance, weighs less and has a wider support network when compared to the Wilksch Airmotive WAM-120. Future developments in diesel engine technology may lead to wide spread adoption if powerplant weight is reduced and the power is increased. However, at this time it is unlikely to see these improvements made in the near future, as the market primarily caters for petrol engines.

For this aircraft, the 915 iS is to be mounted to the aircraft from the rear of the engine using a steel tube truss connected to the firewall. The engine and mounting truss is to be enclosed by cowling that is molded to the aerodynamic shape of the fuselage, with consideration of the cooling requirements of the engine.

6.4 Propeller Selection

Previous analysis of required engine horsepower determined that a propeller diameter of 6.5 ft was optimal. However, since a new engine variant will be used, propeller selection is difficult because the propeller-engine assembly requires a vibration analysis to be conducted to ensure compatibility. The mounting method of the hub also needs to be taken into consideration because some manufacturers build engine-specific propellers. For the sake of interchangeability, a reputable propeller manufacturer will be selected to ensure that a variety of options are available. These manufacturers are also established business' which have refined propeller design processes, advanced testing facilities and continuous component output.

Figure 6.5: Projected Propeller Design

Therefore, Sensenich was selected due to the availability of product data and compatibility with Rotax engines. Taking into account the previous considerations the Sensenich 2-Blade Rotax-variant and the 3-blade Rotax-variant will be available for selection depending on pilot preference and required performance. The 2-blade variant comes in a diameter range from 66 in (5.5ft) to 75in (6.25ft), while the 3-blade variant is available with 68in (5.66ft) diameter. Both of the selected propellers are composite to reduce weight and centrifugal forces. Due to regulatory restrictions both propellers are limited to ground adjustments only. However, since neither of these propellers reach the selected design diameter, an engineering process will be engaged in a joint venture with the company to develop a 6.5 ft propeller that is designed for the Rotax 915 engine. This propeller will not be exclusive to this aircraft, but will give this aircraft its design advantage that is sought with this large propeller.

7. Down Selection from Class I Design Configurations

During the Class I design process, it was found that the most efficient configuration that is competitive in both considered markets has the following characteristics:

- Mid-Monowing
- Tail Dragger
- Tandem Seating
- Conventional Empennage

This set of configuration guidelines allows for lower drag profile, clearer lines in competition, clear control in each of the three axes, smaller fuselage profile, and better stability and control when compared to the other configurations considered.

8. Class II Cockpit and Fuselage Layout

The following section details Class II Cockpit and Fuselage Layouts for the final design concept. After a final arrangement for the fuselage was determined using the weight and balance calculated from Class I, the fuselage was able to be precisely laid out.

8.1 Fuselage Layout

For preliminary design of the fuselage, two pilots were placed in free space oriented in a tandem arrangement. The pilots were placed on the same level to keep the weight distribution of the aircraft as close to the centerline as possible. Placeholder boxes were placed for the engine and payload. An effort was made to make the fuselage look smooth and sleek, providing increased ramp appeal and fulfilling the desire of the RFP for aesthetic appeal.

To better increase the visibility out of the cockpit, transparent panels were placed on the underside of the fuselage near the pilot's feet. This allows pilots flying competition to be able to look down to the ground for reference. It also allows for the pilots to see more clearly the boundaries of the box they fly their routines in. This design feature was found on other top competitive aircraft and was suggested by the pilots interviewed at the Snowbird Classic Aerobatic Competition.

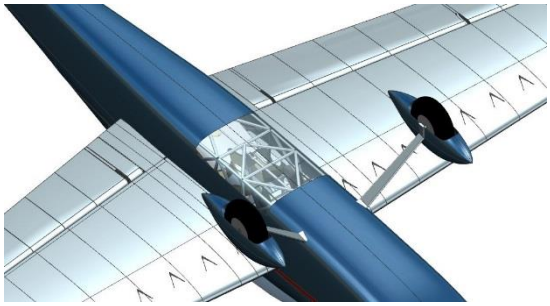

Figure 8.1: Transparent Fuselage Underside

8.2 Cockpit Layout

The cockpit width for the two seat is 29 in, 110 in. in length, and a height of 45 in. This is enough to accommodate a pair of 17x27x30 in seats in a tandem configuration with a seat back angle of 13 degrees, behind the rear seat is 6.5 ft^3 storage space for baggage. The high seat back angle is to alleviate the physical effects of g-forces on the pilot and passenger during aerobatic maneuvers. To the left of each seat is the throttle controller mounting that sits directly adjacent to the pilot and passenger seats.

8.3 Cockpit Instrumentation - Single Seat Variant and Dual Variant Rear Seat

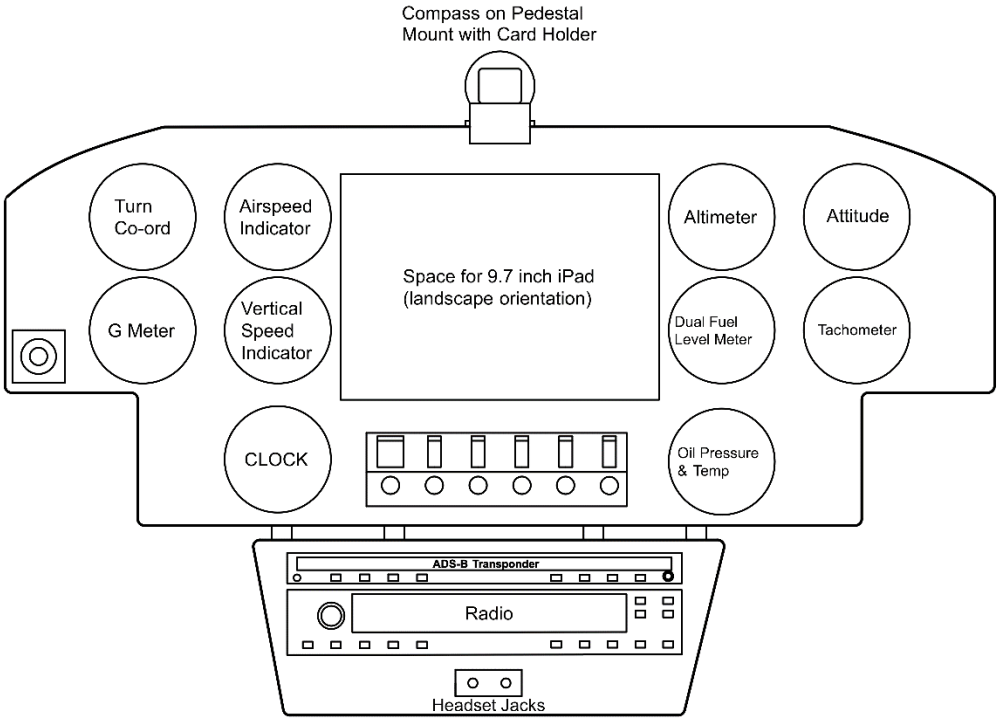

Figure 8.2: Command Seat Schematic

The cockpit dashboard is laid out in four sections: left, center, right, and the communications board. The left and right sides each contain between three and five gauges. The minimum requirement is to have an airspeed indicator (ASI), altimeter, attitude indicator/artificial horizon, vertical speed indicator (VSI), fuel level meter, and oil temperature and pressure gauge. Additionally, a turn coordinator gauge, g-force meter, tachometer, and digital clock can also be added. All of the gauges that satisfy the minimum requirement must comply with the FAR23 requirement for mechanical gauges in general aviation aircraft if sold for GA use.

The center section contains a magnetic compass and space for mountings for a 9.7 in. or smaller tablet. This space is also intend to be at the aerobatic pilots' discretion in terms of placing paper copies of routines for easy viewing during flight. Below the tablet space is the engine starter switch, lighting switch, avionics and electrical system circuit breakers, and the fuel pump on/off switches. The communications board beneath the center section contains a radio slot, ADS-B transponder slot, and intercom plugs.

8.4 Cockpit Instrumentation – Dual Variant Front (Subordinate) Seat

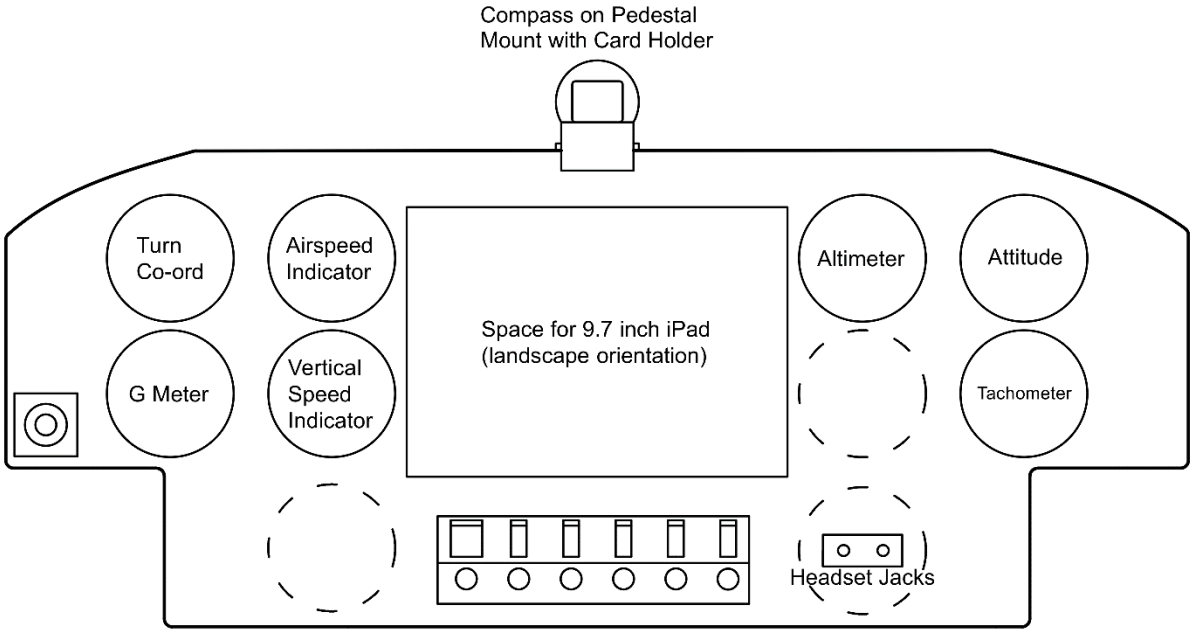

Figure 8.3: Subordinate Seat Schematic

For commonality, the front seat on the two-seat variant is of the same design with omissions to reduce the visual stimulation of the student/passenger and to reduce costs. The student/passenger does not require operational knowledge of the current fuel status, airframe hours, or engine temperature and pressure all of which can be monitored by the more experienced rear pilot. The engine tachometer is retained for the subordinate, as it is crucial for the student to learn to manage propeller speed to prevent over-speed issues. The radio stack is removed to remove clutter and duplication. The headset jacks are relocated and replace the oil temperature and pressure gauge. If the customer has a requirement for a full-sized panel in the subordinate seat, they are able to request a full-sized panel at an additional cost.

8.5 Flight Control Layout

The cockpit flight controls consist of a center stick with a left side throttle controller and rudder pedals with toe brake capability for each seating position providing the most ergonomic control layout possible for high-g aerobatic maneuvers. All three controls operate their associated control schemes mechanically and as such do not require additional feedback mechanisms within the control loop. The flight controls are laid out in their entirety in Section 12.1.

9. Class II Design Procedure

9.1 Wing Design

The following components were investigated further once a low mono-wing configuration was selected as the Class II advanced design.

The vortex generators are based on vortex generator theory developed by Dr. Ron Barrett [8]. They are designed to create counter rotating vortices by allowing flow to "tumble" over the raised edges. These counter rotating vortices allow the boundary layer to be energized and allow for the airflow to be attached at higher angles of attack than a standard NACA 0012 airfoil. As stated above, the vortex generators are designed to be placed at 10% of the wing chord from fuselage to tip. Although the vortex generators will be sized during flight testing, it is determined that each vortex generator is kept at the same size from root to tip. Since the chord length decreases from root to tip, the constant vortex generator size will allow the vortex generator size in terms of percent chord to increase to the tip. As vortex generator percent chord increases, maximum lift coefficient and stall angle also increase. Because the vortex generators have a larger percent chord value at the tip, the outboard sections of the wing will stall at higher angles of attack than the inboard section. This causes the stall cells to grow from root to tip, and allow the pilot to maintain roll control at high angles of attack and low speed. Overall, this gives the wing the inherent effect of maintaining aileron control during high angle of attack stall, an important characteristic for an aerobatic aircraft. An example set of vortex generators are shown in Figure 9.1.

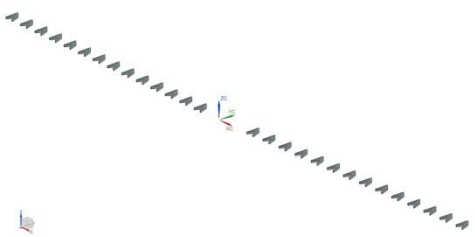

Figure 9.1: Vortex Generators, One Set

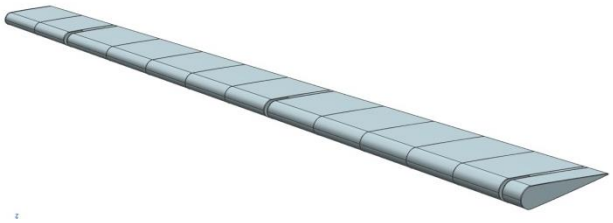

Figure 9.3: Aileron

The aileron by itself is shown in Figure 9.3. The aileron layout for this wing section will be a single aileron per wing that span 82% of the half-span of the wing, and will encompass the rear 33% of the wing chord. The aileron begins 10 inches from the fuselage and terminates 10 inches from the tip of the wing. The aileron is designed to have a rounded nose and is hinged around the 33% aileron chord. This implies that the ratio between the distances from the leading edge of the aileron to the hinge line divided by the distance from the hinge to the trailing edge is 0.5. From Dr. Jan Roskam's Airplane Design Series, Part VI, page 471, Figure 10.65a [15], the balance on a control surface is maximized at the design point described above. This is due to the fact that the weight and aerodynamic forces on the aileron are nearly always balanced, meaning that the unbalancing force is provided only by the pilot. This is to allow for easier control inputs throughout the flight envelop. To provide adequate control authority, the maximum aileron deflection is defined as ±25°. An exploded view of the wing and how the aileron will be integrated is shown in Figure 9.3. The aileron will be integrated using unthreaded bolts connected through three brackets connected directly to the rear spar. This aileron connection scheme was recommended by U.S. Unlimited Aerobatic team member Mark Norwosielski, because it decreases the complexity of connecting the ailerons and increases the life due to no threaded sections rubbing against each other. Two ribs are added on either side of the pin location to increase structural adequacy.

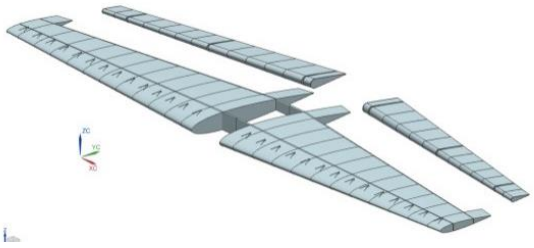

Figure 9.2: Aileron Exploded View

The initial structural configuration is designed as follows: The main spar will be located at the 25% chord location. The main spar is designed to carry the majority of the load of the wing. For main spar sizing, the bending moments associated with a 6g pull up under fully loaded two seat take-off weight conditions are considered. To allow the aircraft to be trailered, the wing is designed to split at the center line of the fuselage. The main and rear spar will both be straight when they are inside the fuselage, allowing for easy placement into the fuselage plugging system. This results in a bolted attachment system being required within the fuselage to lock the wing into place. It should be noted that the main spar travels between the seats of the pilot and passenger while the rear spar stops where it meets the fuselage. Further development of the wing structure is shown in Section 13.3.

9.2 Undercarriage Integration

For the final aircraft configuration, a taildragger landing gear is selected. This is chosen over a tricycle landing gear because it is lighter weight, has lower drag, and is the standard configuration for most aerobatic aircraft. As can be seen in Figure 5.3, the main struts of the tricycle landing gear are forced out to the wings to satisfy the lateral tip-over criteria and therefore require longer, heavier struts increasing both weight and drag. This also increases the weight of the wing because it requires additional structure to support the landing gear. Although there is a possibility of ground loop with a taildragger configuration, it is considered more important to have commonality with other aerobatic aircraft. Since all unlimited class and most other aerobatic aircraft are taildraggers, this will allow for an easy transition from this intermediate level aerobatic aircraft to a higher class of aircraft. Pilots who train for aerobatics will certainly train in a taildragger like a Pitts or a Decathlon, so they will be required to become certified for taildragger aircraft. The final landing gear configuration is sized to fit all tip-over and ground clearance criteria as shown below.

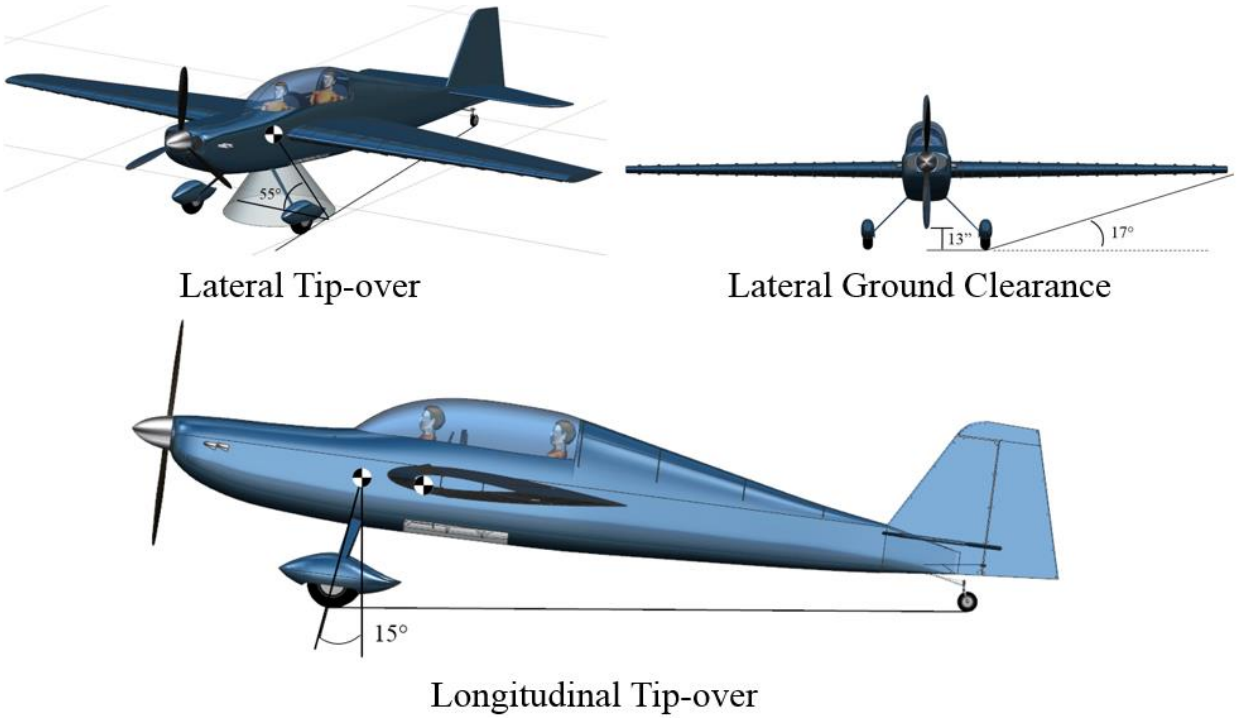

Figure 9.4: Class II Landing Gear Geometric Criteria

The main landing gear strut is of a cantilever spring leaf design. This design provides the necessary shock absorption and is less expensive to manufacture. The design loads are given in Table 9.1, and the main strut is sized

to support the bending moment imparted by the loads at the centerline. A free body diagram displayed in Figure 9.5 is used for the preliminary sizing of the strut and a width of 3.2" resulting in a moment of inertia of 0.111 in^4 is calculated using the yield stress of 41 ksi for 2024 aluminum sheet. The strut will be manufactured from standard ¾" thick aluminum sheet stock and bent to the correct shape using a press brake. Since the bending moment lowers outboard of the centerline, the strut is tapered out to the tire to reduce weight.

The main tire is selected from a selection of B.F. Goodrich tires given in Ref. 14 using the calculated loads. A tire size of 6.00-6 satisfies the loading requirements and also has an inflation pressure of 42 psi, which will allow the aircraft to operate from grass landing strips and other rough terrain.

Table 9.1: Class II Landing Gear Characteristics

Main Landing Gear Strut Characteristics				
Distance from c.g.	l_m	32"	Landing Speed	58.5 kts.
	l_t	182"	Landing Kinetic	1145 ft-lb.
Strut Load	P_m	527 lb.	Energy	
	P_t	185 lb.	Strut Size	3/4" x 3.2"
Main Tire Characteristics				
	W	6.00"	Ply Rating	6
	D	6"	Weight	8 lb.
	$D_{0\ max}$	17.5"	Inflation Pressure	42 psi
Tail Wheel Characteristics				
	W	5.00"	Ply Rating	4
	D	4"	Weight	4 lb.
	$D_{0\ max}$	13.25"	Inflation Pressure	35 psi

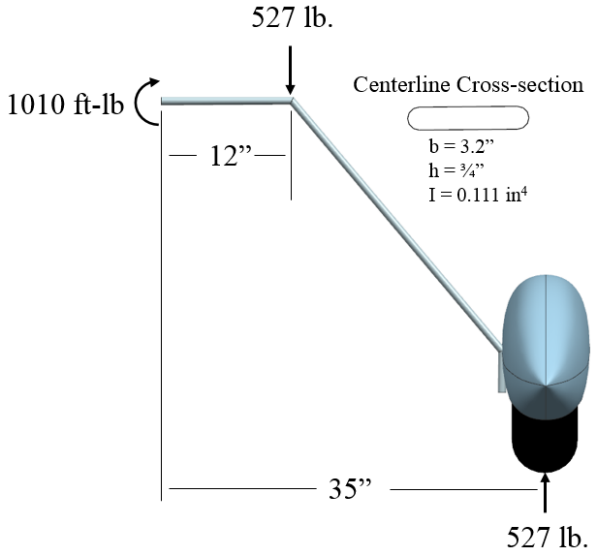

Figure 9.5: Main Strut Free Body Diagram

The tail wheel supports minimal loads and is primarily selected based on similar taildragger aircraft such as the Citabria, given in Ref 13. A tire size of 5.00-4 is selected with an inflation pressure of 35 psi. This is mounted to the structure through a pivot point to allow the tail wheel to be steerable by way of control cables connected to the rudder cables. This feature improves the handling qualities of the aircraft on the ground during taxiing, particularly at low speeds. Also of note is the placement of the strut beneath the main tail structure, preventing a hard landing from damaging the weaker structure of the rudder. Finally, to prevent from scraping the tail on the ground, the tail gear is placed to allow for 20° of clearance on rotation during takeoff.

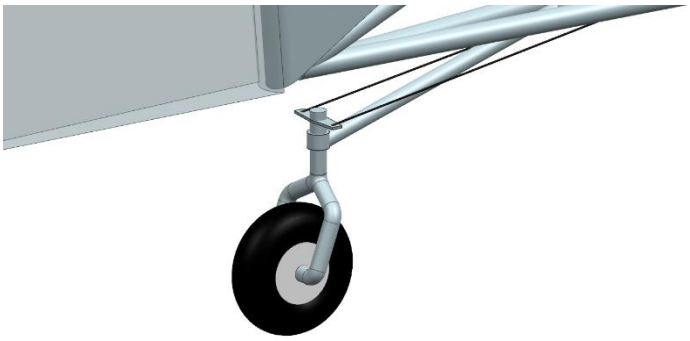

Figure 9.6: Tail Wheel

9.3 Weight and Balance

For the final iteration of the aircraft, a detailed weight and balance summary was performed. The methods used to perform this analysis were taken from Ref. 14 using a combination of the Cessna and U.S. Air Force Methods. These methods were combined since they seemed to be the most appropriate for both LSA design and aerobatics, respectively. Both methods were used for sizing all components, and the most reasonable value was chosen between the two based on preliminary Class I Sizing. The results are shown in the Table 10.2.

Table 10.2: Class II Weight and Balance Analysis

		Two-Seat		Single Seat	
		Weights (lbf)	Xcg (in)	Weights (lbf)	Xcg (in)
1	Wing	137	155	137	155
2	Horizontal Tail	22	299	22	299
3	Vertical Tail	22	317	22	317
4	Fuselage	84	118	84	118
	Nacelle	32	67	32	67
5	Landing Gear				
	Main	20	118	20	118
	Tail	4	323	4	323
6	Engine	164	65	164	65
	Propeller	10	47	10	47
	Fuel System	6	140	6	140
	Trapped Fuel & Oil	7	65	7	65
7	Fixed Equipment				
	Flight Controls	21	170	21	170
	Electrical System	33	85	33	85
	Avionics	66	125	44	125
	Furnishings	30	120	15	120
8	Fuel	80	95	80	95
9	Pilot 1	215	175	245	175
10	Pilot 2	215	137	---	---
11	Payload	30	202	30	202
∑1-7	W_e	658		622	
∑1-7 + 10	W_{oe}	873		867	
∑1-8 + 10	$W_{oe+fuel}$	953		947	
∑1-11	W_{to}	1198		977	
∑1-11 - 8	$W_{oe+pilots+payload}$	1118		897	

Figure 9.7 displays the total shift in the aircraft's center of gravity for max baggage and max pilot weight plus the weight of a parachute, as specified in the RFP. The single pilot column was calculated assuming the forward seat would be vacant. It can be seen that there is approximately 3-4 inches of CG travel in flight, meaning that the aircraft will become more longitudinally stable throughout the flight. Without the payload, the CG travel shifts forward approximately 3 inches, making for an aircraft that responds quicker, but is still stable. A favorable characteristic of this design is the CG travel for the single seat and the two seat are nearly identical. This means the CG placement in the two seat is where the front pilot sits. While this is not as ideal for aerobatic training, it is very good for passengers. Sitting on the CG means they will not feel the motion of the aircraft as strongly as the rear pilot, and they will be less susceptible to feeling motion sickness.

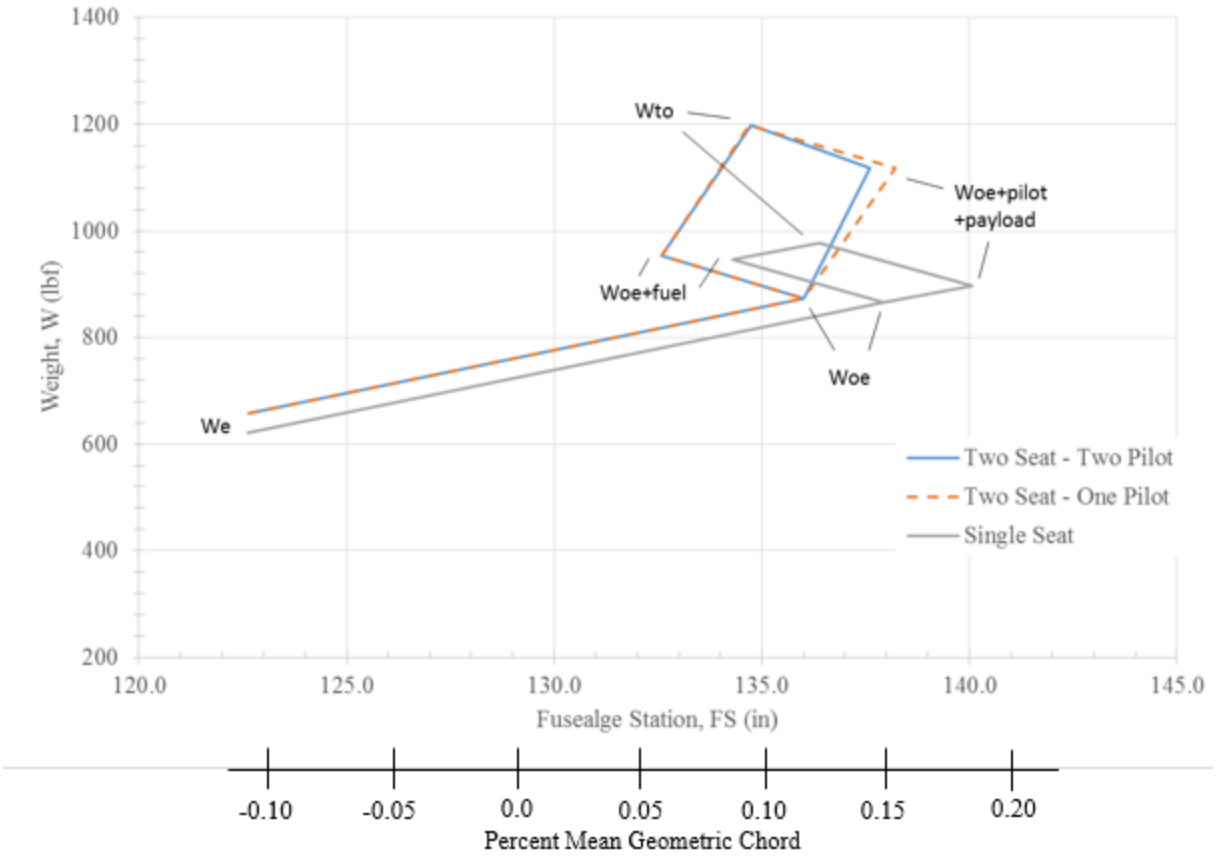

Figure 9.7: Class II Weight and Balance CG Shift, Single and Two Seat (Max Pilot Weights Max Payload)

9.4 Stability and Control

For the Class II Stability and Control derivatives, the static margin was checked to ensure longitudinal stability, using the weights and CG movement generated from Class II calculations. The longitudinal plot in Figure 9.8 shows the final iteration for the aircraft's static margin, determined to be 10% of the wing mean geometric chord. Based on Figure 9.8, the horizontal tail area was increased by 6% to 33 ft^2.

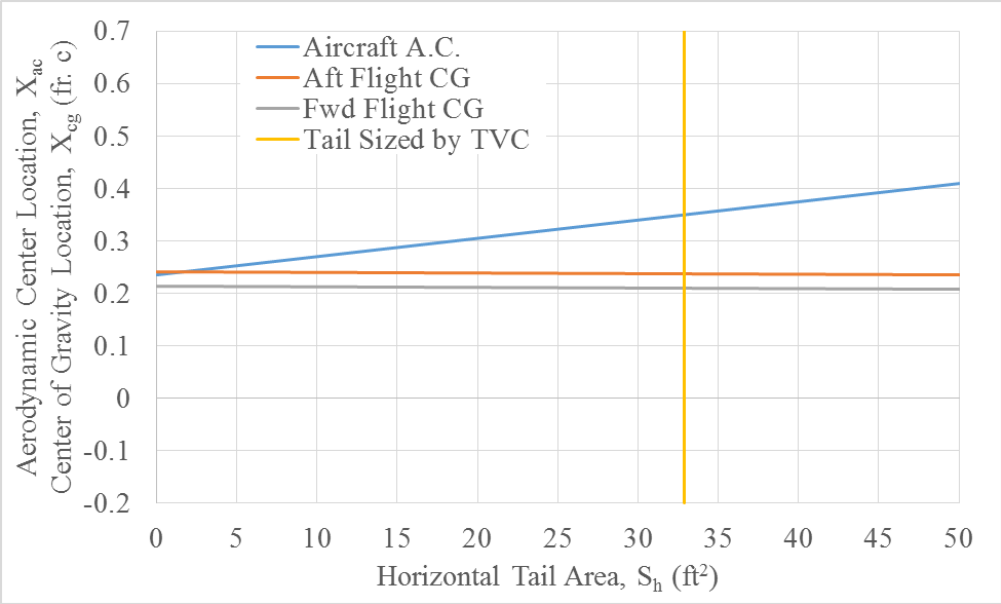

Figure 9.8: Final Static Margin

From Class I to Class II design, the empennage of the aircraft was changed to incorporate a vertical tail that transitions into the fuselage. This motivation was to make an aircraft that is easier to manufacture and more visually appealing, as well as increasing the directional stability. The size of the vertical tail and rudder were kept approximate to the Class I configuration. This resizing also allowed for the vertical tail to drop below the horizontal tail. This is advantageous, as it prevents high alpha blanking of the rudder. This is a common practice on aerobatic aircraft, ensuring rudder effectiveness at all attitudes. Because the Class II rudder is sized larger than the Class I rudder, it can be approximated that the rudder will be at least as effective as the Class I design.

To lower the structural weight of the empennage, a flat plate construction was used. This will allow for a lower weight in the back of the aircraft, and allow for simpler manufacturing of the empennage. This is common practice in light sport aircraft, and is utilized on the Pitts and Christen Eagle aerobatic planes.

For a full stability and control analysis, the program Advanced Aircraft Analysis (AAA) was utilized. AAA is a program written by DARCorp, a company co-founded by Dr. Roskam. The program is based on the Roskam design series, and does analysis of stability and control derivatives as well as flight dynamics given an aircraft geometry and a flight condition. By using the program, the major stability and control derivatives were calculated, as well as the flight qualities of the aircraft for 4 defined conditions.

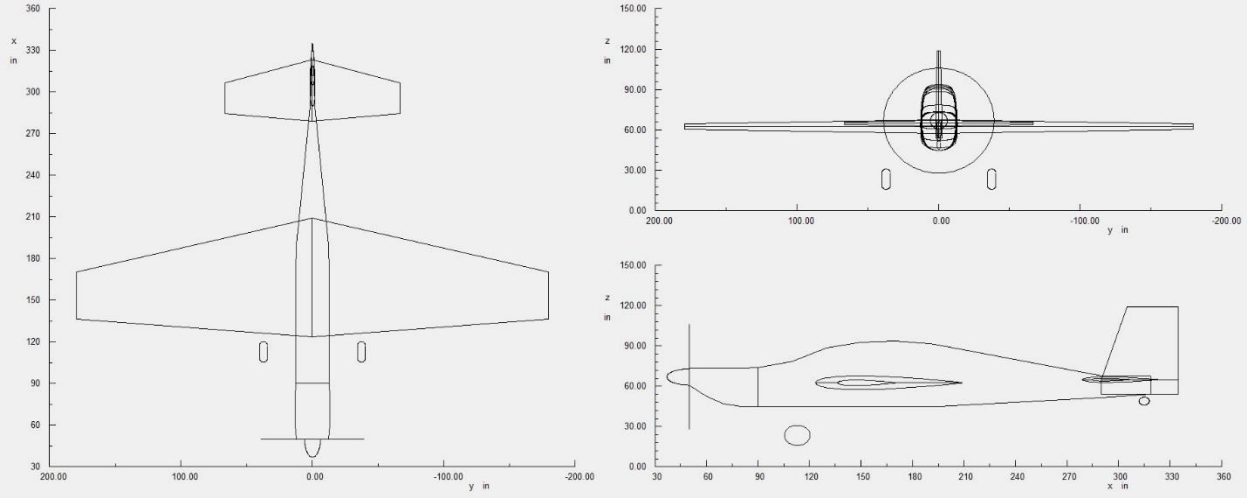

Figure 9.9: Aircraft 3-View in AAA [27]

To verify how stable the aircraft is, the stability and control derivatives were analyzed at cruise condition, the most common flight mode. The cruise condition was defined to be the optimal cruise condition based on the analysis done in Section 10. The condition was defined as being at the max speed at 1,200 lb with the center of gravity in the middle of the c.g range. Table 9.2 displays the derivatives for both longitudinal and lateral states.

Table 9.2: Stability Analysis for Cruise (10,000 ft, 120 kts, 1,200 lb, Mid CG)

Longitudinal				Lateral			
Derivative	**Value**	**Units**	**Stable Range**	**Derivative**	**Value**	**Units**	**Stable Range**
C_{L_0}	-0.0063	--	--	C_{l_β}	-0.0001	deg^{-1}	< 0
C_{L_u}	0.0091	--	> 0	C_{l_p}	-0.0061	deg^{-1}	< 0
C_{L_α}	0.0724	deg^{-1}	> 0	$C_{l_{\delta_r}}$	0.0001	deg^{-1}	> 0
C_{L_q}	0.0918	deg^{-1}	> 0	$C_{l_{\delta_a}}$	0.0047	deg^{-1}	> 0
C_{D_u}	0	--	< 0	C_{y_β}	-0.0063	deg^{-1}	< 0
C_{D_α}	0.0025	deg^{-1}	< 0	C_{y_r}	0.0047	deg^{-1}	> 0
C_{m_0}	0.0056	--	> 0	$C_{y_{\delta_r}}$	0.0034	deg^{-1}	> 0
C_{m_u}	0.0010	--	> 0	C_{n_β}	0.0024	deg^{-1}	> 0
C_{m_α}	-0.0095	deg^{-1}	< 0	C_{n_p}	-0.0005	deg^{-1}	< 0
$C_{m_{\delta_e}}$	-0.0126	deg^{-1}	< 0	$C_{n_{\delta r}}$	-0.0017	deg^{-1}	< 0
C_{m_q}	-0.1315	deg^{-1}	< 0	$C_{n_{\delta a}}$	-0.0002	deg^{-1}	< 0

The flying qualities of an aircraft are defined based on the time constant, damping ratio, and/or natural frequency of each mode. Based on these values, the modes are assigned a level from 1 to 3 describing the flight qualities. Level 1 is adequate flight qualities for the given flight phase. Level 2 is adequate flight qualities, with either an increase in pilot workload or decreased mission effectiveness. Level 3 is an aircraft that is safe to control, but

demands excessive workloads or is unable to complete the mission. Aircraft are required to have level 1 qualities within their normal operating state, since level 2 & 3 qualities have greater chance for failure of crucial systems required for safe flight [15]. The following figure displays the flight qualities for the aircraft in cruise condition. It can be seen that the aircraft meets level 1 flight qualities for every mode.

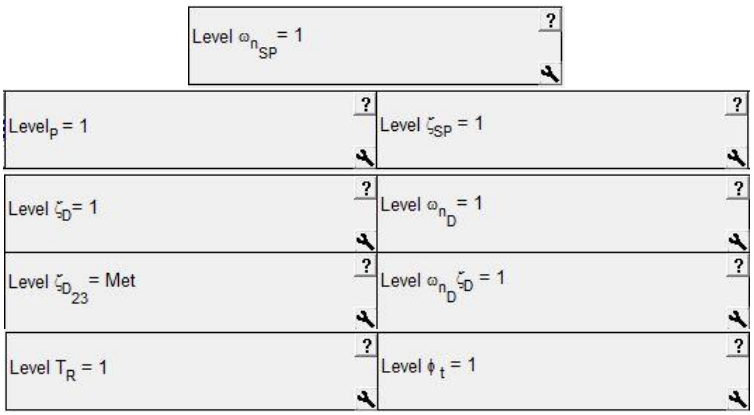

Figure 9.10: Mode Stability Level Output Calculated by AAA [27]

To best display the trim characteristics of the aircraft in cruise conditions, a trim diagram was produced using AAA. The figure below displays the trim diagram for the aircraft at a cruise altitude of 10,000 ft. at max cruise speed of 120 kts and a weight of 1,200 lb. To create the trim diagram, power effects were included, set at the power setting specified in Section 10.

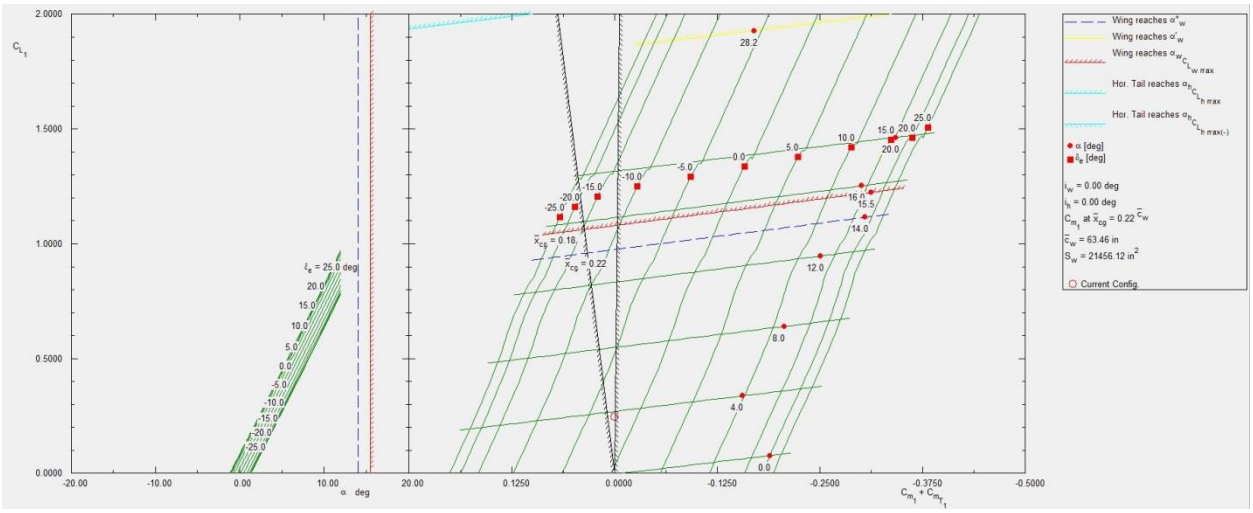

Figure 9.11: Trim Diagram for Cruise Condition [27]

From Figure 9.11 it can be seen that the aircraft flies at an angle of attack at 3.75° and an elevator deflection of approximately 2°. The elevator deflection is able to be trimmed out with the elevator trim tab to relieve the pilot of the stick force for the duration of the flight. The aircraft will need very little trim adjustment during cruise flight due

to the very tight range of in-flight CG movement. The in-flight static margin is calculated to be 12%, approximately what was aimed for in the Class I stability and control analysis. This results in an aircraft that is easy to control for the average pilot, and leans towards being more stable.

To ensure that the aircraft would be controllable in all designed for conditions, analyses were done for 3 other conditions: Takeoff, approach, and 6g pull up. Takeoff and approach were chosen since they are conditions that will be seen at every flight condition. To validate the RFP requirements, the takeoff and approach conditions were analyzed at 5,000 ft MSL at ISA + 10°C (50°F). The 6g pull up was chosen as the maximum maneuvering forces that the aircraft would see. It was evaluated at 3,000 ft, where intermediate aerobatics would take place, at the two seat aerobatic operating weight of 1080 lb. To summarize these conditions, the trim diagrams and flight qualities are displayed in the following figures and table.

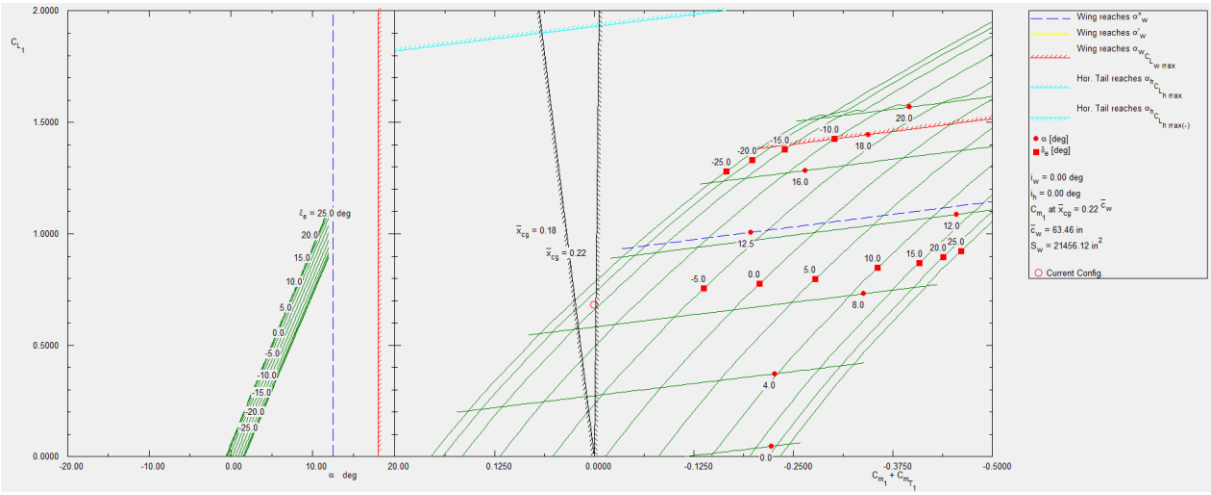

Figure 9.12: Trim Diagram for Takeoff [27]

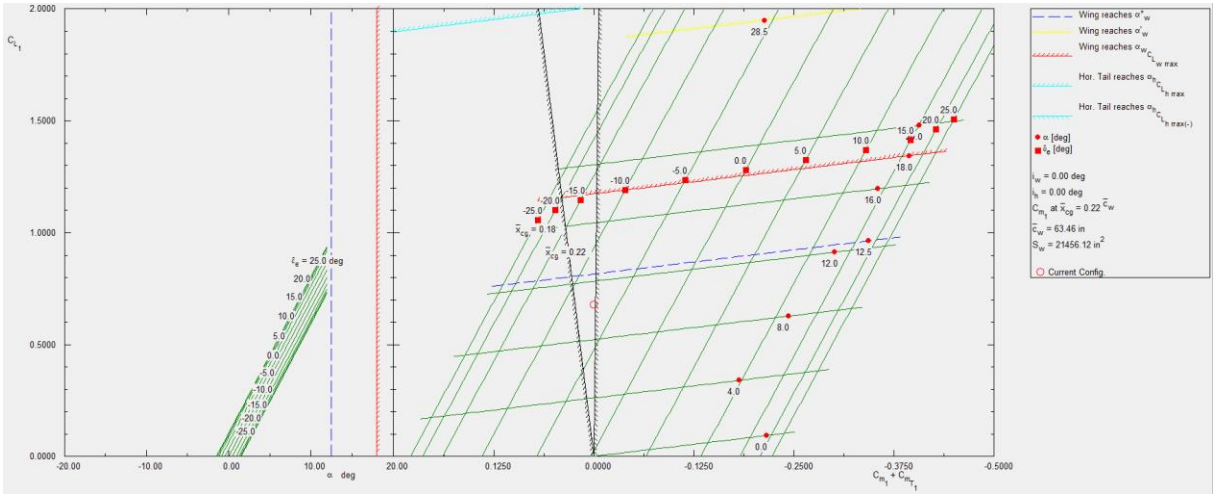

Figure 9.13: Trim Diagram for Approach [27]

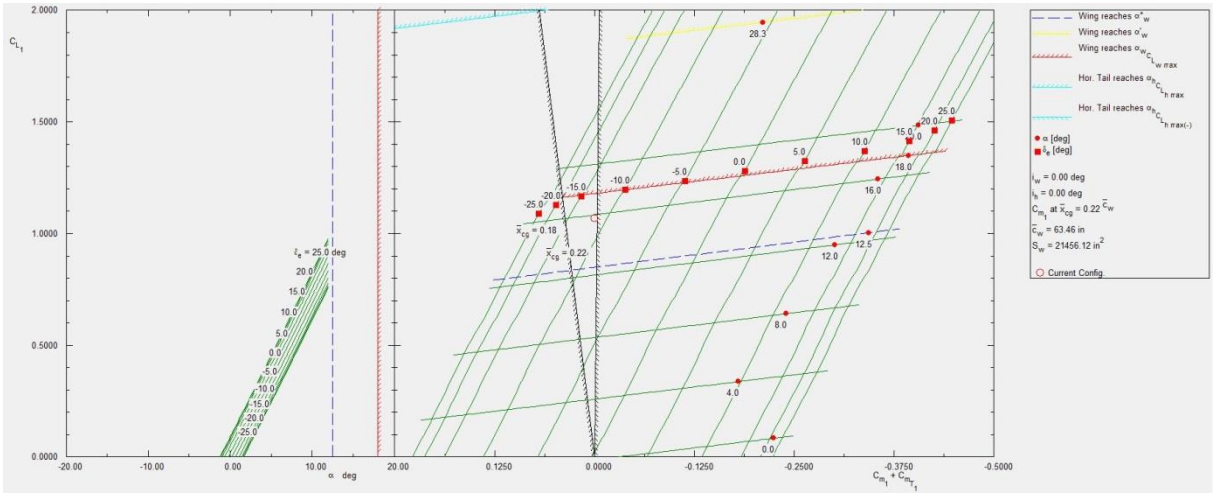

Figure 9.14: Trim Diagram for 6g Pull Up [27]

Table 9.3: Flight Qualities for Takeoff, Approach, 6g Pull Up [27]

	Phugoid	Short Period	Roll	Spiral	Dutch Roll
Takeoff	Level 1	Level 1	Level 1	Level 2	Level 1
Approach	Level 1	Level 1	Level 1	Level 2	Level 1
6g Pull Up	Level 1	Level 1	Level 1	Level 2	Level 1

Based on the trim diagrams, it can be seen that the aircraft is trimmable for all conditions of the flight. The flight qualities are level 1 for all dynamic modes except for the spiral mode. While there are no stringent requirements for civilian aircraft, MIL-SPEC defines Level 2 spiral mode is defined as having a time to double amplitude between 8 and 12 seconds. Spiral mode is heavily influenced by $C_{l\beta}$, which for our aircraft is small. Contributing factors to this are that the aircraft's wing has no dihedral, no wing sweep, and is a mid-wing configuration. Changing these

parameters is not an option for the design since it would compromise the aerobatic qualities of the aircraft. Since each of these flight phases is during a portion of the flight when the pilot is actively working the controls, it is reasonable to assume that any spiral excitement will be neutralized before it becomes uncontrollable.

9.5 Class II Drag

The Class II drag polar for the mid-wing monoplane begins by finding the individual drag increments of each component on the aircraft.

A Class II Drag Polar estimation was performed to confirm and enhance drag profiles found during Class I Drag Polar estimation. The Class II Drag Polar estimation process outlined in Dr. Jan Roskam's Aircraft Design Series, Part VI [15], was utilized for this aircraft. For this estimation, the following components were determined to contribute to the drag of the aircraft:

- Wing;
- Fuselage;
- Empennage;
- Landing Gear;
- Windshield/Canopy.

The Class II zero lift drag coefficient of the wing was found after considering the wing/fuselage interaction, a lifting surface interaction factor, the skin friction coefficient, an airfoil thickness location parameter, the thickness to chord ratio of the wing, and the exposed wetted area of the wing planform. As a conservative estimate, the skin friction drag coefficient was assumed to be 0.01. The other constants were found in Dr. Jan Roskam's Aircraft Design Series, Part VI, Chapter 4, Section 2 [15]. In addition, the vortex generator drag increment must be considered since they are attached during all stages of flight. Using Dr. Ron Barrett's thesis on vortex generator technology [8], it was determined that the vortex generators would add about 4% to the zero lift drag coefficient of the wing. This number is small since the vortex generators are functioning mostly in or near the boundary layer, and don't significantly create drag during operation. The resulting zero lift drag coefficient contribution from the wing was determined to be 0.0208.

The Class II zero lift drag coefficient of the fuselage was found after considering the wing/fuselage interaction, the skin friction coefficient of the fuselage, the geometry of the fuselage, the fuselage frontal area drag, and the fuselage wetted area. As was stated for the wing, a skin friction coefficient of 0.01 was chosen to create a

conservative drag viewpoint. Utilizing the CAD geometry and the methods from Dr. Jan Roskam's Aircraft Design Series, Part VI, Chapter 4, Section 3 [15], the zero lift drag coefficient of the fuselage was found to be 0.0123.

The Class II zero lift drag coefficient analysis of the empennage was split into two parts:

- Horizontal Stabilizer;
- Vertical Stabilizer.

As outlined in Dr. Jan Roskam's Aircraft Design Series, Part VI, Chapter 4, Section 4 [15], the horizontal stabilizer was analyzed as if it were a wing. This included all of the same constants as the Class II wing drag discussed in the previous paragraph, but with different values due to the different geometry. This resulted in a zero lift drag coefficient contribution of 0.0040 for the horizontal stabilizer.

Similarly, the vertical stabilizer was analyzed as a small half wing using the same method described above. This resulted in a zero lift drag coefficient contribution of 0.0015 for the vertical stabilizer.

The Class II zero lift drag coefficient of the landing gear was determined by examining the wetted area and the contouring utilized during design. Since the skirts on the wheels are designed in a streamlined fashion, they contribute smaller amounts of drag when compared to other, more blunt types of wheel skirts. Since the landing gear is designed on two solid supports, rather than a complex truss system, the undercarriage portion contributes smaller amounts of drag coefficient. The result of the above analysis and the methods of Dr. Jan Roskam's Aircraft Design Series, Part VI, Chapter 4, Section 7 [15], the zero lift drag coefficient contribution of the landing gear was determined to be 0.0024.

The final component determined to contribute to the parasite drag is the windshield and canopy. This analysis was performed utilizing Dr. Jan Roskam's Aircraft Design Series, Part VI, Chapter 4, Section 8 [15]. This method involved analyzing the length of fuselage in front of and behind the canopy, as well as the height of the canopy itself. Similarly, an analysis was performed on the windshield of the aircraft to determine the smoothness of the contouring. The resulting contribution to the zero lift drag coefficient due to the canopy and windshield was found to be 0.0055.

The resulting parasite drag that is found by combining each of the individual contributions. The value of the zero lift drag coefficient utilizing the Class II preliminary design methods outlined in Dr. Jan Roskam's Aircraft Design Series, Part VI, Chapter 4 [15], was found to be 0.0466. This parasite drag coefficient is smaller than the Class I estimation. This was determined to be the result of overestimation of the vortex generators contribution to drag. By utilizing Dr. Ron Barrett's thesis information [8], a more accurate drag estimate was found. This resulted in a lower

parasite drag value, and a more efficiently flying plane. Since the vortex generators were determined to be nearly identical to a clean wing, no specific determination is made on the drag polar graph shown below.

Utilizing the technique that the maximum lift to drag ratio occurs when the induced drag is equal to the parasite drag, a lift to drag maximum value was calculated for this aircraft. The maximum lift to drag ratio occurs at $C_L = 0.86$. This results in a maximum lift to drag ratio of 9.27. The Class II drag polar utilizing the new parasite drag value is shown below.

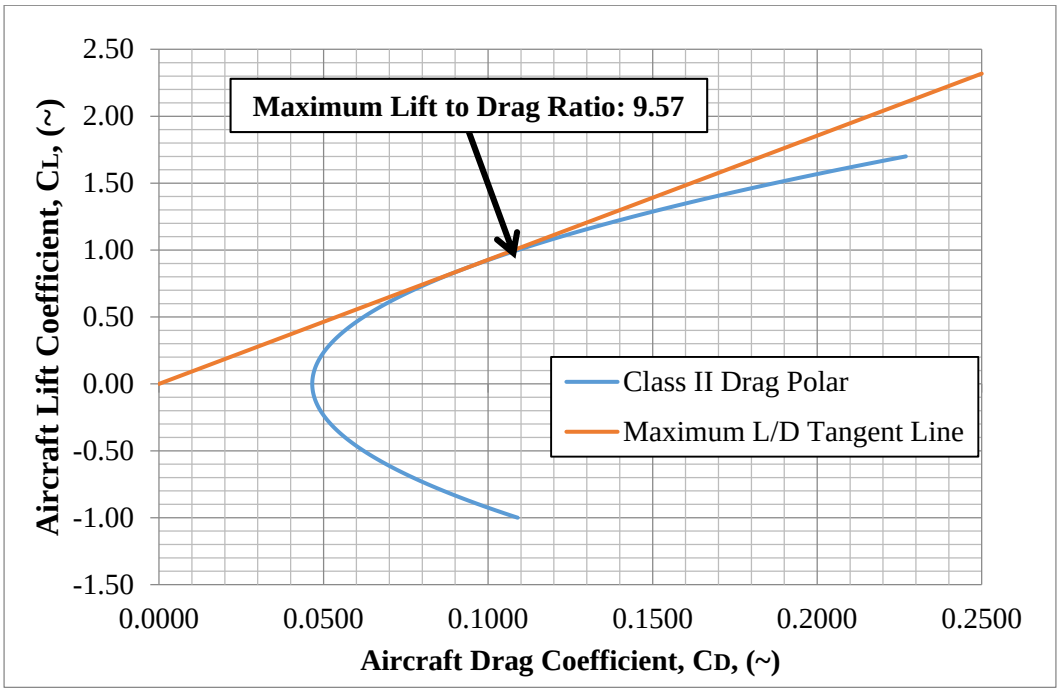

Figure 9.15: Class II Drag Polar and L/D_{max}

10. Class II Propulsion Performance

The best cruise altitude and speed depend primarily on the engine selected, and at what engine setting it achieves its best specific fuel consumption (SFC). For the Rotax 915, it achieves an SFC of 0.465 lb/hp*h at 5500 RPM [31]. This is assumed to be the most efficient level the engine can run at. To account for the propeller effects, a prop efficiency of 0.85 was assumed. This placed our power available at 115 hp. To determine the possible speeds and altitudes that the aircraft can fly at, the power required was plotted compared to the power available. Power required was calculated using the following equation taken from Anderson [40]. The prop efficiency was added on to get the total power required.

$$P_R = \eta VD = \eta\, {}^1\!/_2\, \rho V^3 \left(C_{D_0} + \frac{\left(\frac{2W}{\rho V^2 S}\right)^2}{\pi A e} \right) S \tag{13.1}$$

The power available and power required were plotted to show what the limitations of altitude imposed on speed for the aircraft. Figure 10.1 displays the curve plotted for the different altitudes that are in the aircraft flight envelope.

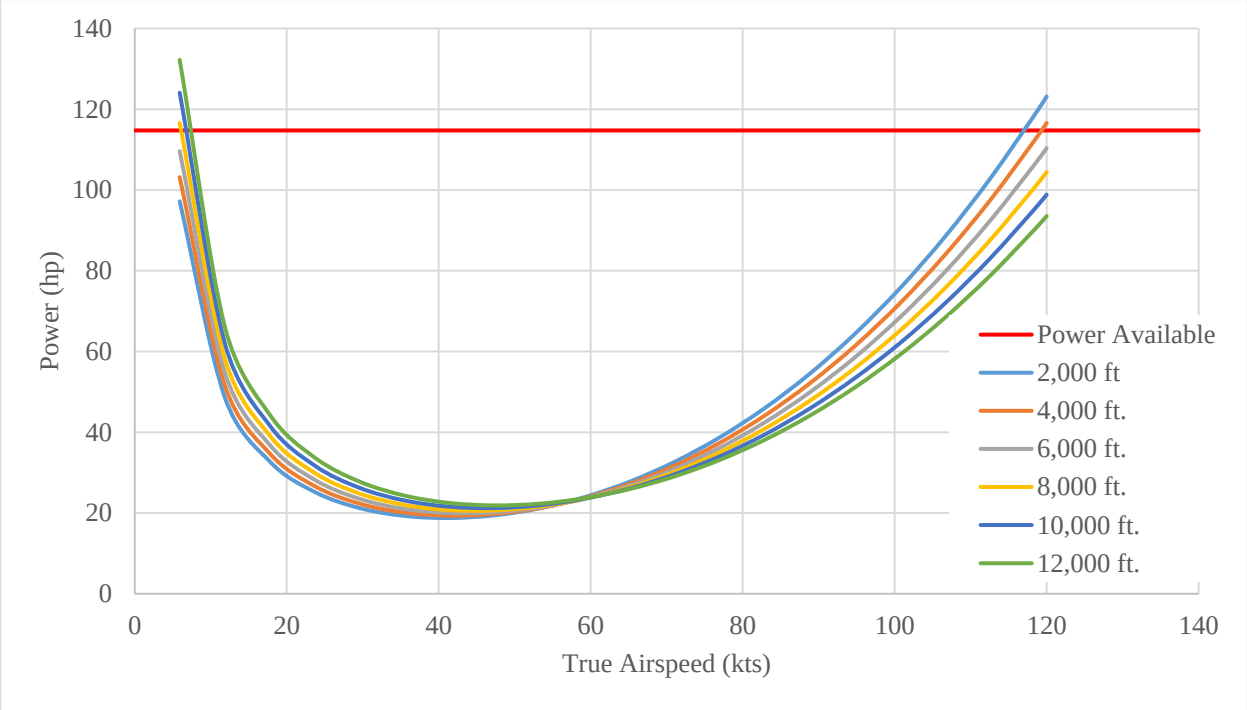

Figure 10.1: Power Required vs. True Airspeed for Varying Altitudes

From Figure 10.1, the power available only limits the aircraft when it is at 4,000 ft. It is free to fly at the max level flight speed of 120 kts at an altitude above 12,000 ft. However, this may be uncomfortable for pilots due to the oxygen limitations. For long duration flights, the pilot may desire to cruise at a lower altitude for comfort. It would also be detrimental to the range of the aircraft. If the max speed at altitude is desired, the following chart displays the maximum speed that can be achieved at a given altitude for a certain throttle setting. The plots were determined by using Eq. 13.1, above, to determine an airspeed for a given altitude and throttle setting.

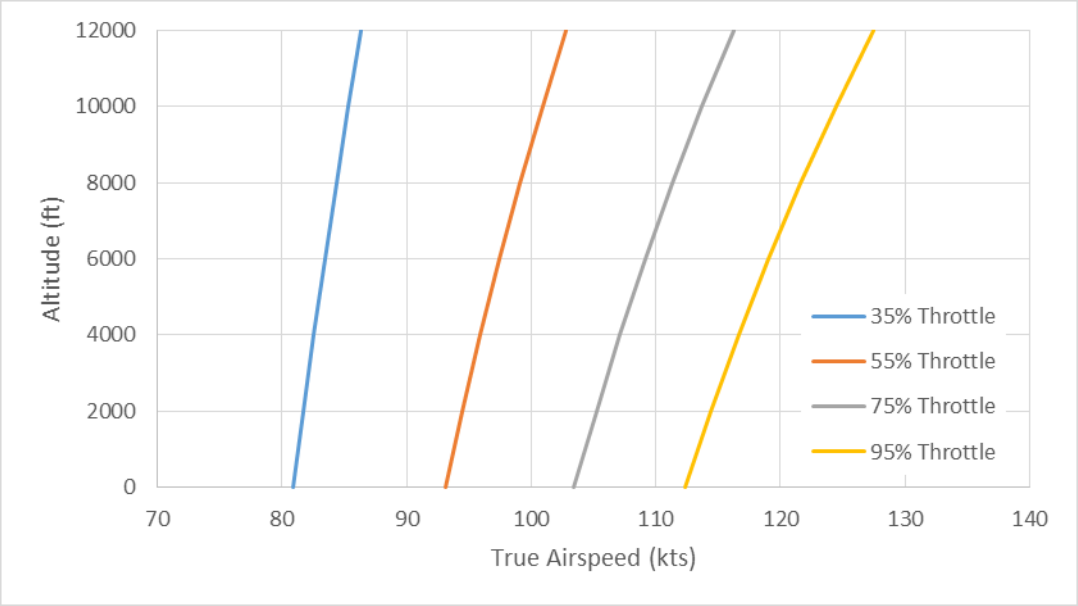

Figure 10.2: Cruise Performance – Max Takeoff Weight (1260 lb.)

11. Performance Verification

From the RFP, the following performance requirements were outlined for the one and two seat variants. To verify these parameters, multiple methods were used to ensure that the aircraft were adequately designed to achieve these performance requirements.

Table 11.1: Performance Requirements

	Single	Double
Ferry Range	300 nmi + 30 minute fuel reserve	250 nmi + 30 minute fuel reserve
Climb Rate	1,500 fpm at sea level	800 fpm at sea level
Takeoff and Landing (over 50’ obstacle)	1,200 ft.	1,500 ft.
Minimum Roll Rate	180°/s	180°/s

11.1 Climb Rate

The climb rate was calculated by using the following equation from Ref. 40:

$$RC = \frac{P_A - P_R}{W} \tag{14.2}$$

Because the two seat has the highest weight, it was decided that if it could outclimb the requirement for the single seat, then the single would be able to climb faster due to a lower max takeoff weight. To verify the climb rate at sea level ISA + 10°C, the P_A and P_R curves in Figure 10.1 were used with the density corrected for the increased

temperature. Climb velocity was assumed to be 1.5 time the stall speed. For the two seat aircraft, the rate of climb was determined to be 2173 ft/min. This exceeds the expectations for the single seat and far exceeds the expectation for the two seat. The climb rate for the single and the two seat aircraft are displayed below at max payload and max pilot weight.

Table 11.2: Climb Rate – Maximum W_{TO}, Sea Level, ISA + 10°C, Max Power

	Climb Rate (fpm)
Single Seat	2250
Two Seat	2170

11.2 Takeoff and Landing

Takeoff performance was calculated using the following equation from Ref. 40:

$$s_{TO} = \frac{1.44W^2}{g * \rho * S * C_{Lmax}\{T - [D + \mu_r(W - L)]_{av}\}} \quad (14.3)$$

To evaluate the takeoff performance at 5,000 ft. ISA + 10°C, the density at 5,000 ft. was calculated for + 10° C. This density value was used in all calculations for takeoff and landing. The thrust was calculated assuming the maximum available power for takeoff. To account for the average drag across the takeoff run, Anderson suggests that the velocity be set to 0.7 times liftoff velocity, which was assumed to be 1.2 times stall speed. Lift was calculated with the velocity found for drag. The coefficient of rolling friction was set to 0.10, corresponding to a grassy field. Because this equation accounts only for the takeoff ground roll, the result was multiplied by 1.66 to determine the total takeoff distance over a 50 ft. obstacle [11].

Landing was evaluated at the same condition as takeoff, with minor modifications. The speed was assumed to be 1.3 times V_{stall}. The coefficient of rolling friction was assumed to be 0.4, assuming brakes would be applied. The equation below comes from Ref. 40:

$$s_L = \frac{1.69W^2}{g * \rho * S * C_{Lmax}[D + \mu_r(W - L)]_{av}} \quad (14.3)$$

As a verification of the results, AAA was used to calculate both takeoff and ground run distances. The takeoff run was set to use max power, while the landing condition was specified to have no power. The results of all methods can be seen in Table 11.3. While AAA estimates the ground run to be shorter than Anderson does, the distances to clear 50 ft obstacle are very similar. This verifies the performance, and puts the two seat within the performance range of the single seat.

Table 11.3: Takeoff and Landing Distances

	Ground Run		Clearance of 50 ft obstacle	
	Anderson	AAA	Anderson	AAA
Takeoff (ft.)	400	330	670	680
Landing (ft.)	550	370	1060	1010

11.3 Roll Rate

The roll rate for the aircraft was estimated using AAA. While the RFP does not specifically state that the two seat variant will need to meet the 180°/s roll rate requirement, it is assumed that the aircraft should have similar performance characteristics. Therefore the two seat variant was analyzed for roll rate. The roll rate was calculated for 120 kt CAS. The result is shown below:

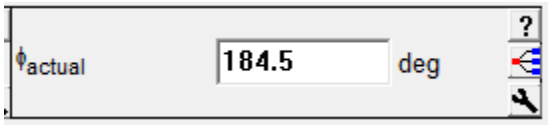

Figure 11.1: Roll Rate Determined by AAA

11.4 Payload-Range Diagram

To analyze and clearly show the ferry range capabilities of both variants of aircraft, payload/range diagrams were created. To craft a payload/range diagram, four points are needed for each aircraft. These points are defined as follows:

A: This point is defined as the operating empty weight of the aircraft (structure, trapped fuel/oil, pilots) plus the maximum available payload. For the 1-seat variant, this is 30 pounds of cargo plus a 15 pound parachute, or 45 pounds. For the 2-seat variant, this is 30 pounds of cargo plus two 15 pound parachutes, or 60 pounds.

B: This point is defined as the aircraft fully loaded with payload (point A), but filled to the maximum takeoff weight with fuel. For the 1-seat variant, this corresponds to 970 pounds, 55 pounds of which is fuel. For the 2-seat variant, this corresponds to 1,320 pounds, also with 55 pounds of fuel. Since the aircraft is now loaded with fuel, the range for each case was able to be calculated using the Breguet range equations. The range of both variants was calculated assuming 30 minutes of reserve fuel. The weight of the reserve fuel was calculated through the Breguet endurance equations. The 1-seat reserve fuel is 4 pounds; the 2-seat reserve fuel is 6 pounds. These in combination result in range values as follows:

- 1-Seat Range (Point B): 298 nautical miles;
- 2-Seat Range (Point B): 209 nautical miles.

C: This point is defined as the aircraft fully fueled to the volumetric limits of the tank. In this case, filling the tanks to full capacity exceeds the maximum takeoff weight. This requires the payload to be partially removed in both aircraft variants. The fuel tank equipped on both aircraft has a fuel capacity of 80 pounds, leaving 20 pounds of cargo space in the 1-seat aircraft and 35 pounds of cargo space in the 2-seat aircraft. Since there is more fuel onboard the aircraft, a larger range was found for each aircraft. As in Point B, range was calculated assuming 30 minutes of reserve fuel. The resulting range values for each aircraft under the lower payload configuration are as follows:

- 1-Seat Range (Point B): 450 nautical miles;
- 2-Seat Range (Point B): 318 nautical miles.

D: This point is defined as the aircraft fully fueled to the volumetric limits of the tank with 0 pounds of cargo or payload on board. Since the overall weight of the aircraft has been reduced with the same fuel capacity, slightly higher ranges were found. These zero-payload ranges are defined as the ferry ranges of the two aircraft. As in Point B and C, range was calculated assuming 30 minutes of reserve fuel. The resulting range values for each aircraft under the zero payload configurations are as follows:

- 1-Seat Range (Point B): 460 nautical miles;
- 2-Seat Range (Point B): 327 nautical miles.

Since Point D corresponds to the ferry range of the aircraft, it can be seen that the minimum ferry distance of 300 nautical miles for the 1-seat aircraft is met, and the ferry distance of 250 nautical miles for the 2-seat aircraft is met. Although the ferry range found is higher than the specification and the fuel tank size could be reduced, it was determined through pilot interviews that fewer stops on the way to a competition or airshow are desirable. With this in mind, the fuel tank remained the same size after payload/range analysis. The payload/range plots are shown in Figures 11.2 and 11.3. The vertical axis displays payload weight only, the fuel weight is not shown in this diagram.

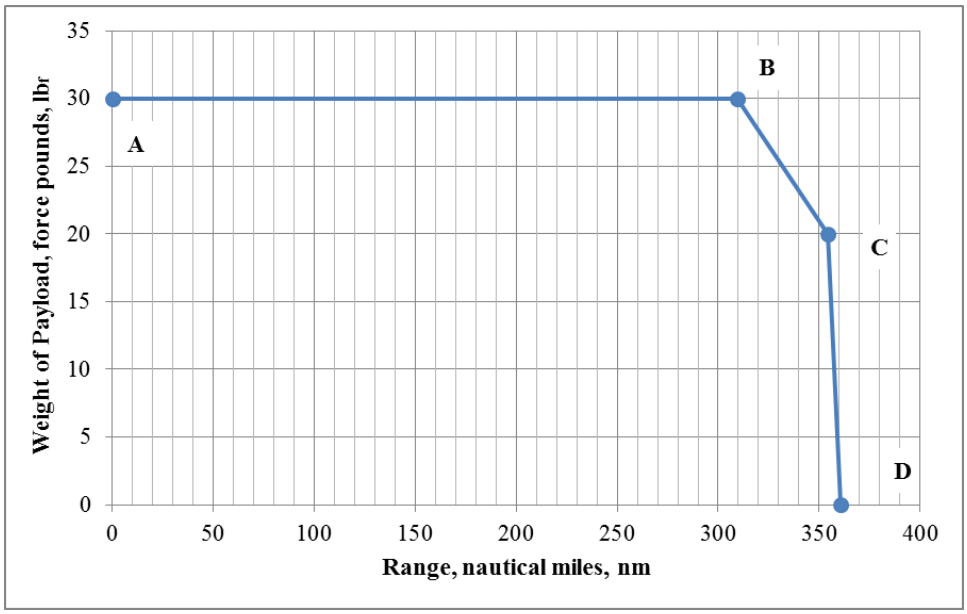

Figure 11.2: Two Seat Payload/Range Diagram

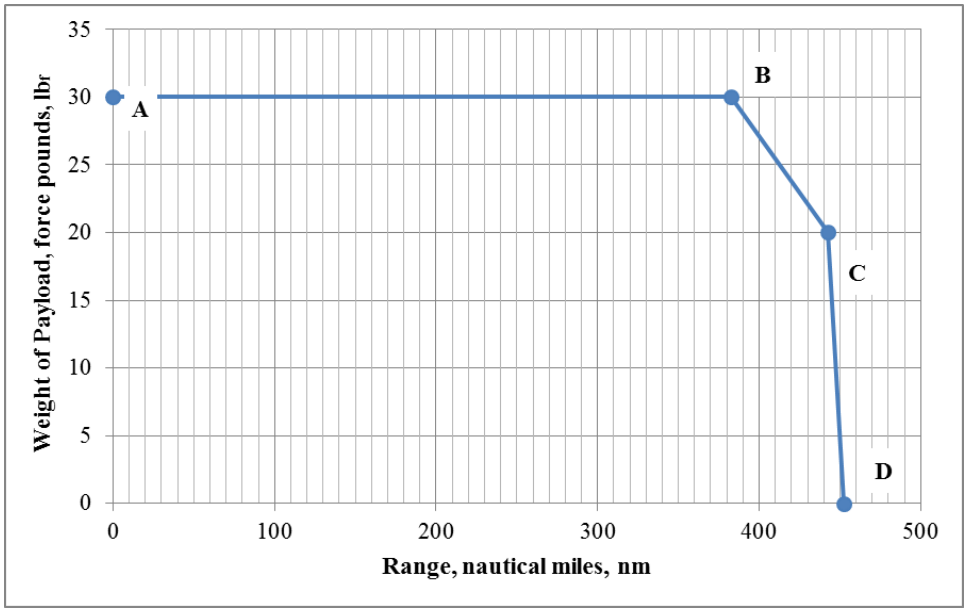

Figure 11.3: One Seat Payload Range Diagram

To ensure compliance with the RFP, the figure below displays the cargo space of the aircraft directly behind the pilots. The cargo space will not change between the two seat and single seat aircraft.

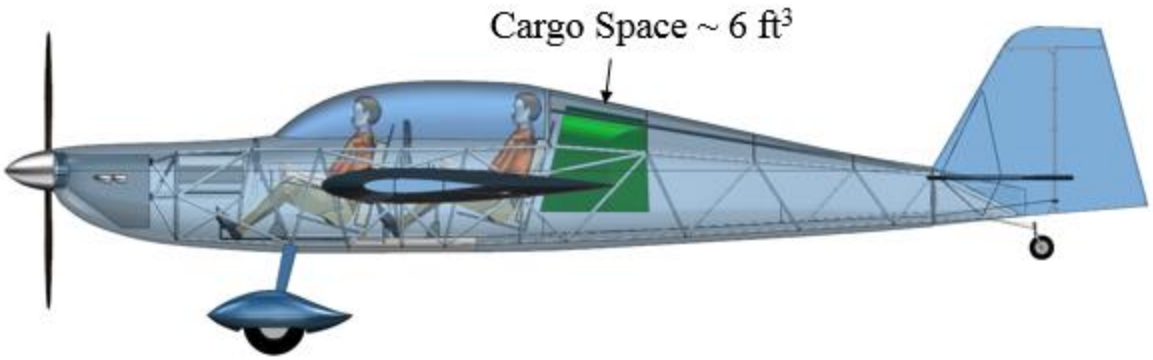

Figure 11.4: Verification of Cargo Space

11.5 V-n Diagram

A Velocity/Load Factor, or V-n diagram, was constructed for this family of aircraft to display the prescribed capabilities. The process to create a V-n diagram followed Dr. Jan Roskam's method outlined in the Aircraft Design Series, Part V, Chapter 4, Section 2 [14]. The V-n diagram was constructed based on a FAR 23 certified aircraft. The values of stall velocity, V_S, design cruising speed, V_C, design diving speed, V_D, and design maneuvering speed, V_A, were calculated. Also, the highest positive and lowest negative load factors were also determined for cruise, dive, and maneuver. The values constraining maneuverability were prescribed to be +6/-5 g for the 1-seat aircraft. Lastly, the gust lines and associated load factors were found and plotted. The resulting V-n diagram is shown below.

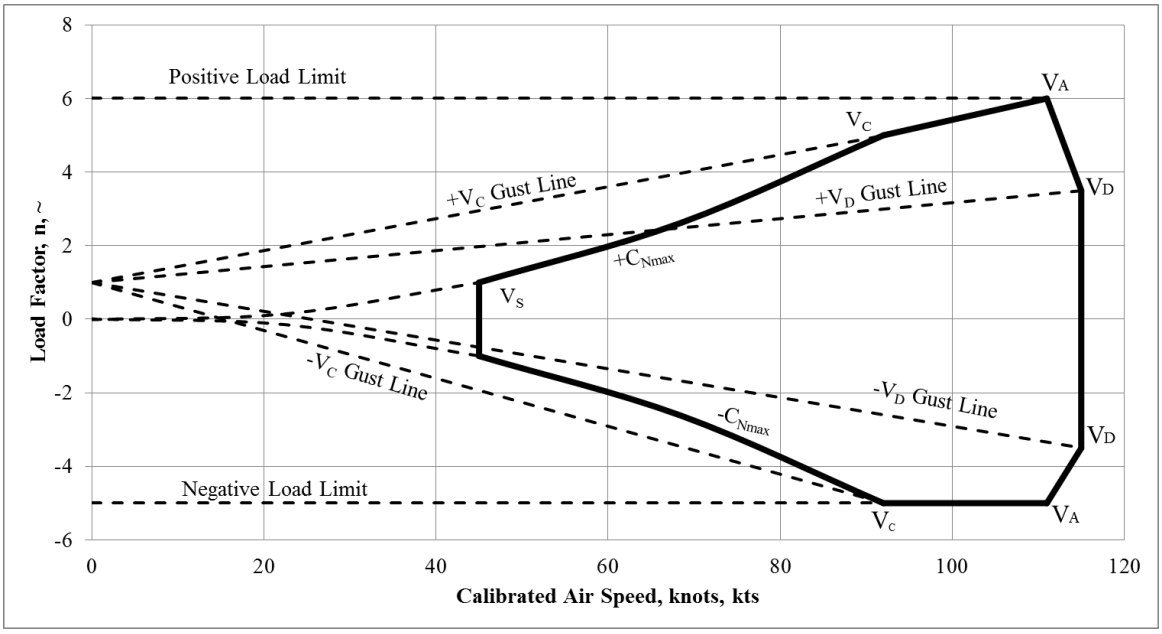

Figure 11.5: Aircraft V-n Diagram

12. Systems and Subsystems Layout

The layout of the systems for the aircraft includes the following:

- Flight Controls
- Fuel System
- Hydraulic System
- Electrical System
- Environmental System

Each system is described in detail in the following sections.

12.1 Flight Controls

The two possibilities considered for the flight controls system of this aircraft are reversible and irreversible controls. The factors differentiating the two are response time, cost and pilot preference. The response time for a pushrod reversible system is nearly instantaneous and therefore matches the possible response of an irreversible system. The complexity of an irreversible control system would be higher because it requires additional electronics and triple redundancy for safety. It is preferred that it is easy to maintain and an electronic irreversible system would be more difficult for the typical homebuilder to maintain than a pushrod system. Of greatest importance is pilot preference; all aerobatic pilots contacted while gathering information for this report stated that reversible flight controls are absolutely necessary. The pilots fly by the feel of the stick, and without it they would consider themselves to be at a significant disadvantage.

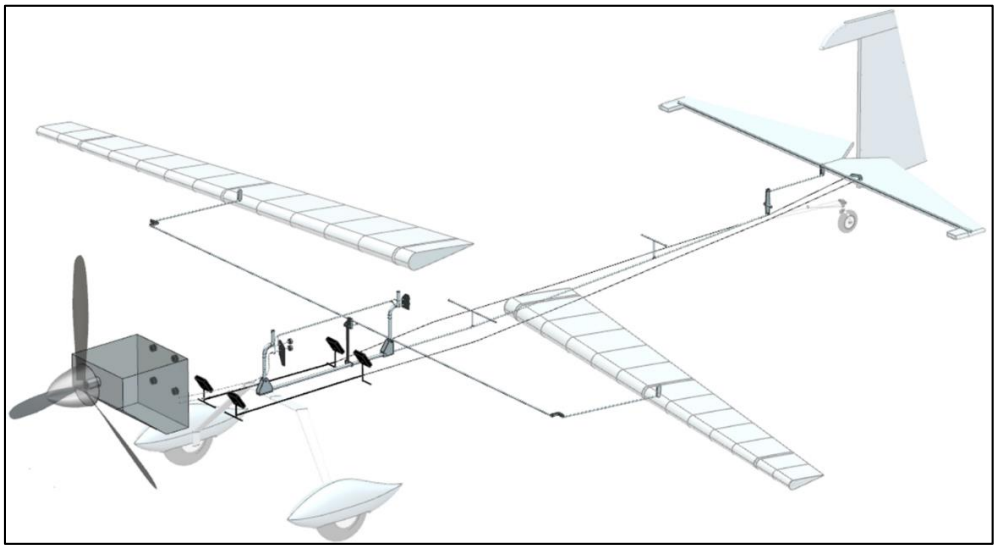

Figure 12.1: Flight Controls Layout

For aileron control, the stick pivots around a torque tube which is connected to both pilot's control sticks. Based on the space available in the cockpit, the stick can pivot 15° left and right. The rotation caused by the stick must then be transferred from the deck of the cockpit to the mid-wing position of the ailerons. This is accomplished with a pushrod connected to a bellcrank. The motion is then transferred out through the wing to a second bellcrank. The control rod is routed in front of the main spar for support and to allow for easier access. The bellcrank at the wing is positioned at a rib to provide structural support and transfers the motion to the aileron. This results in an aileron deflection of up to ±25°.

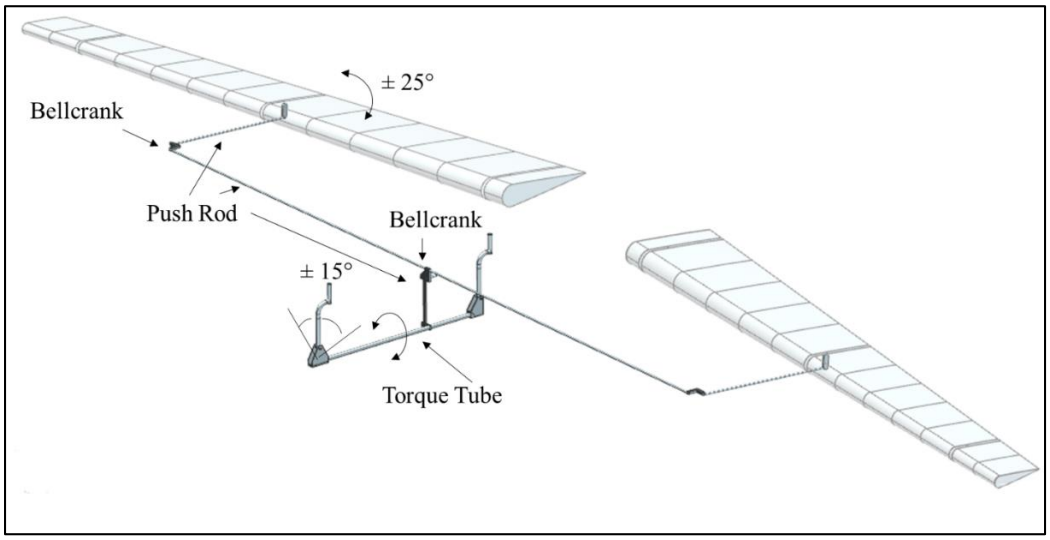

Figure 12.2: Aileron Controls Layout

The elevator controls are connected to each other with a pushrod inside the torque tube. The bend in the control stick is incorporated to allow for ±20° forward and aft movement inside the cockpit. The pushrods transfer the motion all the way to the elevator and are supported every 3-5 ft. by bellcranks. The motion is then transferred up to the elevator using a crank arm and results in ±25° of deflection. To balance the elevator, a full horn is used.

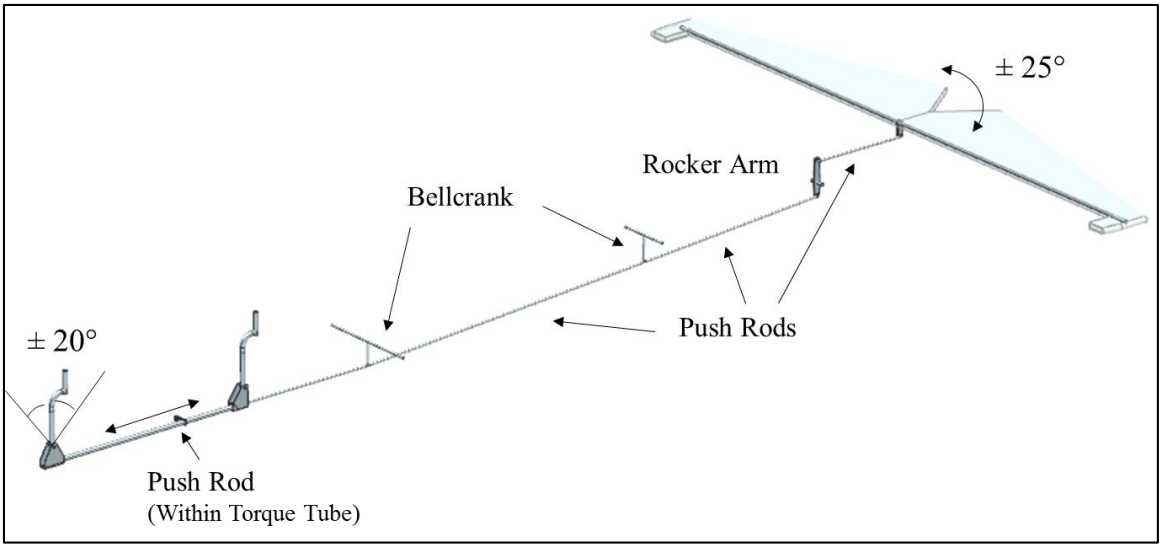

Figure 12.3: Elevator Controls Layout

The two pairs of rudder pedals are connected to each other by way of control rods. These rods are connected to cables which are routed through the fuselage to the rudder. The cables are guided along the bottom interior of the fuselage by fairleads mounted at several points along the truss. Pulleys are not used because the path is relatively short and straight and this method reduces weight. Also, this is the same method used to guide the rudder cables on other aerobatic aircraft such as the Extra 300 [15] and therefore is proven to function effectively. The cables are also spliced to control the tail wheel to provide steering control on the ground. For balancing purposes, the rudder also has a full horn and movement in the rudder pedals can result in up to ±25° of rudder deflection.

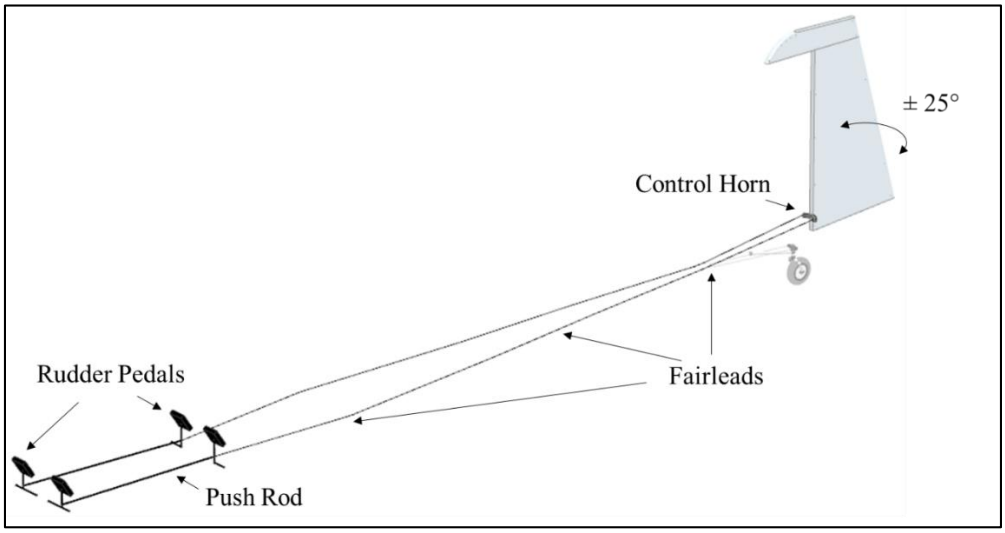

Figure 12.4: Rudder Controls Layout

12.2 Fuel System

The fuel system consists of the required 13.3 gallon fuel tank and the accompanying inverted flight kit. This requires a flop tube within the tank which is a weighted fuel line that follows the fuel when the aircraft goes inverted. Since the engine is fuel injected it does not need a special carburetor, but it does need an inverted oil system. This system prevents oil from leaking out of the vent for blow-by gases while inverted. A system such as the Christen 801 Inverted Oil System will need to be used; however, since the Rotax 915 is not yet in production, there is not an inverted oil system designed for it.

The fuel tank is placed in the fuselage between the engine and the front pilot. This placement is selected because it fulfills requirements for aerobatics and is this safest position given the options. This tank placement is standard among many aerobatic aircraft such as the Edge, Extra and Pitts, because it reduces the moment of the inertia of the aircraft and allows for a higher roll rate. In considering safety, since the wings are detachable, it will be safer to place the fuel tank within the fuselage than the wings because of the likelihood of loose fuel lines, which could lead to a potentially catastrophic accident. This leaves three options within the fuselage; in front, beneath or behind the pilots. Placing the fuel tank beneath the pilot is a safety hazard if the landing gear should ever collapse during a landing, and placing it behind the pilot increases the cg travel. If it is placed in front, then to rupture the fuel tank would require flying the nose into the ground and collapsing the frame around both the tank and the pilot meaning that the fire would not cause the most serious injury. Therefore, for performance and safety reasons the fuel tank is placed between the pilot and the engine.

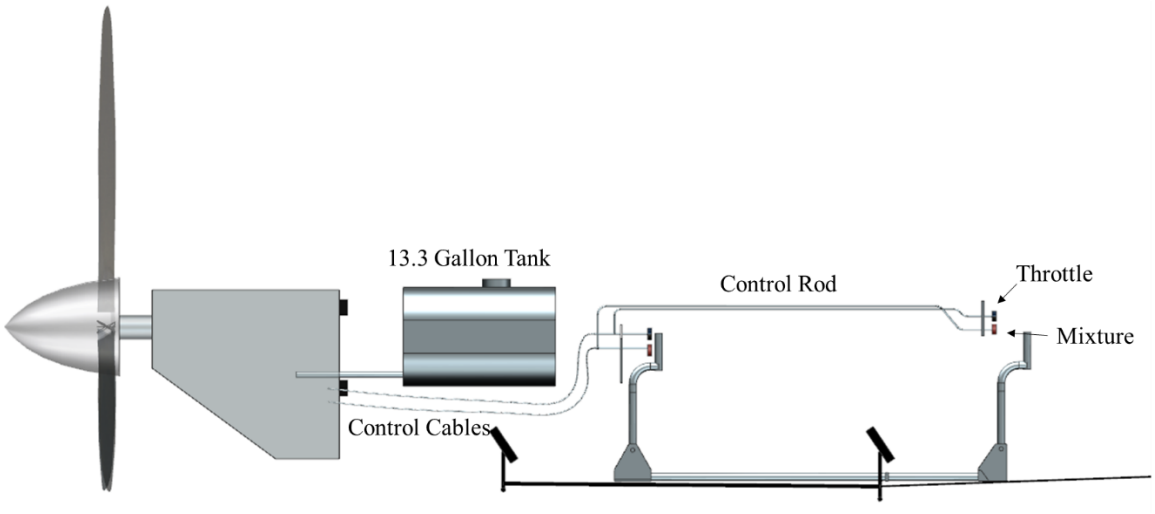

Figure 12.5: Fuel System

12.3 Hydraulics System

A hydraulic system is required for the hydraulic disc brakes installed on the main landing gear. These brakes are operated by the toe pedals attached to the rudder pedals. The hydraulic lines run directly from the pedals to the disc brakes and therefore do not require a hydraulic reservoir or pump.

12.4 Electrical System

The electrical system consists of the battery and alternator on the engine. The battery will be mounted in the engine compartment ahead of the firewall and can be accessed through the cowling. It will only be used to start the engine and power the radio, instrument panel and required lights.

12.5 Environmental System

Due to the simple construction of the aircraft and the fact that it cannot be flown in poor weather conditions, the only environmental control available for the cockpit will be a heater. An air conditioning system is not practical due to the added weight. Air heated by the exhaust will be utilized to heat the cabin on cold days. Ventilation can be controlled by opening a small port in the canopy.

13. Structures, Manufacturing, & Production

The factors which have the greatest impact on the selection of the structural configuration and corresponding materials are weight, ease of manufacturability, and cost. Also taken into consideration is the need to sustain the +6g/-5g loading from aerobatic maneuvers. To meet these requirements, the structure must be as light as possible to remain below the 1,320 lb. weight limit, but still remain structurally sound during maneuvers. Ease of manufacturability is considered to allow the aircraft to be sold in kit form and be constructed as a homebuilt. By regulation, 51% of the aircraft must be built by the owner to be certified by the FAA as an amateur built aircraft. Acquisition costs of the materials and manufacturing costs must remain low for the aircraft to be marketable in the light sport market. Reparability is also an important consideration for aircraft in this market because it is preferred that the owner can affordably and easily make minor repairs.

The other important design goal for the aircraft is the detachability of the wings. This allows owners to be able to trailer their aircraft and drive to competitions if weather is unfavorable. To achieve this, the wing and fuselage

must be interfaced in such a way that it does not add significant weight and is still simple to attach and remove. The design of this connection and the initial sizing of the spar to support 6g loads is given in the following sections.

The final important design goal is to maintain 75 % commonality by weight between the one and two seat variants. This is achieved by using the same fuselage, wing and empennage sections for each. The only major difference between the two is the addition of a seat, instrument panel, set of dual controls and a larger canopy for the two seat variant. A fairing will be designed to cover the front seat opening and support the canopy for the one seat variant.

Each of these factors have been taken into consideration for the development of the fuselage, wing and empennage structures, and the final configuration is shown in Figure 13.1.

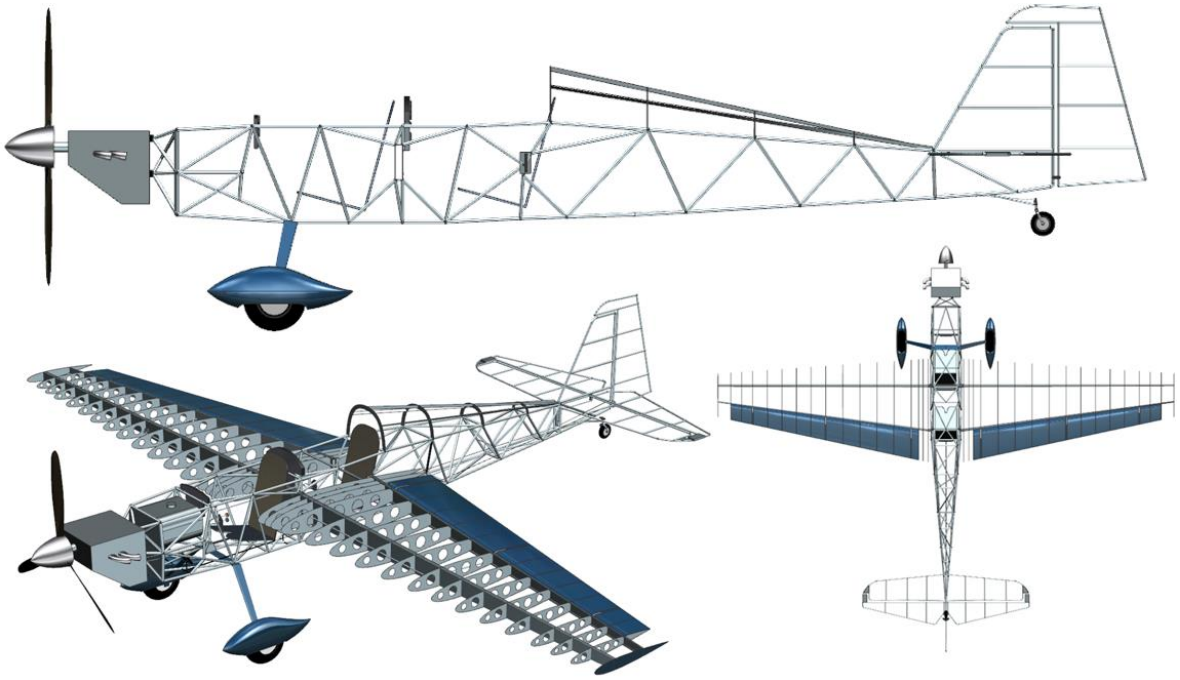

Figure 13.1: Structural Configuration

13.1 Materials Selection

The overall configuration will be composed of aluminum, steel and fabric. Aluminum and steel were selected instead of composites for the primary structure for their savings in cost and to lower the skill requirements to manufacture the aircraft. While the use of composites would save weight, it can require several expensive machines such as an autoclave or large oven and freezer for material storage as well as skilled labor. These manufacturing costs will be difficult for a small light sport aircraft company to overcome and still make a profit. It will also be more difficult to sell as a kit and only perform 49% of the manufacturing prior to sale. This would require that much of the

aircraft be bolted together or connected in some way that could be completed inside a garage without a complex cure cycle. In addition, a composite structure would be more difficult for the owner to repair if it is damaged. Instead, the fuselage will be composed of a welded 4130 steel frame. This material can be acquired in standard sizes and is easy to weld. It will be slightly heavier than an aluminum structure would be, but there are few types of aluminum that are weldable and that also requires more skilled labor. Riveted 2024 Aluminum sheet will be used to construct the internal wing structure for the ease of manufacturing.

To shed some of the weight gained by using a metallic structure, much of the exterior of the aircraft will be covered be fabric. Since the primary load bearing structure in the fuselage is designed as the truss, much of the skin is not load bearing. Fabrics have been used on aircraft since the very beginning and are still used today in smaller aircraft categories such as light sport, aerobatic, agricultural and other small utility and general aviation aircraft. Fabric used to be stitched to the proper shape, sewn to the structure and shrunk to size using dope, however recent advances in materials have allowed simpler and longer lasting fabrics to be developed. The fabric is cut to shape and attached to the structure using adhesive. After setting for 24 hours, the fabric is heated using a heat gun to shrink the fabric until taught. Three of the most common modern fabrics in use are Ceconite [16], Poly-Fiber [17] and Oratex [18]. The first two fabrics use a toxic chemical for the adhesive and require protection when it is being applied, however the more recently developed Oratex does not. The Oratex fabric is also ¼ of the weight with a similar strength to the others. For these reasons this fabric will be used to cover portions of the wings and fuselage. The only disadvantage is that it is certified in Europe but is currently not certified by the FAA. It is expected to be certified by the entry into service date of this aircraft and will therefore be used.

Table 13.1: Material Properties [19]

	F_{tu} (ksi)	F_{ty} (ksi)	F_{cy} (ksi)	E (Msi)	Poisson's Ratio	Density (lb/in^3)
AISI 4130 Chrome Moly Steel	95	75	75	29.0	0.32	0.283
2024-T3 Aluminum Sheet	64	47	39	10.5	0.33	0.1
	Tensile Strength					
	Lengthwise (N/ 50 mm)	Crosswise (N/ 50 mm)	Burst Strength (psi)	Shrinkage	Melting Point	Weight (oz/ft^2)
Oratex6000 Fabric	1600	1400	145	9-13%	482°F	0.459-0.524

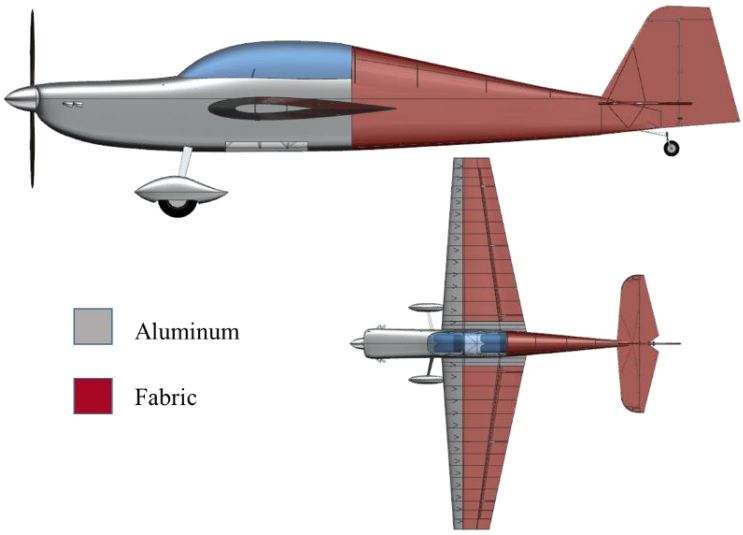

Figure 13.2: External Materials Selection

13.2 Fuselage

The fuselage truss is designed around the major load locations of the wing engine mounts and landing gear. For the fuselage a truss structure is selected over the more traditional longeron and ring frame construction. The advantages of this structure are reduced complexity and it allows the internal structure to take most of the loads while the external structure can be made as light as possible. The truss is designed to place the main supports at the engine mount, wing connection and landing gear connection. Supports are placed diagonally to take torsional loadings and are placed within the cockpit to support the wing and landing gear as much as possible without interfering with the pilot. Aluminum skin will be used from the nose to the cockpit for damage tolerance and to protect the engine. Meanwhile fabric will cover the aft portion of the fuselage to save weight. Ring frames and small longerons are used to maintain the shape of the fuselage aft of the cockpit and support the fabric.

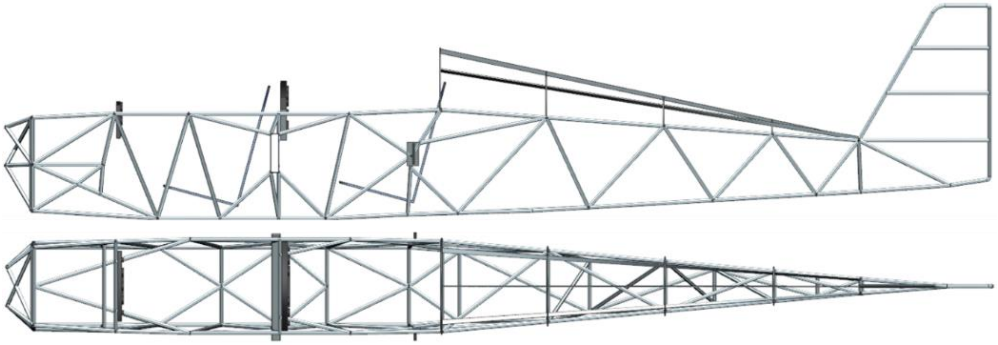

Figure 13.3: Fuselage Truss Structure

13.3 Wing

For initial sizing of the wing the main spar is sized to take the full load of a 6g pull up. The loading is determined using the assumption that the lift along the span of the wing is distributed linearly based on the chord. The shear and moment diagrams are shown following with a maximum shear of 3,720 lb. and a maximum moment of 286,500 in-lb, both of which occur at the root. The location of the rear pilot does not allow for a continuous rear spar. Instead, it will be bolted to the fuselage using a single bolted connection. Therefore, the rear spar will be designed to support only the shear caused by the twisting moment. Otherwise additional fuselage structure would be required to support a torsional load, possibly requiring a ring frame passing through the canopy

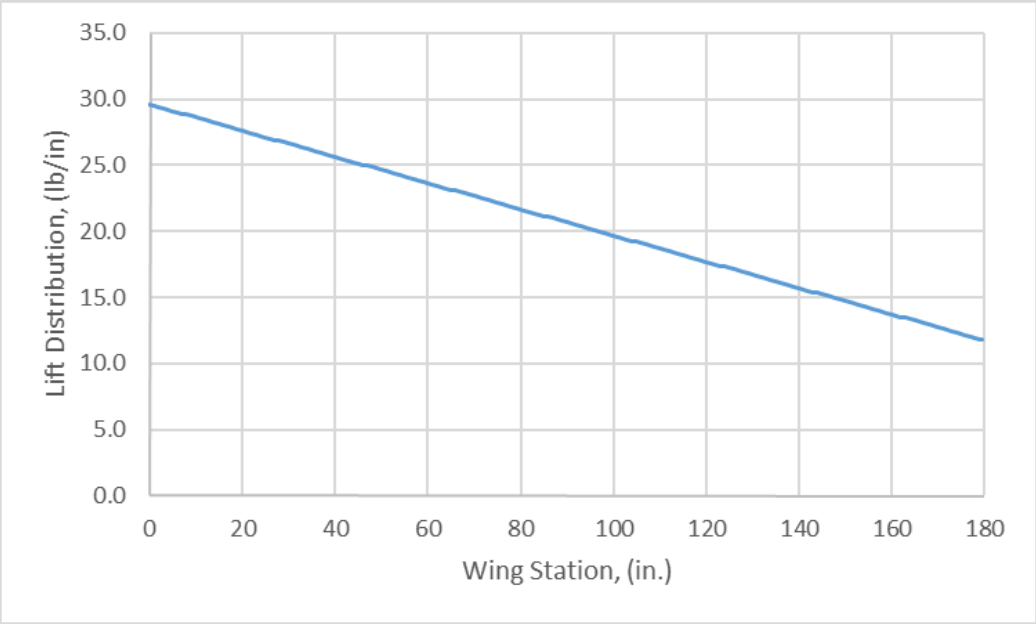

Figure 13.4: 6g Wing Lift Distribution

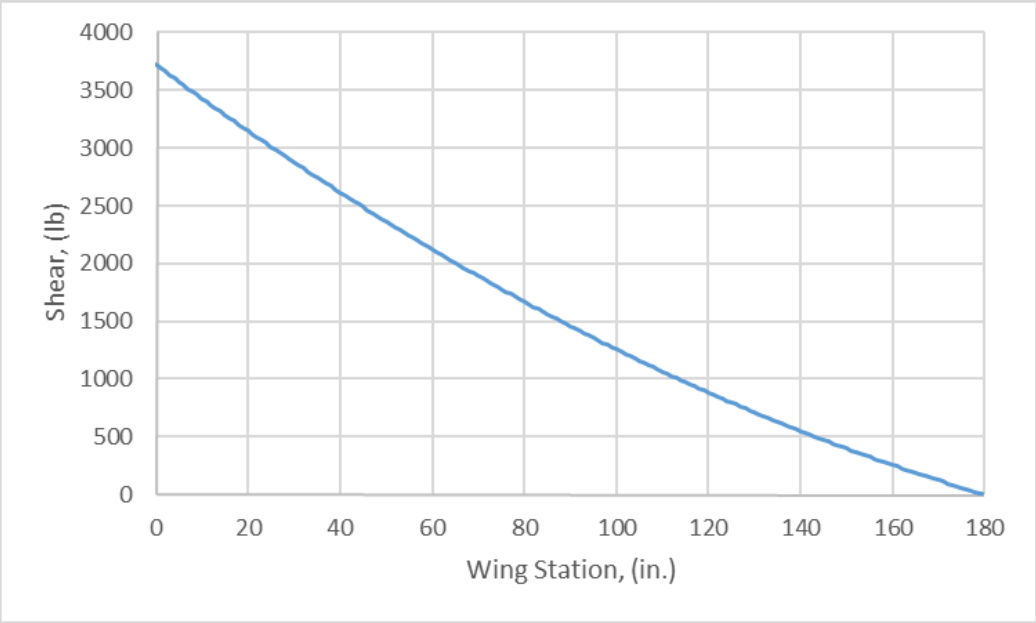

Figure 13.5: 6g Wing Shear Diagram

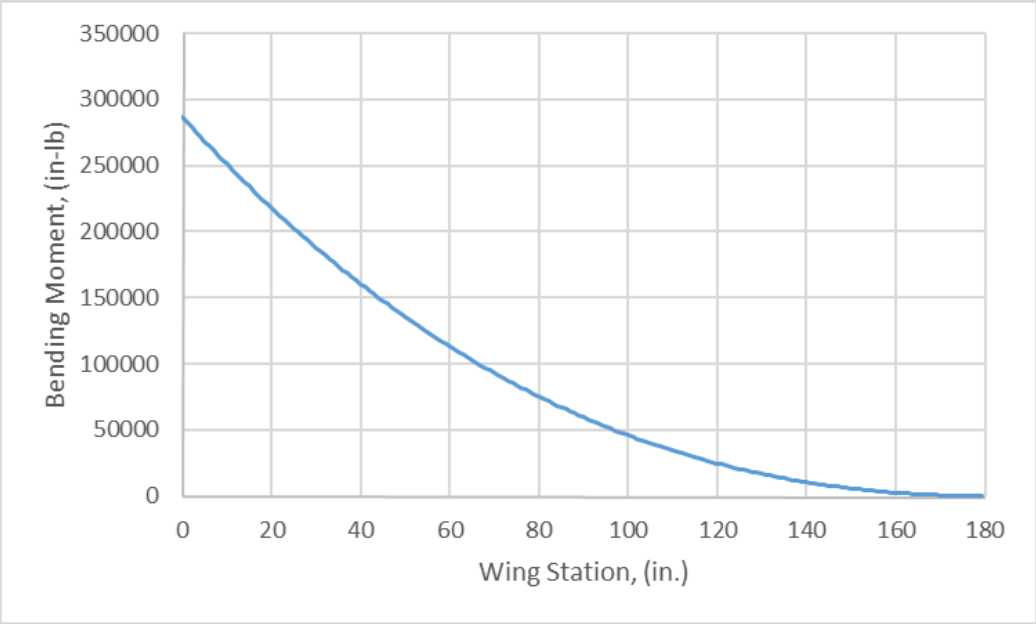

Figure 13.6: 6g Wing Bending Moment

An initial size for the main spar was determined using the calculated maximum bending moment. A spar with a c-cross-section was selected to increase the moment of inertia and for manufacturing purposes. With further integration of the distributed load curve, the wing is estimated to have a 6 in. deflection under a maximum 6g load. This calculation is based on the assumption that the wing is a cantilevered beam and only the moment of inertia of the main spar is considered.

The ribs are spaced 8-12 in. apart to provide support for the fabric covering to preventing wrinkles and provide plenty of surface for the fabric to adhere to. Rib flanges, not shown in Figure 13.7, will be included to support the fabric. The ribs are also spaced so that one rib is placed at each aileron hinge to provide structural support for the aileron. It is expected that lightening holes will be added to both the ribs and spars to save weight and allow space for the aileron pushrods to pass through.

The skin will primarily be fabric for the weight savings. The only portions not covered be fabric are the leading edge and the root section between the fuselage and the aileron. The leading edge is aluminum for damage tolerance and to allow access to the aileron pushrods without damaging the fabric. This will also support the mounting of the vortex generators. The inboard section is aluminum and includes ribs with closer spacing because the pilots will need to step here to enter the aircraft and this section will be handled often to attach and detach the wing.

For manufacturing, the 2024 aluminum spars will be cut to size and then the flanges will be bent to shape using a press brake. These will be riveted together in the final assembly. With the internal structure completed the aluminum skin can be attached and then the fabric adhered to complete the wing.

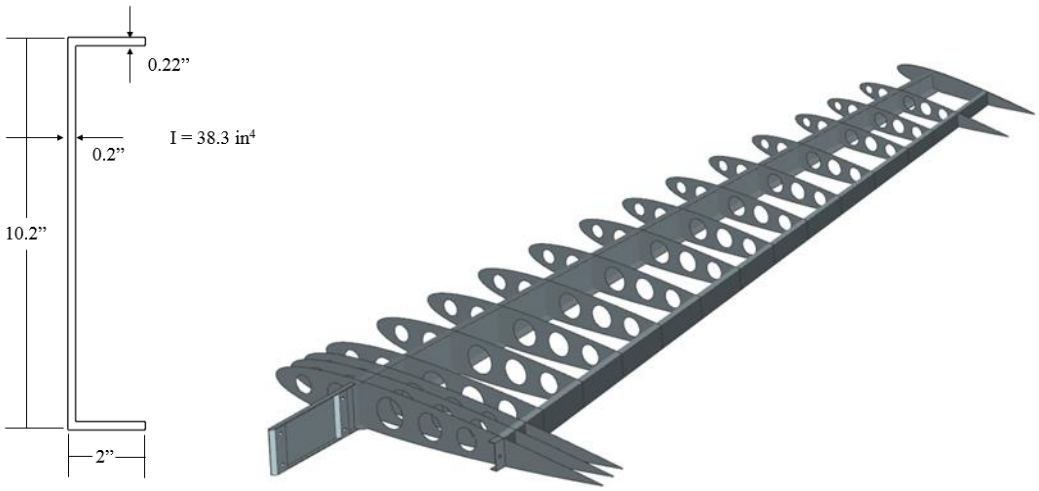

Figure 13.7: Wing Structure and Main Spar Root Cross Section

13.3.1 Wing-Fuselage Interface

Since the aircraft has a mid-wing, the full wing cannot be detached from the top or bottom of the fuselage in one piece; it must instead be disconnected at the half span. Several joint methods were considered for this intersection, such as insertion of the main spar into a sleeve, a butt joint with a bolted connection to the fuselage frame, and a lap joint. Of the possibilities, a lap joint within a rectangular sleeve was chosen for the lower weight and ease of attachment. If the main spar of both wings are not connected directly to each other and instead transfer load through the fuselage, the fuselage structure at this point will significantly increase in size to support the additional loads and will likely require an additional ring frame through the canopy. This method of attachment differs very little from a full span spar and adds only the weight of the mounting box and a solid insert within the c-channel to maintain the structural integrity of the spar.

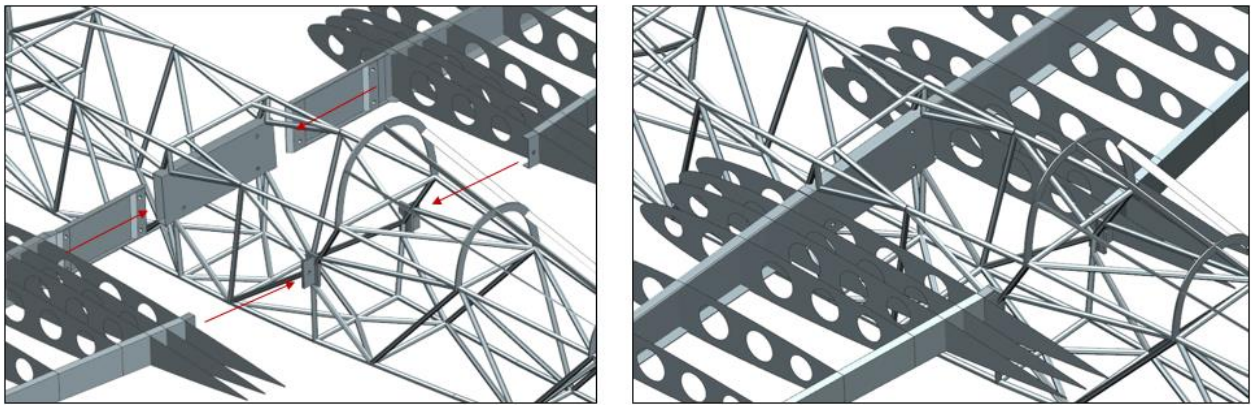

Figure 13.8: Connection of Wing to Fuselage

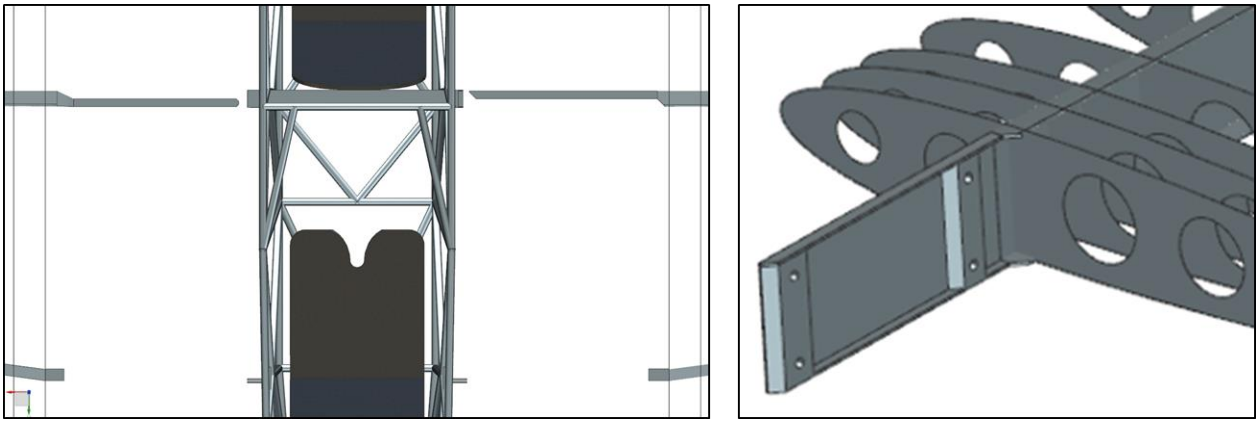

Figure 13.9: Spar Lap Joint Detail

To make the c-cross section stable under torsional loads, a solid insert is added at the points where the bolt holes intersect the spar. This will maintain the stability of the spar until it can be mounted in the box within the fuselage. It will also help to transfer the load in the flange of the spar down into the bolt. What will likely size the inboard portion of the spar and the solid support within the c-channel is the handling loads associated with inserting and removing the wing from the fuselage.

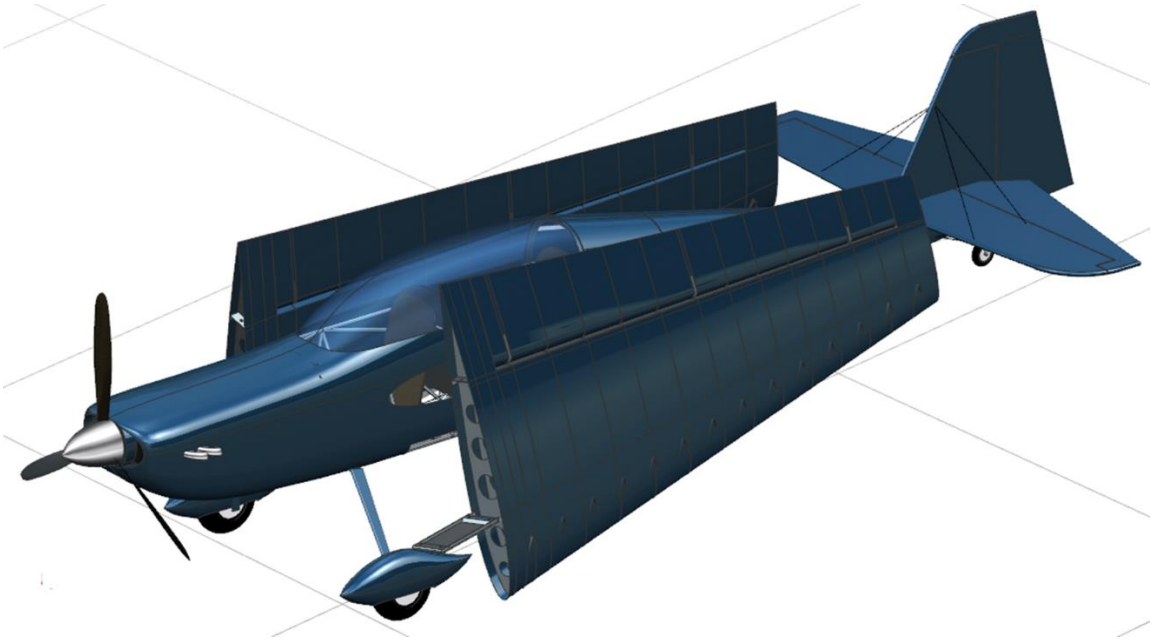

Figure 13.10: Aircraft with Detached Wings for Trailering

13.4 Empennage

The empennage structure is designed similar to the fuselage structure. It is composed of bolted aluminum tube substructure and fabric skin. The aluminum tubing will be bolted together so that the more complex welding of aluminum will not be required. Four support rods added to the tail to decrease the required structure and therefore the weight. Once again to save weight, the empennage will be covered by fabric. The curved leading edge is added purely for aesthetic appeal, although it adds some complexity to the manufacturing process. It is considered worthwhile because it differentiates the profile of the aircraft from the sharp leading edges of the Extra 330 or the Edge 540, but looks sharper and faster than a Pitts.

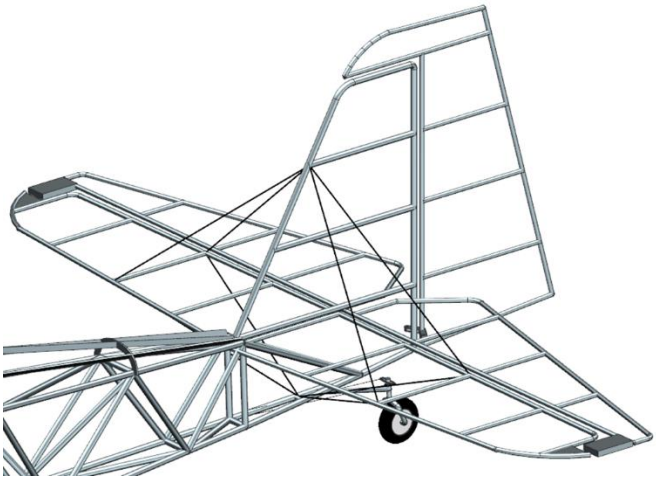

Figure 13.11: Empennage Structure

14. Cost Estimation

Major aircraft manufacturers in the USA, such as Cessna and Piper, have attempted Light Sport Aircraft designs with little success or market penetration. This is due to the high purchase price of the designed aircraft when compared to the Light Sport Aircraft market. Major manufacturers attempted to primarily market the aircraft as a cheap alternative to Part 23 certified aircraft. This was the hubris of both major manufacturers as the LSA market is generally the market for potential aviators to enter the aviation sphere rather than stepping down from Part 23 certified aircraft.

Therefore, the aircraft is primarily targeted at pilots that have obtained their sport pilot certificate, looking for the next challenge and are searching for an aerobatic aircraft. A secondary market is identified as pilots that are looking for an alternative to Part 23 certified aerobatic aircraft, but as stated before, this is not a large market.

Since the introduction of the Light Sport Aircraft category in 2005, the General Aviation Manufacturers Association (GAMA) reports between 2005 and 2015 the affiliated manufacturers have sold 17,898 aircraft where 1,492 were LSA's and 525 were aerobatic [33].

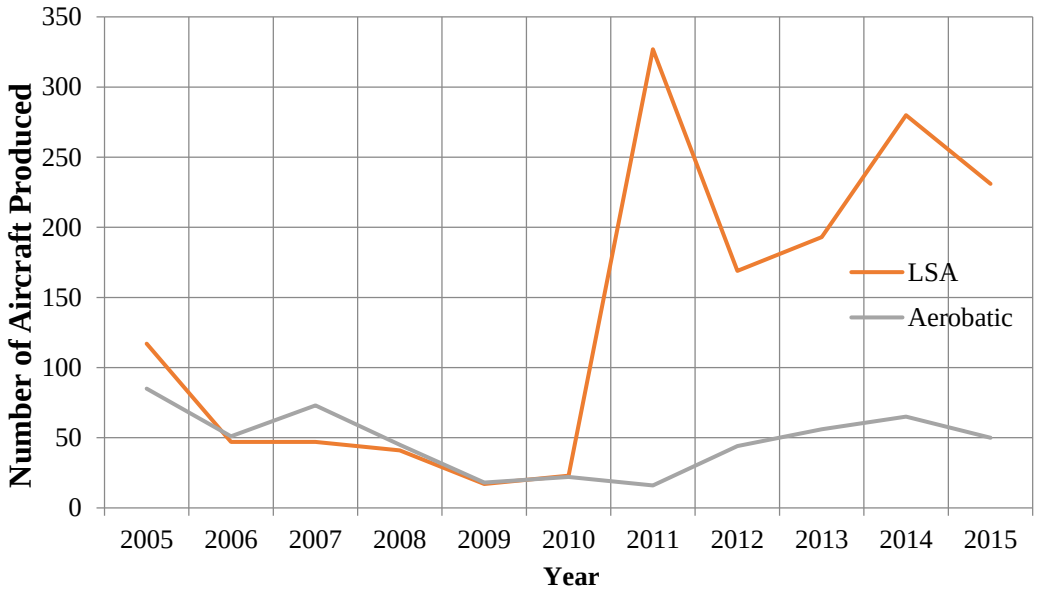

Figure 14.1: Number of Aircraft Deliveries [33]

From Figure 14.1 it can be seen that the yearly deliveries of LSA's is volatile but has grown between 2005 and 2015 at a rate of 11.4 aircraft per year. Deliveries in 2015 totaled at 19.25 aircraft per month from eleven manufacturers resulting in a production rate of 1.75 aircraft per month, per manufacturer. Due to the volatility in the market and that the aircraft opens a new market placed both in the LSA and Aerobatic categories, a conservative initial production rate of 1 (either single or two seater) aircraft per month total to break into the market.

To supplement sales of the ASTM certified aircraft, a popular option is to offer the aircraft as a 49% pre-built kit. This allows pilots that are interested to be involved in the manufacturing process to construct 51% of the aircraft and register as an experimental/amateur-built LSA [34]. It is expected that the sales of the kit version would not exceed 1 every six months.

It is difficult to accurately cost LSA designs, as many successful manufacturers in the Light Sport Aircraft market started as enthusiasts that designed an aircraft for themselves and later went into production or initially modified older, well-known, and proven designs such as the Piper J-3 Cub [35].

From discussion with David Pilkington the authors were advised that often the designer, as a hobby, conducted the engineering for no immediate remuneration and built a prototype under the experimental homebuilt legislation. Due to the relatively low cost to construct an aircraft, the designer kept a running total of costs and estimated cost for subsequent aircraft and further used that data to estimate a profitable production rate.

For the purpose of this report estimates for costing were derived from Raymer [25]. The method is derivative of DAPCA IV which is used for military programs. To calibrate the Raymer method for civil designs the final results are divided by four. The Eastlake model [36] for cost was used to calibrate or outright replace values from the Raymer method where the estimation was extreme.

The Raymer civil method is limited to large civilian projects and did not correlate well to existing Light Sport Aircraft designs. While still utilising the data created, the Raymer civil method was used to estimate the percentage of cost from engineering, tooling, manufacturing, quality control, development support, and flight-testing to improve cost estimation. This was reasoned as sufficient cost allocation could be made for each sub-category in regards to an estimated aircraft cost, excluding the engine, avionics systems and any miscellaneous items that can be costed as separate entities.

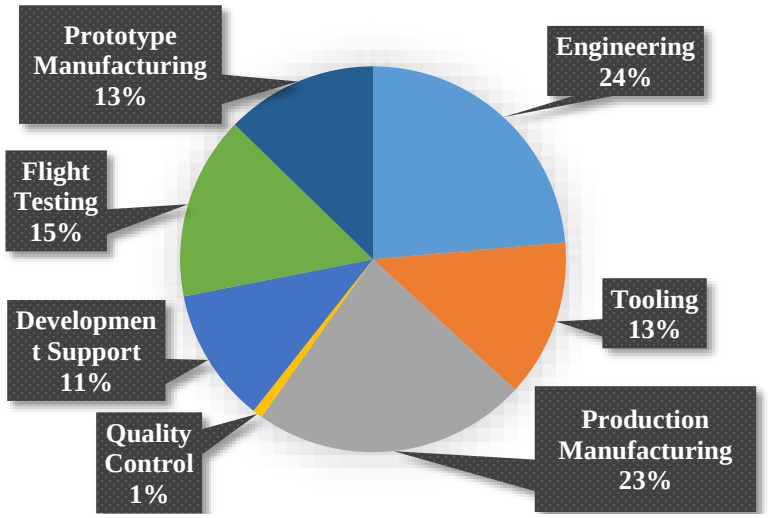

Figure 14.2: Typical Engineering and Manufacturing Cost Percentages [38]

14.1 Certification Cost

At a minimum production of 60 aircraft, the non-recurring costs of the program are listed in the table below.

Table 14.1 - Non-recurring Costs

	Man-hours	Rate, $/hr	Total Cost
Engineering	2,514	$92.00	$238,226.64
Development Support			$159,478.50
Flight Test Operations			$24,018.08
Tooling/Machinery	8,812	$61.00	$553,651.35
Certification Cost			**$975,374.57**

Engineering costs and flight test operations were estimated via the Eastlake method [36]. Development Support and the tooling/machinery were estimated using Raymer [25].

14.2 Flyaway Cost

Due to the high similarity between designs, costing was conducted for the two-seat variant, as the majority of manufacturing processes are common. The discount provided by the single seat variant is a reduction of cost in avionics, a removal of a seat. Although the canopy is of reduced size it is expected that the complexity of manufacturing would remain and that the price would not drop. For non-recurring costs a payback period of 5 years is assumed. Costing for Development Support and Manufacturing Labour has been determined by the estimation methods presented in Raymer [25]. Costing for Engineering has been determined by the Eastlake model presented in Ref. 36. The engine and avionics were priced at market value or were adjusted for a future value if the product was still in development but would be available by 2020. The avionics were priced with data from online retailers such as Aircraft Spruce [44]. As there is no estimated price for the Rotax 915iS, the price has been estimated from a similar product, the Rotax 914, and the price scaled by horsepower.

Table 14.2: Fly-Away Costs for Single and Two Seat Variants

	Single Seat	Two Seat
Engineering	$3,970.44	$3,970.44
Development Support	$2,657.97	$2,657.97
Flight Test Operations	$400.30	$400.30
Tooling	$9,227.52	$9,227.52
Manufacturing Labor	$25,234.60	$25,234.60
Quality Control	$1,640.25	$1,640.25
Materials/Equipment	$4,628.14	$4,628.14
Fixed Landing Gear Discount	-$7,500.00	-$7,500.00
Engine	$33,165.39	$33,165.39
Propeller	$3,239.35	$3,239.35
Avionics	$5,084.94	$10,169.88
Total Cost to Produce	**$81,748.91**	**$86,833.85**

14.3 Profitability

The program can be 10% profitable at any production rate if the aircraft have a 10% premium placed upon cost. While this is unrealistic from the RFP, a plot showing the total program cost and revenue created by the sale of these aircraft at a range of price-points was produced. This shows the number of factory-built aircraft required to be produced at a given price-point to generate a profit.

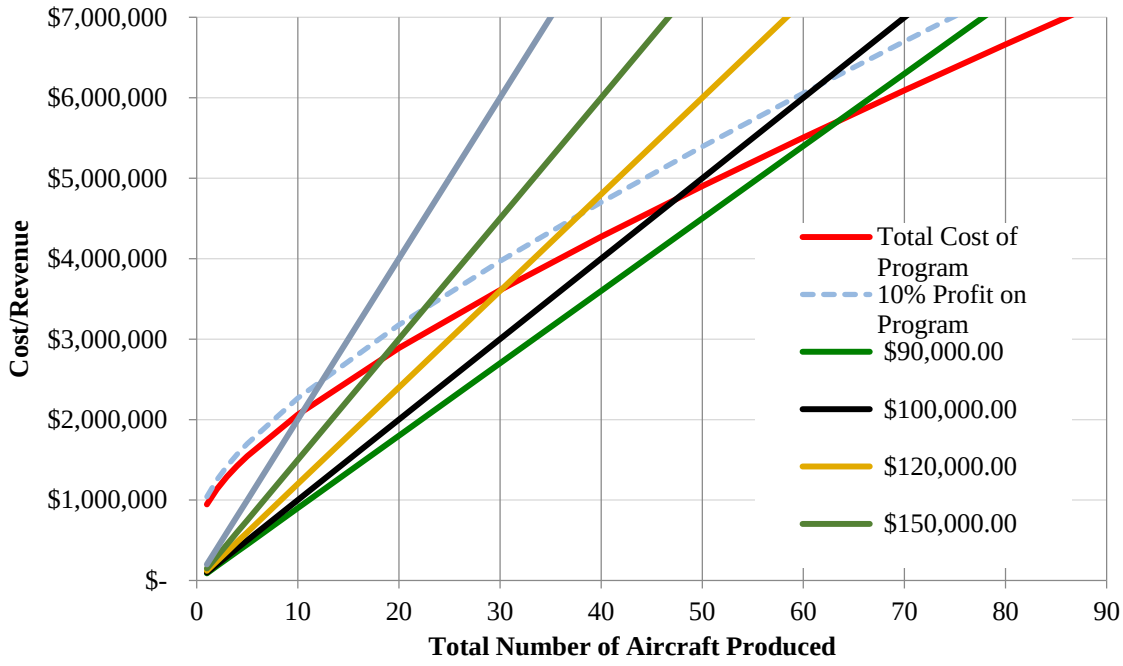

Figure 14.3: Program Break-Even Analysis

It can be seen quite clearly that a higher price-point per factory-built aircraft produces a profit quicker but this trend needs to be tempered with market expectation. While the aircraft may be priced at $200,000 and offers profits after the eleventh aircraft, the market may not pay $200,000 for such an aircraft and if the aircraft is not marketable, it will never be profitable.

From a quick market survey it was found that a two-seat base-model aircraft in this class is reasonably expected to be priced at $100,000 with a single-seat variant priced at about $95,000. At this price, every aircraft produced after the 48th aircraft would be profit and after the 60th aircraft the program would be generating more than 10% net profit. At initial production rates, the 60th aircraft would be 5 years after the launch of the first aircraft.

Table 14.3: Aircraft Sales Price

	Single Seat	Two Seat
Aircraft Cost	$81,748.00	$86,833.85
Sales Price	$95,000.00	$100,000.00
Profit	$13,252.00	$13,166.15

Certain extras are expected to be fitted to the aircraft that some pilots may elect to purchase. The installed price is listed below. A greater list of future extras/retrofits would be expected that require further engineering and design, such as, carbon fiber skin retrofit kits.

Table 14.4 - Optional Extras

Interchangeable Leather Seat (per seat)	$780.00
EFIS Upgrade (per seat)	$15,021.27
Autopilot	$2,171.00
Audio and speakers	$1,950.00
External Lights for Night Flying	$1678.66
Smoke System	$1354.63
Long-range fuel tanks (per set)	$422.50
Possible increase on Sales Price	**$24,158.06**

To generate a 10% profit on aircraft kits they would be priced at $30,684 + Shipping. The aircraft kits would be 49% pre-built by the factory to meet the 51% amateur-built FAA ruling [34]. The aircraft kits would be all parts required to build the aircraft minus the engine, propeller, and avionics which the builder is expected to purchase at a later stage of manufacturing due to the cost and service life of the components.

The kit-built aircraft are not included in the cost analysis as the kit-built market is even more volatile than the LSA market. Any profits from the sales of aircraft kits would be seen as supplemental and cannot be considered, at least initially, a viable source of income.

14.4 Maintenance Costs

The maintenance costs of an aircraft are a continual associated cost that will directly affect the consumer. Typically, LSA's are owned privately which creates an impetus for aircraft that are not only affordable to purchase, but affordable to fly and maintain. Aircraft with low running costs are more popular which would see an increase in the production of the design.

The Raymer method uses material cost/flight hours and material cost/flight cycle as two parameters to determine maintenance cost [25]. Regulations state that all light aircraft must have a routine inspection every 100 flight hours and costing was executed upon this basis [24].

The calculations done are assuming each year 100 flight hours will be completed. This was given in 33.3 cycles, giving an average flight time of 3 hours. All prices estimated from Raymer [25].

Table 14.5 - Maintenance Costing

	Man-hours or units	Rate, $/hr	Cost
Maintenance Labour	30	$36.00	$1,080.00
Material (Flight Hours)	100	$2.34	$234.00
Material (Cycles)	33.3	$19.60	$652.68
Annual Maintenance Cost			**$1,966.68**

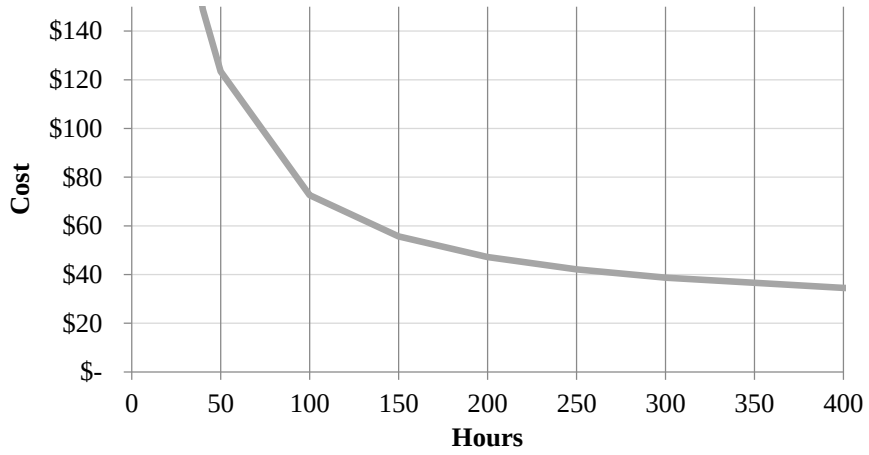

Figure 14.4: Direct Operating Costs per Hour

The fuel costs were priced from an average consumption of 5.7 gal/hr from the Rotax 914 and the average national automobile fuel price [45]. The oil consumed was priced from the maximum allowable oil consumption of the Rotax 914 and priced using aviation grade oil from Aviation Spruce [44]. The annual inspection pricing was estimated earlier in the report from Raymer [25]. Oil change, overhaul, unscheduled maintenance, insurance, and tie down are priced from Ellis [38]. The FAA registration fees are direct from the FAA website [39].

Table 14.6: Variable and Yearly Fixed Costing

Variable		**Fixed (Yearly)**	
Item	Cost per hour	Item	Cost
Fuel	$12.16	Annual Inspection	$1,966.88
Oil Consumed	$0.65	Unscheduled Maintenance	$1,500.00
Oil Change	$3.00	Insurance	$1,000.00
Overhaul	$6.00	Tie Down	$900.00
		FAA Registration	$5.00

15. Salient Characteristics & Final Three-Views

Table 15.1: Common Values between Single and Two Seat

Parameters	***Value***
Fuselage Length	360 in.
Power	135 hp
Propeller Size	6.5 ft.
Thrust Attainable	813 lb.
Wing Area	150 ft^2
Wingspan	30 ft.
Horizontal Tail Area	29 ft^2
Vertical Tail Area	15.3 ft^2
Stall Speed	45 kt

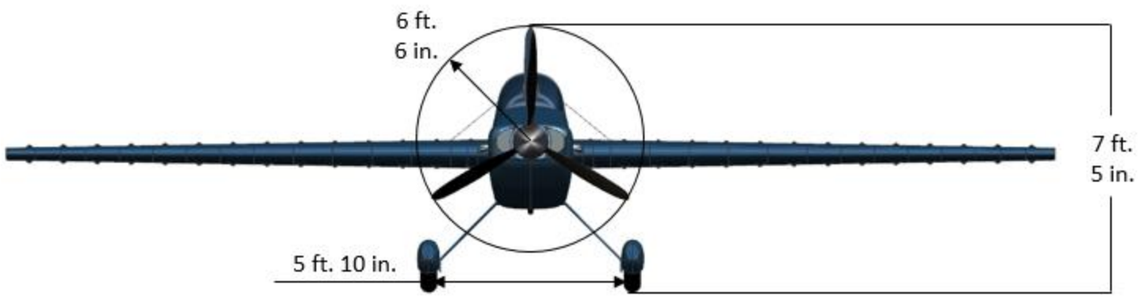

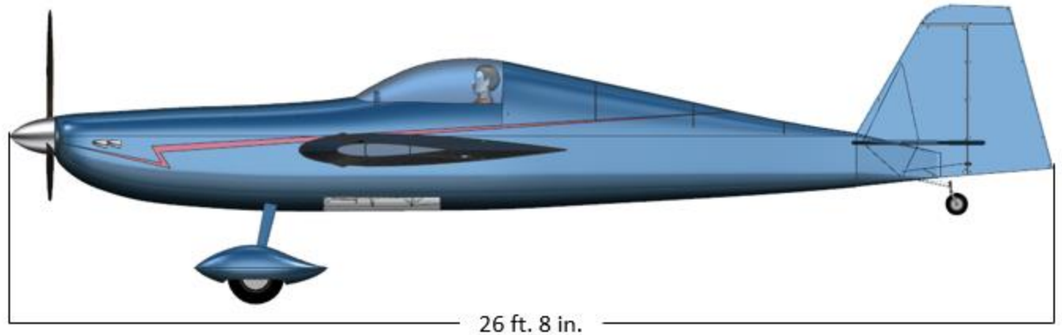

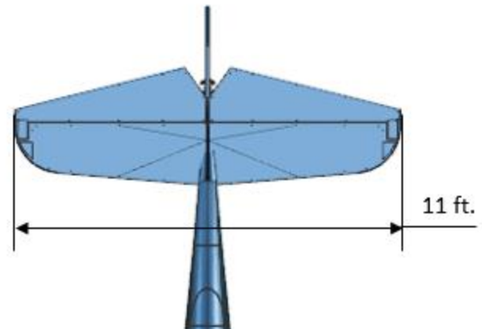

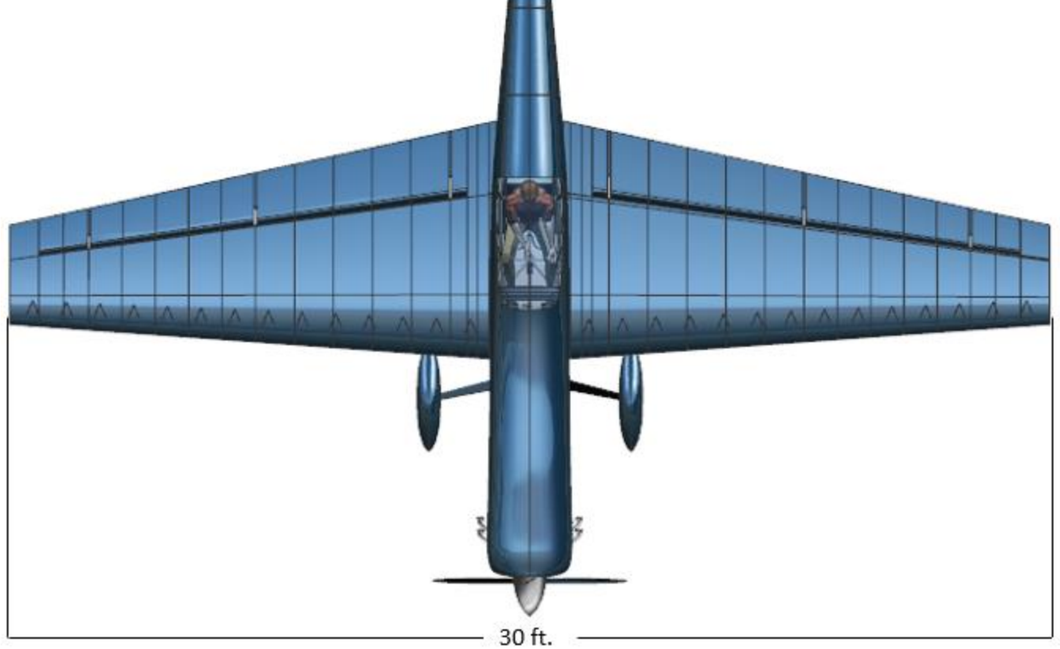

Single Seat Characteristics	
Max Takeoff Weight	980 lb.
Aerobatic Weight	880 lb.
Range	460 nmi.
Takeoff Field Length	680 ft.
Climb Rate	2,250 fpm
Roll Rate	185 °/s
Cost	$95,000

Figure 15.1: Final 3-View – Single Seat

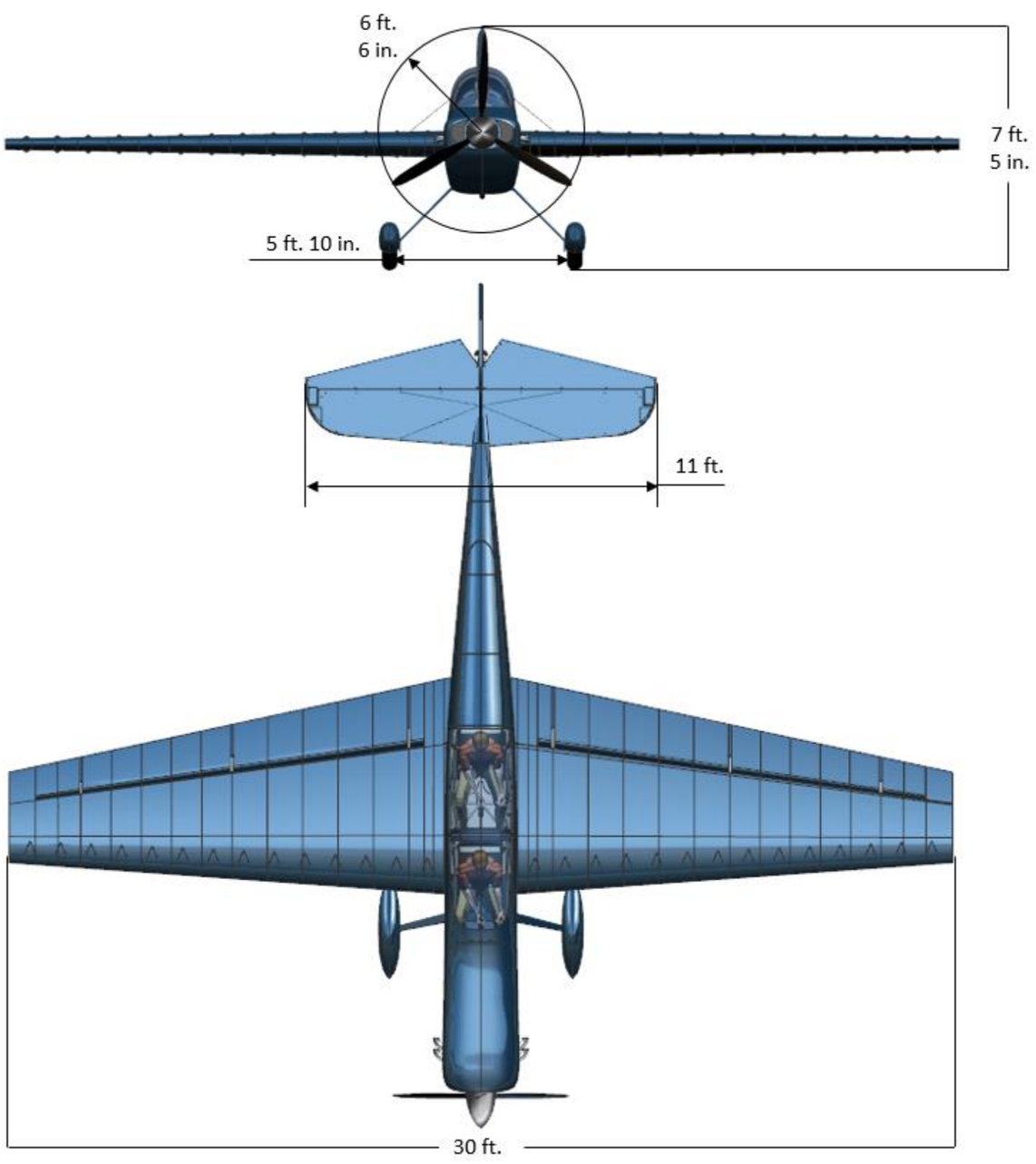

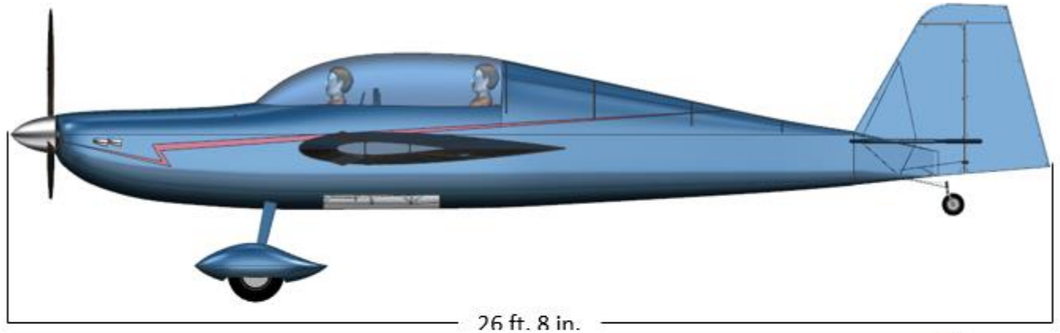

Two Seat Characteristics	
Max Takeoff Weight	1,200 lb.
Aerobatic Weight	890 lb.
Range	327 nmi.
Takeoff Field Length	1,010 ft.
Climb Rate	2,170 fpm
Roll Rate	185 °/s
Cost	$100,000

Figure 15.2: Final 3 View – Two Seat

16. References

1. Orr, Matt, *2015-2016_Undergraduate_Team_Aircraft_Design_Competition*, Reston: American Institute of Aeronautics and Astronautics, 23 Aug 2015, PDF.
2. Anon, "Airdrome Aeroplanes" ~ Holden, MO", airdromeaeroplanes.com, Airdrome Aeroplanes. 2011. Web. February 16, 2016.
3. Anon, "WW1 Wings of Glory Airplane Packs Preview – Sopwith Camel – Part 2", *aresgames.eu*, Ares Games Srl. 2015. Web. February 16, 2016.
4. Davisson, Bud. "Flying Leo's Stephens Akro", *Air Progress*, Oct 1973: Web. February 16,2016.
5. Anon, "Zenith Aircraft Company", *zenithair.net*, Zenith Aircraft Company, 2016. Web. February 16, 2016.
6. Anon, "U.S. Civil Airman Statistics", *faa.gov*, Federal Aviation Administration, 2016, Web, May 11, 2016.
7. Wheeler, Gary, *U.S. Patent Application for Low Drag Vortex Generators*, Publication Number US5058837A, published 22 October 1991, filed 7 April, 1989.
8. Barrett, Ronald, *An Experimental Evaluation of Smart Tetrahedral Vortex Generators*, University of Kansas, Lawrence KS, 1993.
9. Maliniemi, Mikko, *Christen Eagle*. 2004, Photograph, www.airliners.net, Jamijarvi, Finland.
10. Desrosier, Walter, Doug Macnair, Peter While, "PAFI: Piston Aviation Fuels Initiative; Future Unleaded Aviation Gasoline", *EAA AirVenture 2015*, FAA. Oshkosh, Wisconson, July 21, 2015.
11. Roskam, Jan, *Airplane Design Part I: Preliminary Sizing of Aircraft*, DARcorporation, Lawrence KS, 1985.
12. Roskam, Jan, *Airplane Design Part II: Preliminary Configuration Design and Integration of the Propulsion System*, DARcorporation, Lawrence KS, 1985.
13. Roskam, Jan, *Airplane Design Part IV: Layout of Landing Gear and Systems*, DARcorporation, Lawrence KS, 1985.
14. Roskam, Jan, *Airplane Design Part V: Component Weight Estimation*, DARcorporation, Lawrence KS, 1985
15. Anon, *Service Manual Extra 300L Doc. No: EA-06702*, Extra Flugzeugproductions-und Vertriebs-GMBH, Hünxe, Germany, 2009.
16. Anon, *Ceconite Fabric Product Data Sheet 2014-1*, Randolph Aircraft Products, 2014, Available: http://www.ceconite.com/fabrics.htm.
17. Anon, *Poly-Fibre Fabric Product Data Sheet 2014-1*, Poly Fiber Aircraft Coatings, 2014, Available: http://polyfiber.com/stits/index.htm.
18. Anon, *Oratex Speifications and Technical Data*, Better Aircraft Fabric, Available: http://www.betteraircraftfabric.com/specifications.html.
19. Anon, "*Military Handbook Metallic Materials and Elements for Aerospace Vehicle Structures*, Department of Defense, United States, 1998.
20. Roskam, Jan, *Airplane Design Part VI: Preliminary Calculation of Aerodynamic, Thrust, and Power Characteristics*, DARcorporation, Lawrence KS, 2008
21. Roskam, J. *Airplane Flight Dynamics and Automatic Flight Controls*, DARcorporation, Lawrence, KS, 1995.
22. Sadraey, M. H. *Aircraft Design: A Systems Engineering Approached.*, Wiley: 2012.
23. Weir, R. J. *"*Ducted propeller design and analysis,*" Sandia National Laboratories, Albuquerque*, 1987.
24. Küchemann, D., and Weber, J. *Aerodynamics of Propulsion*, McGraw-Hill: 1953.
25. Raymer, D. P. *Aircraft Design: A Conceptual Approached.* The American Institute of Aeronautics and Astronautics. 2013.
26. Gudmundsson, S. *General Aviation Aircraft Design: Applied Methods and Procedures. 1 ed., Elsevier Science: 2013.*
27. Roskam, Jan, and Willem Anemaat. *Advanced Aircraft Analysis*. Vers. 3.6. Lawrence: DARCorporation, 2014. Computer software.
28. Staffell, I., *Energy and Fuel Datasheet*. 2011, University of Birmingham: United Kingdom.
29. Miller, D.J., *Energy Storage: Current Status and Future Trends*. 2013, Argonne National Laboratory.
30. McKissock, B., P. Loyselle, and E. Vogel, *Guidelines on Lithium-ion Battery Use in Space Applications*. 2009, NASA Glenn Research Centre. p. 3-24.
31. Anon, "Rotax 915 IS/ISC – Rotax Aircraft Engines" *flyrotax.com*, Bombardier Recreational Products, 2016. Web. May 2, 2016.
32. Anon, "WAM 4 Cylinder Diesel Aero Engine", *wilksch.net*, Wilksch Airmotive, 2016. Web. May 2, 2016.

33. Anon, "Shipment Database | GAMA - General Aviation Manufacturers Association", *Gama.aero* Available: https://www.gama.aero/media-center/industry-facts-and-statistics/shipment-database.
34. Anon, "Amateur-Built Aircraft Kits", *Faa.gov* Available: https://www.faa.gov/aircraft/gen_av/ultralights/amateur_built/kits/.
35. Anon, "CubCrafters | adventure included", *Cubcrafters.com* Available: http://www.cubcrafters.com/.
36. Gudmundsson, S., *General aviation aircraft design*, Oxford: Butterworth-Heinemann, 2014.
37. Anon, "AAA's Daily Fuel Gauge Report", *Fuelgaugereport.com* Available: http://www.fuelgaugereport.com/.
38. Ellis, J., *Buying and owning your own airplane*, Newcastle, Wash.: Aviation Supplies & Academics, 2006.
39. Anon, "Aircraft Certification – Light Sport Aircraft Registration", *Faa.gov* Available: https://www.faa.gov/licenses_certificates/aircraft_certification/aircraft_registry/light_sport_aircraft/.
40. Anderson Jr., John D., "Elements of Airplane Performance," *Introduction to Flight*, 7th ed., McGraw Hill, New York, 2012, pp. 440-529.
41. Renz, Ron. "Alligator, Inc. – Lawrence, KS – Company Information, Partners, Links", *Airplanetest.com*, Alligator, Inc, 2005. Web. May 6, 2016.
42. Taylor, H., *The elimination of diffuser separation by vortex generators*. 1947, United Aircraft Corporation.
43. Lin, J.C., *Review of research on low-profile vortex generators to control boundary-layer separation*. Progress in Aerospace Sciences, 2002. 38(4–5): p. 389-420.
44. Anon, "Pilot Supplies and Parts from Aircraft Spruce", *Aircraftspruce.com*. Available: www.aircraftspruce.com.
45. Anonymous, "AAA's Daily Fuel Gauge Report", *Fuelgaugereport.com* Available: http://www.fuelgaugereport.com/.